

For Reference

NOT TO BE TAKEN FROM THIS ROOM

Ex libris
UNIVERSITATIS
ALBERTAENSIS



For Reference

NOT TO BE TAKEN FROM THIS ROOM

THE UNIVERSITY OF ALBERTA
THE Hg $6(^3P_1)$ PHOTSENSITIZATION OF
CARBON AND SILICON HYDRIDES

by



ERNEST JAKUBOWSKI

A THESIS

SUBMITTED TO THE FACULTY OF GRADUATE STUDIES
IN PARTIAL FULFILLMENT OF THE REQUIREMENTS FOR THE DEGREE
OF DOCTOR OF PHILOSOPHY

DEPARTMENT OF CHEMISTRY

EDMONTON, ALBERTA

October, 1968

1968 (F)
45 D.

UNIVERSITY OF ALBERTA
FACULTY OF GRADUATE STUDIES

The undersigned certify that they have read, and
recommend to the Faculty of Graduate Studies for acceptance,
a thesis entitled THE Hg $6(^3P_1)$ PHOTSENSITIZATION OF CARBON
AND SILICON HYDRIDES submitted by Ernest Jakubowski in partial
fulfilment of the requirements for the degree of Doctor of
Philosophy.

ABSTRACT

The primary processes in the mercury-photosensitized decomposition of propane and three deuterated propanes have been studied at low pressures.

Primary radicals were trapped by methyl radicals, from the in situ decomposition of dimethyl mercury, and the products measured by gas chromatography. The trapping technique was checked by using 1-chloropropane and 2-chloropropane as propyl radical sources. Butane yields were observed to be representative of the primary radical yields.

The ratio of isobutane to n-butane from the propane reaction was found to be dependent on light intensity. The ratio varied between 0.3 (at high intensity) and 8.5 (at low intensity). Numerical values for the isopropyl to n-propyl split in the primary step for the propanes are ($C_3H_8=9.1$), ($CH_3-CD_2-CH_3=0.6$), ($CD_3-CH_2-CD_3 >30$) and ($C_3D_8=7.0$).

An investigation of the primary processes involved in the mercury-photosensitized decomposition of cyclopropane at low pressures has also been carried out. Results of experiments using methyl radicals as scavengers indicate that decomposition to a cyclopropyl radical and a H-atom is not an important process. The major primary step is probably the formation of an electronically excited cyclopropane, possibly the ground state triplet of trimethylene, with a large excess of vibrational energy.

A study of the unimolecular isomerization of chemically activated methylcyclopropane has also been conducted. The chemically activated species were produced by the recombination of cyclopropyl and methyl radicals. These radicals were produced through the mercury-photosensitization of dimethyl mercury, cyclopropylbromide mixtures.

Unless excess energy is removed from the activated methylcyclopropane molecules via collisional deactivation, isomerizations to butenes occurs. A pressure study, using helium as a third body, has yielded data which are concordant with the results of previous studies in which chemical activation was initiated by other methods.

Studies of the mercury-photosensitized decomposition and 2700 Å photolysis of phenylsilane have yielded data concerning the relative reactivity of a silyl substituted aromatic compound as compared to alkyl substitution.

The mercury-photosensitized decomposition of phenylsilane has been found to take place via C-Si as well as Si-H cleavage. This is the first reported instance of C-Si bond rupture in the mercury sensitization of organosilicon compounds. Decomposition is observed to occur with a quantum yield of unity.

When phenylsilane is photolyzed at 2700 Å, decomposition takes place via C-Si cleavage. Measurements of Φ_{SiD_4} for this reaction indicate that the quantum yield of decomposition should be near unity.

Studies of the secondary radical processes in the sensitization and direct photolysis experiments indicate that silyl radicals do not

recombine to form disilane, their major reactions being abstraction and disproportionation.

Arrhenius parameters for the abstraction reactions of methyl radicals with SiH_4 , SiD_4 , Si_2H_6 , Si_2D_6 and $\phi\text{-SiD}_3$ have been measured. Silanes are more reactive than their hydrocarbon counterparts. The increased reactivity is due to lower activation energies, the A-factors for the analogous carbon and silicon compounds being similar.

Experimental values of E_a have been compared to energies calculated by the Bond-Energy-Bond-Order method using a simple three-mass-point model.

Comparisons of experimental and calculated kinetic isotope effects, based on absolute reaction rate theory, imply that tunneling effects may be significant in these abstraction reactions.

ACKNOWLEDGEMENTS

The author wishes to express his sincere gratitude to Drs. H. E. Gunning and O. P. Strausz for their guidance and assistance throughout the course of this investigation.

Special thanks go to Dr. P. Kebarle for his advice and assistance with the construction and operation of the mass spectrometric system.

The conscientious efforts of Mr. W. Duholke during some of the experimental work, are gratefully acknowledged.

The author would like to express his special appreciation to Dr. H. S. Sandhu for his invaluable assistance in carrying out many of the calculations involved in this manuscript.

Thanks go to Dr. D. C. Dobson for the use of his computer program.

The author would like to thank Mr. B. Woods, Mr. M. deSorgo, Dr. S. Penzes. Mr. R. E. Berkley, Mr. J. Campbell, Mr. B. O'Callaghan and Mr. T. Pollock of the photochemistry group for their helpful advice and criticism.

The invaluable help of the technical staff of the department is acknowledged.

The diligent efforts of Mrs. A. Andrech in the typing of this thesis is appreciated.

The financial assistance provided by the University of Alberta

and the National Research Council of Canada during the course of this work is gratefully acknowledged.

TABLE OF CONTENTS

	<u>Page</u>
ABSTRACT.....	i
ACKNOWLEDGEMENTS.....	iv
LIST OF TABLES.....	x
LIST OF ILLUSTRATIONS.....	xi
CHAPTER I INTRODUCTION.....	1
1) The Hg 6(³ P ₁) Photosensitization of Alkanes.	
2) The Hg 6(³ P ₁) Sensitized Decomposition of Cyclopropane.	
3) The Photochemistry of Silicon Compounds.	
4) The Reactions of Methyl Radicals with Silanes.	
CHAPTER II EXPERIMENTAL.....	18
FAST FLOW SYSTEM	
1) Mass Spectrometer.	
2) Reactor.	
3) The Mercury Lamp.	
4) Sampling Leak.	
5) Operating Procedure.	
STATIC SYSTEM	
1) Vacuum System.	
2) Analytical System.	
3) Photolytic System.	
AUXILIARY EQUIPMENT	

CHAPTER III	THE Hg $6(^3P_1)$ PHOTSENSITIZATION OF PROPANE.....	40
-------------	---	----

RESULTS

- 1) Decomposition of Chloropropanes.
- 2) Decomposition of Propane.
- 3) Deuterated Propanes.
- 4) The Role of H-atoms.

DISCUSSION

- 1) Trapping of the Propyl Radicals.
- 2) Photosensitization of Propane.
- 3) Light Intensity.
- 4) Secondary Decomposition of Primary Radicals.
- 5) The Role of H-atoms.
- 6) Primary Radical Distribution.

CHAPTER IV	THE Hg $6(^3P_1)$ PHOTSENSITIZED DECOMPOSITION OF CYCLOPROPANE.....	76
------------	--	----

RESULTS

- 1) Decomposition of Cyclopropane.
- 2) Decomposition of Cyclopropyl Bromide.

DISCUSSION

THE PRIMARY PROCESSES IN THE $Hg^* +$ CYCLOPROPANE
REACTION

THE UNIMOLECULAR REACTIONS OF CHEMICALLY ACTIVATED
METHYLCYCLOPROPANE.

- 1) Thermochemistry of the Methyl Plus Cyclopropyl
Reaction.

- 2) Isomeric Distribution of Butene Products.
- 3) Miscellaneous Products.
- 4) Calculation of Rate Constants.
- 5) Evaluation of the Technique.

CHAPTER V THE PHOTOCHEMISTRY OF SILICON COMPOUNDS..... 100

RESULTS

- 1) Flow System ($\text{Hg } 6(^3\text{P}_1)$ photosensitization).
- 2) Static Photolysis.

DISCUSSION

$\text{Hg } 6(^3\text{P}_1)$ PHOTSENSITIZATION.

- 1) The Decomposition of Benzene, Toluene and Phenylsilane- d_3 .

- 2) Secondary Reactions.

THE PHOTOLYSIS OF PHENYLSILANE- d_3 .

- 1) 2700 Å Photolysis.
- 2) Summary and Comparison with Benzene and Toluene.
- 3) The Reactions of Silicon Containing Free Radicals.

CHAPTER VI THE REACTIONS OF METHYL RADICALS WITH SILANES... 125

RESULTS

- 1) SiH_4 and SiD_4 .
- 2) Si_2H_6 and Si_2D_6 .
- 3) $\text{C}_6\text{H}_5\cdot\text{SiD}_3$.

DISCUSSION

- 1) SiH_4 and SiD_4 .
- 2) Si_2H_6 and Si_2D_6 .
- 3) Phenylsilane- d_3 .
- 4) Calculated and Observed Activation Energies.
- 5) Primary Kinetic Isotope Effect.

BIBLIOGRAPHY.....	152
APPENDIX A.....	158
APPENDIX B.....	160
APPENDIX C.....	162
APPENDIX D.....	168
APPENDIX E.....	171

LIST OF TABLES

<u>TABLE</u>		<u>Page</u>
I	Propyl Radical Yields from the Mercury- Photosensitized Decomposition of Propane.....	9
II	G. L. C. Operating Conditions and Relative Retention Data.....	33
III	Materials Used.....	36
IV	Decomposition of Chloropropanes.....	44
V	Product Yields from the Decomposition of a 1:1 Mixture of 1- and 2-chloropropane with Excess Hg (CH ₃) ₂	45
VI	Decomposition of Propane and Dimethyl Mercury Mixtures.....	47
VII	Decomposition of Deuterated Propane plus Dimethyl Mercury Mixtures.....	57
VIII	Products from the Mercury-Photosensitized Decomposition of Chloropropane, Dimethyl Mercury-d ₆ and Hydrogen Mixtures.....	62
IX	Butane Ratios from the Decomposition of 1- and 2-chloropropane Mixtures with Added Dimethyl Mercury and Hydrogen.....	63
X	Propyl Radical Yields from the Hg 6(³ P ₁) Photosensitized Decomposition of Propane and Deuterated Propanes.....	74

TABLEPage

XI	Product Yields from the Photosensitized Decomposition of 0.5-1.0 mtorr Cyclopropyl Bromide and 15 mtorr of Dimethyl Mercury.....	78
XII	Product Ratios from Methyl and Cyclopropyl Radical Reaction as a Function of He Carrier Gas Pressure..	82
XIII	Lifetime and Energies of Activated Molecules and Butene Isomer Distribution.....	92
XIV	Photolysis of Phenylsilane-d ₃	106
XV	The Reactions of Methyl Radicals with Monosilane.....	129
XVI	The Reactions of Methyl Radicals with Disilane.....	132
XVII	The Reactions of Methyl Radicals with Phenylsilane-d ₃	134
XVIII	Reactions of Methyl Radicals.....	141
XIX	Calculated and Experimental Energies of Activation for H-atom Abstraction by Methyl Radicals.....	149
XX	Input Parameters for BEBO Calculations.....	178
XXI	Properties of the Activated Complex for Three-Atom-Model Obtained by BEBO Method.....	180

LIST OF ILLUSTRATIONS

<u>Number</u>		<u>Page</u>
1)	Flow System.....	20
2)	Lamp Designs.....	22
3)	Emission Spectrum of Low Pressure Hg-arc.....	23
4)	Construction of Sampling Leak and Reaction Zone.....	24
5)	High Vacuum System.....	28
6)	Analytical System.....	29
7)	Static Photolysis System.....	30
8)	Propylene/Butane Yields as a Function of % Conversion/Pass.....	43
9)	Isobutane/ <u>n</u> -Butane as a Function of % Conversion/Pass.....	51
10)	Energy Levels of Mercury.....	53
11)	Isobutane/ <u>n</u> -Butane as a Function of % Conversion/Pass.....	59
12)	Isobutane/ <u>n</u> -Butane as a Function of % Conversion/Pass.....	60
13)	Isobutane/ <u>n</u> -Butane as a Function of % Conversion/Pass.....	61
14)	C ₄ H ₁₀ Product Ratios as a Function of Pressure.....	84
15)	Butene Ratios as a Function of Pressure.....	85
16)	Product Ratios as a Function of Pressure.....	86
17)	Butene/Methylcyclopropane vs. ω^{-1}	87
18)	Reactions of Methyl Radicals with Monosilanes.....	135

<u>Number</u>		<u>Page</u>
19)	Reactions of Methyl Radicals with Disilanes.....	136
20)	Reactions of Methyl Radicals with Phenylsilane-d ₃	137
21)	Kinetic Isotope Effect, Log k_H/k_D vs. 1000/T, for Methyl Radical plus Monosilane System.....	150
22)	Kinetic Isotope Effect, Log k_H/k_D vs. 1000/T, for Methyl Radical plus Disilane System.....	151

CHAPTER I

INTRODUCTION

- 1) The Hg $6(3P_1)$ Photosensitization of Alkanes.
- 2) The Hg $6(3P_1)$ Sensitized Decomposition of Cyclopropane.
- 3) The Photochemistry of Silicon Compounds.
- 4) The Reactions of Methyl Radicals with Silanes.

INTRODUCTION

Most chemical bonds are of the order of magnitude of 40 or more kcal mole⁻¹. For this reason photochemistry deals primarily with light of wavelength less than 7000 Å. In normal one-quantum absorption processes it is only quanta of these wavelengths which are sufficiently energetic to rupture bonds and produce chemical changes. In special cases of relatively long-lived intermediates and very high, laser-like light intensities, biphotonic processes can initiate chemical reactions with near infrared radiation.

Radiant energy can be introduced into the reactant species (the molecule, radical, etc., which is to undergo chemical change), by either of two processes:

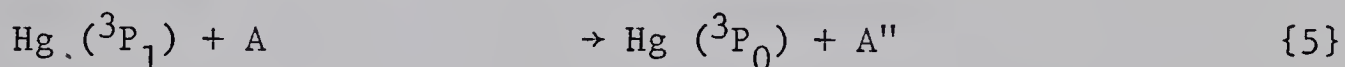
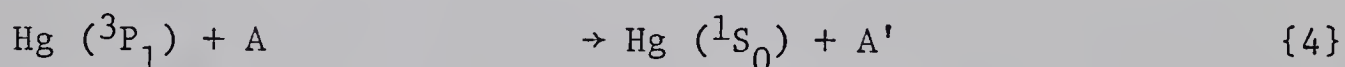
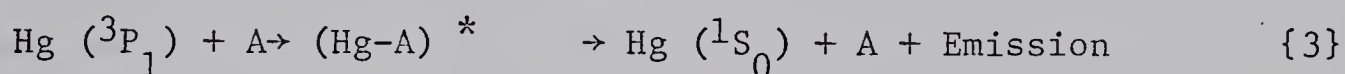
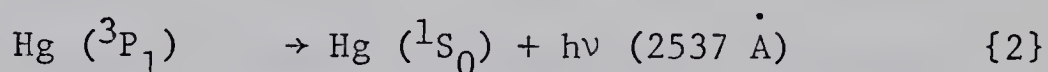
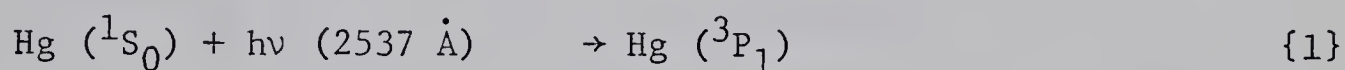
- a) Direct Photolysis - The exciting photon is absorbed directly by the species which is to undergo chemical change.
- b) Photosensitization - The exciting photon is absorbed by some species other than the principal reactant. This excitation energy is then transferred to the principal reactant by a "collision of the second kind" (collisions in which energy of excitation is converted either to other energy of excitation or into kinetic energy).

This technique is particularly valuable in the case where the reactant species does not absorb light in the appropriate spectral region. For instance, the lower molecular weight alkanes absorb in the vacuum

ultraviolet region below 1800 Å. These are energies in excess of 159 kcal mole⁻¹ and are much higher than the 104 kcal mole⁻¹ necessary to rupture the C-H bond in methane, the strongest known for alkanes. Through the technique of photosensitization it is possible to introduce lesser amounts of energy into these molecules.

1) The Hg 6(³P₁) Photosensitization of Alkanes:

The absorption and dissipation of radiant energy by a mercury atom takes place via the following mechanism:



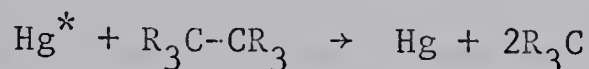
A represents the quenching gas. For alkanes reaction {4} leads to immediate C-H bond scission. The primary quantum efficiency is defined as:

$$\Phi_{\text{Primary}} = \frac{(\text{radicals or H-atoms}) \text{ produced via } \{4\}}{\text{quanta absorbed via } \{1\} - \text{quanta emitted via } \{2\}}$$

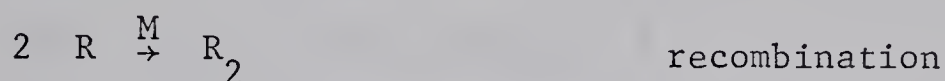
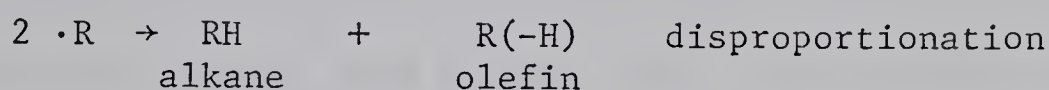
Reaction {5} does not lead to decomposition of the quencher as only 5 kcal mole⁻¹ of energy is transferred.

Early studies (1) on the mercury photosensitization of paraffins have shown the only primary step to be carbon-hydrogen bond cleavage.¹

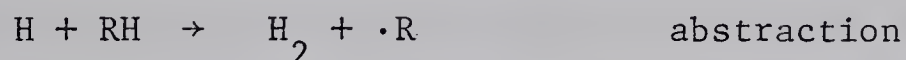
Carbon-carbon bond cleavage was conspicuously absent.



The alkyl radicals formed undergo disproportionation and recombination reactions,



and the hydrogen atoms recombine or abstract hydrogen from the parent paraffin to give H_2 .

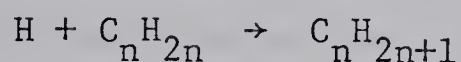


With the exception of the two spherically symmetrical molecules methane and neopentane, primary quantum efficiencies were reported to be quite high.

More recent studies have established primary quantum efficiencies

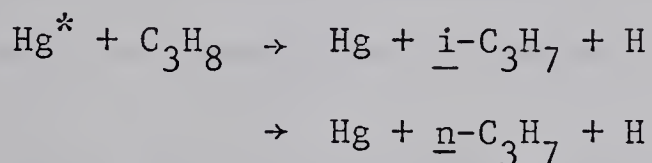
¹ In this thesis, Hg^* will refer to a mercury atom in its $6(^3\text{P}_1)$ electronic state containing $112 \text{ kcal mole}^{-1}$ of electronic excitation energy.

near unity and have pointed out the significance of internal scavenging of H-atoms by the olefins formed through disproportionation reactions.



For a comprehensive review of mercury photosensitization to 1963, consult the excellent article by Cvetanovic', published in the series "Progress in Reaction Kinetics" (2).

The primary process in the Hg^* plus propane reaction is the cleavage of C-H bonds to give H-atoms and n- and isopropyl radicals.



The end products are hydrogen, propylene, 2,3-dimethylbutane, 2-methylpentane and n-hexane. The main constituent of the hexane fraction is 2,3-dimethylbutane, its yield being over 90%. This however, cannot be accepted as unequivocal evidence for a predominant secondary C-H bond cleavage in the primary step for two reasons: (a) the importance of the reaction



has not been clarified and (b) the extent of the self-scavenging reaction



varies with the experimental conditions.

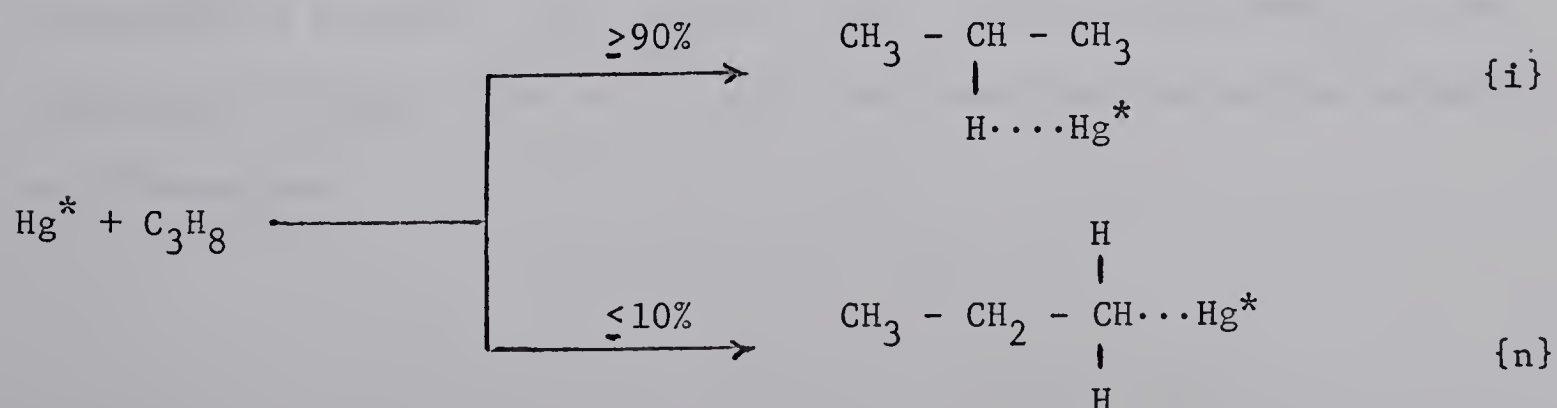
To elucidate the nature of the primary step in the mercury sensi-

tization of paraffins, Woodall and Gunning (3), studied the propane reaction using nitric oxide as a trap for the primary radicals. By gas chromatographic separation of acetoxime and propanal oxime, they obtained values believed to be representative of the primary radical distributions.

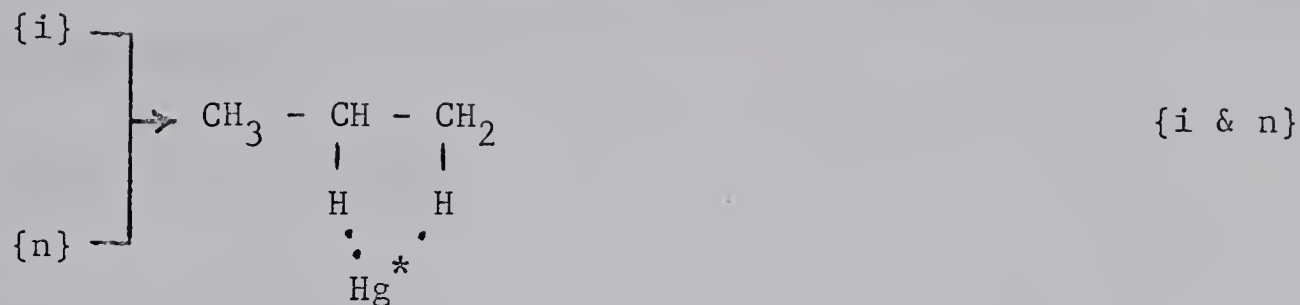
Concurrently, the propane reaction was also studied by Kebarle and Avrahami (4), at low pressures and high light intensities by a mass spectrometric technique. The propyl radicals were trapped by methyl radicals and from the measured yields of the n- and isobutaneproducts they also deduced values for the isomeric distribution of the primary radicals. These two vastly different techniques led to surprisingly concordant results, which are summarized in Table I.

These results were unexpected as quenching rate measurements by Darwent, recently confirmed by the deuterium-labelling technique (5), clearly established that at least 90% of the quenching efficiency was due to the methylene moiety of the molecule. Yet, according to the radical trapping experiments, the primary C-H bond cleavage was 42% of the total, or since the primary quantum efficiency is near unity, Φ (primary C-H) = 0.42.

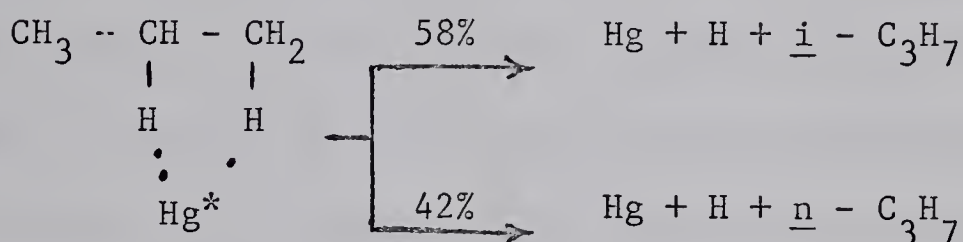
As a reconciliatory explanation for the quenching and radical trapping data, a cyclic transition complex was postulated between an excited mercury atom and the paraffin molecule (6).



The initial interaction is then immediately followed by the cyclization process,

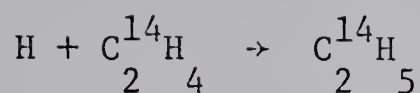


The rate of formation of this complex could be governed by the interaction with the methylene group but transfer of energy and consequent bond cleavage could occur with nearly equal probability at the methylene or methyl hydrogens.

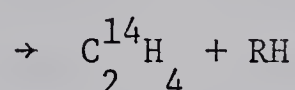
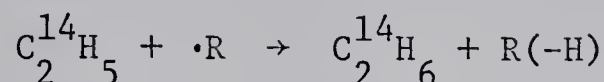
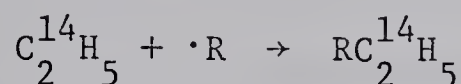


This structure appeared to be the only reasonable alternative, to the internal flow of energy through the carbon skeleton of the paraffin, which allowed for pumping energy into it at one point and breaking bonds at another, without cleavage of the weaker C-C bond.

Shortly after these studies appeared, Holroyd and Klein (7), reported their work with the "ethylene sampling" technique. This technique employs ethyl-C¹⁴ radicals as scavengers for radicals formed in the primary decomposition reaction. The labelled ethyl radicals are formed by the addition of H-atoms, from the mercury photosensitization of the paraffin, to C¹⁴-ethylene.



The labelled ethyl radicals then recombine or disproportionate with other radicals in the system.



Product yields were measured and an estimation of the relative importance of the various C-H bond cleavages was made. For propane, this estimation was based primarily upon the relative yields of isopentane- C^{14} and n-pentane- C^{14} . Table I contains the final value for the estimated secondary to primary C-H bond cleavage for propane. This value is in serious conflict with the previous studies and appears to be in close agreement with the relative quenching site in the molecule.

By mass spectrometry and methyl scavenging, Palmer and Lossing (8), studied the decomposition of isobutane. The result was in agreement with those from the ethylene sampling and nitric oxide trapping techniques.

Chesick (9), has repeated some of Holroyd and Klein's experiments and has obtained similar results (Table I).

To resolve this discrepancy, it was decided to carefully reexamine Kebarle's original experiments on the propane reaction.

Propyl radical yields from the mercury-photosensitized decomposition of
propane

Propane	Isopropyl/ <u>n</u> -Propyl		Reference
CH ₃ -CH ₂ -CH ₃	1.38 ^a	1.38 ^b	3
CH ₃ -CD ₂ -CH ₃	0.22 ^a	0.31 ^b	""""
CD ₃ -CH ₂ -CD ₃	2.12 ^a	2.92 ^b	""""
CD ₃ -CD ₃ -CD ₃	0.79 ^a	1.04 ^b	""""
CH ₃ -CH ₂ -CH ₃		1.2	4
CH ₃ -CD ₂ -CH ₃		0.2	""""
CD ₃ -CH ₂ -CD ₃		6.8	""""
CD ₃ -CD ₂ -CD ₃		0.9	""""
CH ₃ -CH ₂ -CH ₃		9.0	7
CH ₃ -CH ₂ -CH ₃		9.9	9
CH ₃ -CD ₂ -CH ₃		0.55	""""

(a) NO used as a radical trap.

(b) NO in combination with butene-1 used as a radical trap.

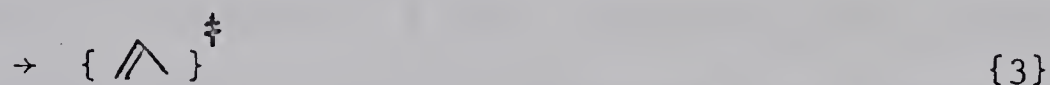
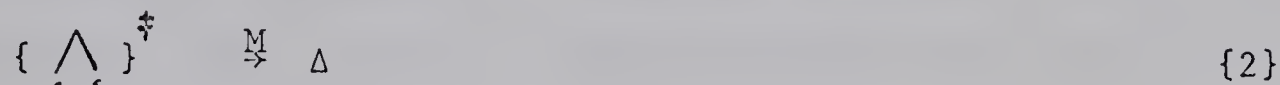
The mass spectrometric technique of mercury photosensitization employs reaction conditions which are much different from those ordinarily used in photosensitization studies. In this system the partial pressure of reactants are only a few mtorr and the partial pressure of mercury is much higher. A large excess of helium is present. The incident light intensity is much greater than is customary. The low substrate pressures insure less reaction of the primary radicals (formed by photosensitization) with the original reactants. The reactions are carried out in a fast-flow system, with contact times of the order of 1 - 2 milliseconds, removing the possibility of secondary decomposition of reaction products via mercury photosensitization. These factors make conditions more favorable for determining primary processes. The technique of saturating the system with methyl radicals, thus forcing the primary radicals formed to terminate their existence as methyl derivatives also facilitates the determination of primary processes.

2) The Hg $6(^3P_1)$ Sensitized Decomposition of Cyclopropane:

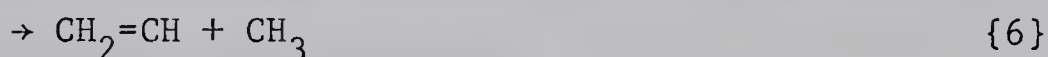
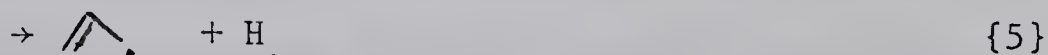
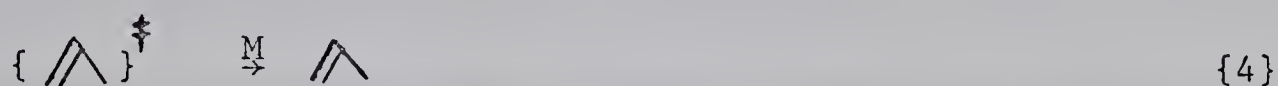
Several studies (10 - 15) of this system have been reported in the literature. The particularly interesting feature of the reaction is the primary quenching act. Unlike the higher cycloparaffins which in general comply with the behavior of alkanes, in that the primary quenching act results in C-H bond cleavage, two basic modes appear possible for cyclopropane. Excited mercury atoms can quench into the C-H bonds to give a cyclopropyl radical plus H-atom {1a} or interact with the carbon skeleton resulting in the formation of a vibrationally excited triplet trimethylene {1b}.



The intermediate trimethylene species formed in {1b} could then undergo the following reactions.



The propylene product formed via {3} may contain up to 121 kcal mole⁻¹ of excess energy and may undergo further reactions.



Attempts have been made to determine what radical intermediates are formed in the primary quenching process.

Ford, Kozak and Gunning (12) observed that in the presence of carbon tetrachloride, allyl chloride and n-propyl chloride are formed. Cyclopropyl chloride was not detected. These results indicated the presence of n-propyl and allyl radicals. The authors postulated that the initial quenching reaction proceeds via {1a} giving cyclopropyl radicals plus H-atoms, with the former isomerizing in subsequent recombination and abstraction processes.

Sester, Rabinovitch and Spittler (13) studied the mercury photosensitization of trans-cyclopropane-d₂. These authors concluded

that cyclopropane quenches predominantly by the formation of an excited molecule, most likely a vibrationally excited triplet biradical.

Holroyd and Klein have also investigated the reaction using the ethylene- C^{14} sampling technique (14). The major products observed were 1-pentene and n-butane, indicating the presence of allyl radicals and H-atoms. Small amounts of ethylcyclopropane were also observed (ethylcyclopropane- C^{14} /1-pentene- C^{14} = 0.08). The conclusion reached in this study was that either allyl or cyclopropyl plus H-atoms were produced in the primary decomposition. The authors proposed that if cyclopropyl radicals were the major radical intermediates formed, they must undergo rapid subsequent isomerization to allyl. It was suggested that under high light intensity conditions, radical concentrations may be sufficiently high enabling a greater proportion of the cyclopropyl radicals to be scavenged.

Strausz et al, studied the reaction in a static and rapid flow system (15). It was found that polymerization, which is the major process under static conditions, could be suppressed by rapid flow, in which case propylene appears as the major product. The addition of nitric oxide to the system led to the generation of propenaldoxime and acrylonitrile as principle products, indicating the presence of allyl radicals. The formation of an electronically excited cyclopropane, possibly the vibrationally excited ground state triplet of trimethylene, was proposed as the major primary step.

Because of its unique conditions of high light intensity and high radical concentrations, it was thought that the mass spectro-

metric technique employing methyl radicals as scavengers could provide additional data concerning the primary processes.

3) The Photochemistry of Silicon Compounds:

The photochemistry of silicon compounds has not received the widespread attention afforded the carbon compounds.

An early study by Emeleus and Stewart (16) concerning the mercury photosensitized decomposition of SiH_4 , revealed hydrogen and a brown polymeric silicon hydride as products.

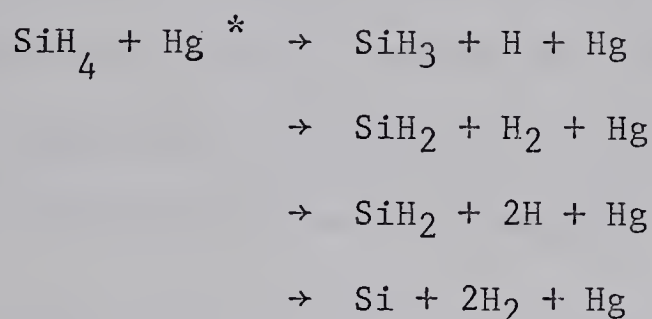
A more extensive study of the $\text{SiH}_4 + \text{Hg } 6(^3\text{P}_1)$ reaction was conducted by Niki and Mains (17). The important products were found to be hydrogen, disilane and trisilane, with quantum yields of 1.8, 0.6 and 0.06 respectively. Noticeable amounts of polymer were also observed.

A similar study by Nay et al. (18), using SiD_4 , confirmed a quantum yield greater than unity for deuterium. Φ_{D_2} was found to be ~10 in a newly cleaned reaction vessel and dropped to ~3 after prolonged irradiation, indicating a surface dependent reaction. Di-, tri-, and tetrasilane in addition to polymeric silicon hydride were also detected as products. The reactions of excited mercury with a series of methylsilanes were also studied in this investigation. The primary process was found to be exclusive Si-H bond scission. For molecules in which Si-H bonds were absent, C-H cleavage was observed.

White and Rochow (19) have used the technique of mercury photosensitization to synthesize various organosilicon compounds. Mixtures

of SiH_4 with various unsaturated compounds were sensitized and the organosilicon compounds were separated from the product mixture by fractional distillation.

The data available to the present time are not sufficient to conclusively establish the primary process (or processes) involved in the reaction of Hg^* with monosilane. To explain the large value of ϕ_{H_2} the following reactions have been proposed (17).



These steps, when followed by H-atom abstraction common to hydrocarbon systems, still could only provide a maximum of 2 for the quantum yield of hydrogen. Under these circumstances it seems that some sort of disproportionation or displacement reactions peculiar to silicon containing radicals must be responsible for the abnormally high yields of hydrogen.

Very little quantitative kinetic data exists concerning the photolysis of silicon containing compounds. Most of the studies reported deal with the preparation of organosilicon compounds.

A recent kinetic study of the 1470 Å photolysis of methylsilane has revealed the involvement of the methylsilene ($:\text{SiH}-\text{CH}_3$) diradical as the principal radical species (20). This radical has shown a preference for Si-H insertion relative to C-H.

The above is a brief summary of the photochemistry of silicon containing compounds. In order to supplement this limited information the photolysis and mercury photosensitization of phenylsilane- d_3 ($C_6H_5 \cdot SiD_3$) was studied. This compound was chosen for two reasons:

- a) The Hg $6(^3P_1)$ sensitized and direct photolysis studies should yield information concerning the photochemistry of the electronically excited triplet and singlet states of a silyl substituted benzene. These results can then be compared to the existing data regarding the photochemistry of benzene and alkyl substituted benzenes. From this comparison, correlations and discrepancies relating to alkyl vs. silyl substitution can be attempted.
- b) Very little is known about the general reactivity of silicon containing free radicals. Decomposition of phenylsilane- d_3 via Si-D or C-Si bond cleavage would produce $C_6H_5 \cdot SiD_2$ and SiD_3 radicals respectively. A study of the secondary radical-radical, radical-molecule reactions should yield additional data concerning the reactions of silyl radicals.

4) The Reactions of Methyl Radicals with Silanes:

Quantitative kinetic data for the gas phase reactions of alkyl radicals with silicon containing compounds are sparse.

Kerr, Slater and Young (21, 22) studied the reactions of methyl radicals with various chlorinated, fluorinated and methylated silanes. Their data led them to conclude that though silicon compounds are more reactive than paraffins, the increased reactivity is not indicative

of particularly weak Si-H or C-H bonds but arises from abnormally high A-factors.

Cheng and Szwarc (23) studied the reactions of trifluoromethyl radicals with tetramethylsilane and mono-, di- and trichloromethyl silanes at 180° C. They found CF_3 to be more reactive with the silicon compounds than with neopentane. These authors questioned the abnormally high A-factors reported by Kerr et al. (21, 22).

Bell and Johnson (24) also studied the reaction of trifluoromethyl radicals with trichlorosilane. They showed that CF_3 abstracts only H-atoms but not Cl-atoms and obtained Arrhenius parameters.

Mono- and disilane are the simplest silicon compounds containing abstractable hydrogens. The study of their reactions with methyl radicals is essential to the basic understanding of the reactivity of Si-H bonds with alkyl radicals. Polarization effects such as those possible with chlorinated, fluorinated and methylated silanes previously studied are absent.

Quantitative data concerning isotope effects for silicon containing compounds are almost nonexistent. A study of the mercury photosensitized decomposition of methylsilane using CH_3SiH_3 and CH_3SiD_3 indicated that the H/D isotope effect for this reaction is less important than that for hydrocarbons (18).

In the present investigation, the reactions of methyl radicals with light and perdeuterated mono- and disilane were examined in order to obtain the Arrhenius parameters for the reactions and the magnitude

of the primary H/D kinetic isotope effect.

To the present time, no calculations concerning the abstraction of H or D by alkyl radicals from silicon containing compounds have been reported. Johnston and co-workers have reported a "Bond-Energy-Bond-Order" (BEBO) method for obtaining the potential energies of activation and the properties of activated complexes for H-atom abstractions. Results obtained using this method have been found to be in reasonable agreement with values obtained from London-Eyring-Polanyi-Sato (LEPS) calculations (25).

In the present study, BEBO calculations based upon an ultrasimple three-mass-point model for the activated complex have been carried out. Values for the potential energy of activation and the primary kinetic isotope effect have been evaluated and are compared to the experimental measurements.

One of the major characteristic differences between the chemistry of carbon and silicon is the inability of the latter to form multiple bonds of the type so common to carbon chemistry (26). A limited type of $d_{\pi} - p_{\pi}$ bonding is, however, possible with silicon. This arises from the ability of silicon to withdraw electron density into its empty 3d-orbitals. This phenomenon has been observed in the case of phenylsilane (27).

In order to examine the effect of phenyl substitution on the hydrogen donating ability of the Si-H bond, the reactions of methyl radicals with $C_6H_5 \cdot SiD_3$ were studied.

CHAPTER II

EXPERIMENTAL

FAST FLOW SYSTEM

- 1) Mass Spectrometer.
- 2) Reactor.
- 3) The Mercury Lamp.
- 4) Sampling Leak.
- 5) Operating Procedure.

STATIC SYSTEM

- 1) Vacuum System.
- 2) Analytical System.
- 3) Photolytic System.

AUXILIARY EQUIPMENT

Two major pieces of apparatus were used to obtain the experimental data for this thesis.

FAST FLOW SYSTEM

A flow system attached to the sampling inlet of a mass spectrometer was used. A schematic illustration of the experimental arrangement is given in Figure 1. The design of the reactor system was originally developed by Lossing et al. (28), with subsequent modifications by Kebarle (29).

1) Mass spectrometer:

The mass spectrometer used was an Associated Electronics MS 10 instrument. This instrument analyzes the ions electromagnetically, the magnet being a 1800 gauss permanent magnet. The detector consists of a direct current amplifier (with Faraday cup).

2) Reactor:

The reaction system consisted of a mercury saturator kept at 65°C, a stripper kept at 55°C to ensure saturation of the reaction mixture with mercury vapor, and a reaction zone consisting of a length of 9 mm i.d. quartz or vycor tubing surrounded by an annular low pressure mercury resonance lamp. The body of the lamp and reaction zone were kept at a constant temperature of 55 - 60°C by means of a cylindrical pyrex water jacket which surrounded the lamp. An all glass water circulating system supplied water at a constant temperature to the water jacket. The jacket had a hole in the bottom which was slightly larger than the outside diameter of the reactor tubing. A rubber O-ring was

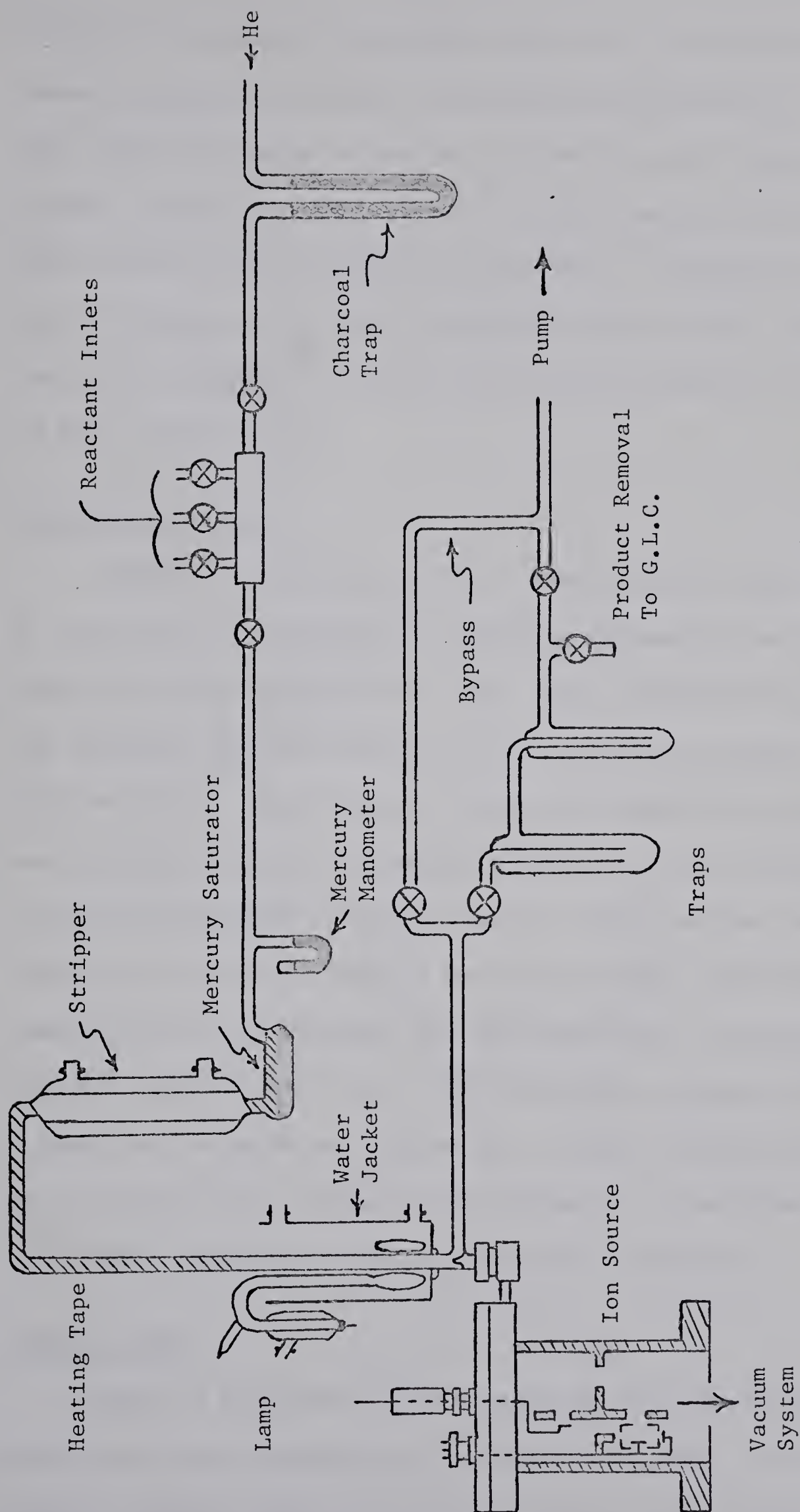


Figure 1. Flow System.

fitted to the bottom of the water jacket (G. E. RTV-102 white silicone rubber adhesive) to provide a watertight seal around the reactor tube. This allowed movement of the lamp and water jacket along the reactor tubing. Tubing from the saturator to the reaction zone was kept at 55°C with the use of flexible heating tape. Immediately following the reaction zone, a quartz cone containing a small orifice opening to the ionization chamber of the mass spectrometer served as a sampling probe of the reaction stream.

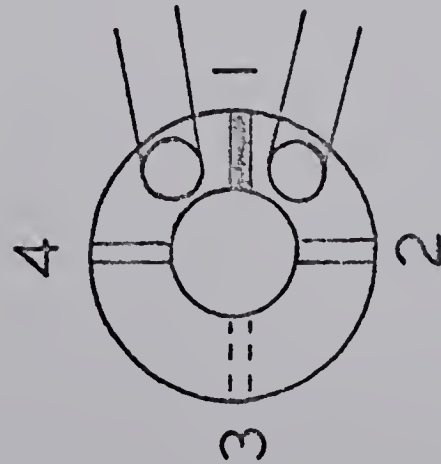
3) The Mercury lamp:

Figure 2 is an illustration of the designs of lamps used. Type A, was found to be superior in providing the maximum unreversed 2537 Å radiation to the reaction zone. The lamps used were constructed by the chemistry glassblowing shop. The following procedure was used to fill the lamps. Each lamp was thoroughly outgassed by heating, mercury was distilled into the condensers to serve as electrodes and the lamp was then filled with 1.5 torr of neon. After starting the lamp and letting it run hot for about 1 hour the neon was pumped out and a fresh charge was put in. The lamp was then sealed off and ready for use. The lamp was operated from a 220 V d.c. source through a series resistor. A Tesla Coil or an Osram starter (No. Z 5103) was used to fire the lamp. At a current of 6 - 7 amperes the voltage drop across the lamp was 100 V. Figure 3 shows the emission spectrum of the lamp.

4) Sampling leak:

Figure 4 illustrates how the sampling leak was constructed. The quartz cone was obtained from the glassblowing shop. An electrolyte solution (dil HCl, NaCl, etc.) was prepared. Some of the electrolyte

Top View



Interior Partitions

- 1. Full Length of Cell.
- 2. & 4. Space at Bottom.
- 3. Space at Top.

Side View

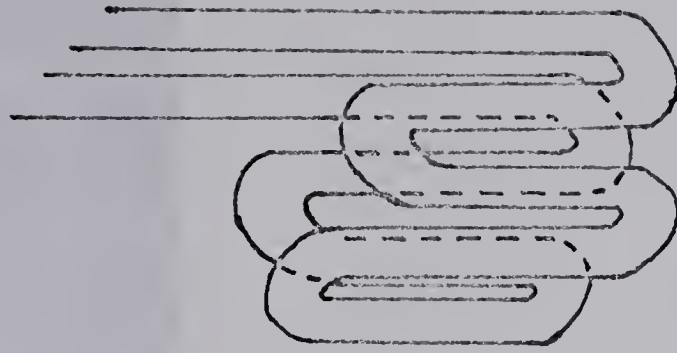
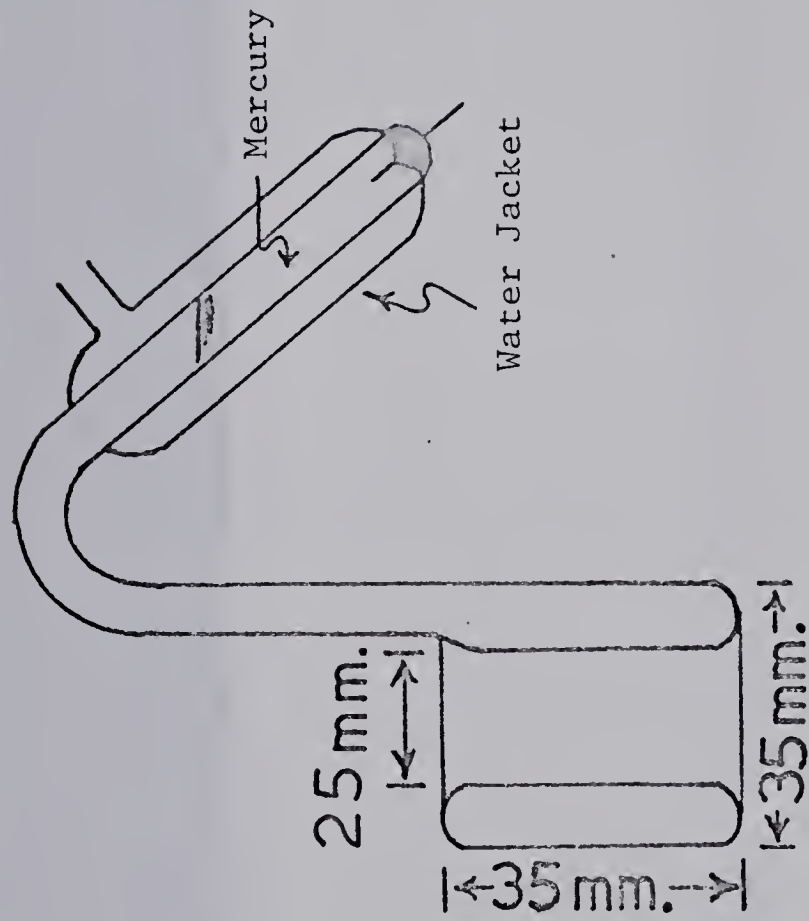


Figure 2. Lamp Designs.



Figure 3. Emission spectrum of low pressure Hg-arc.

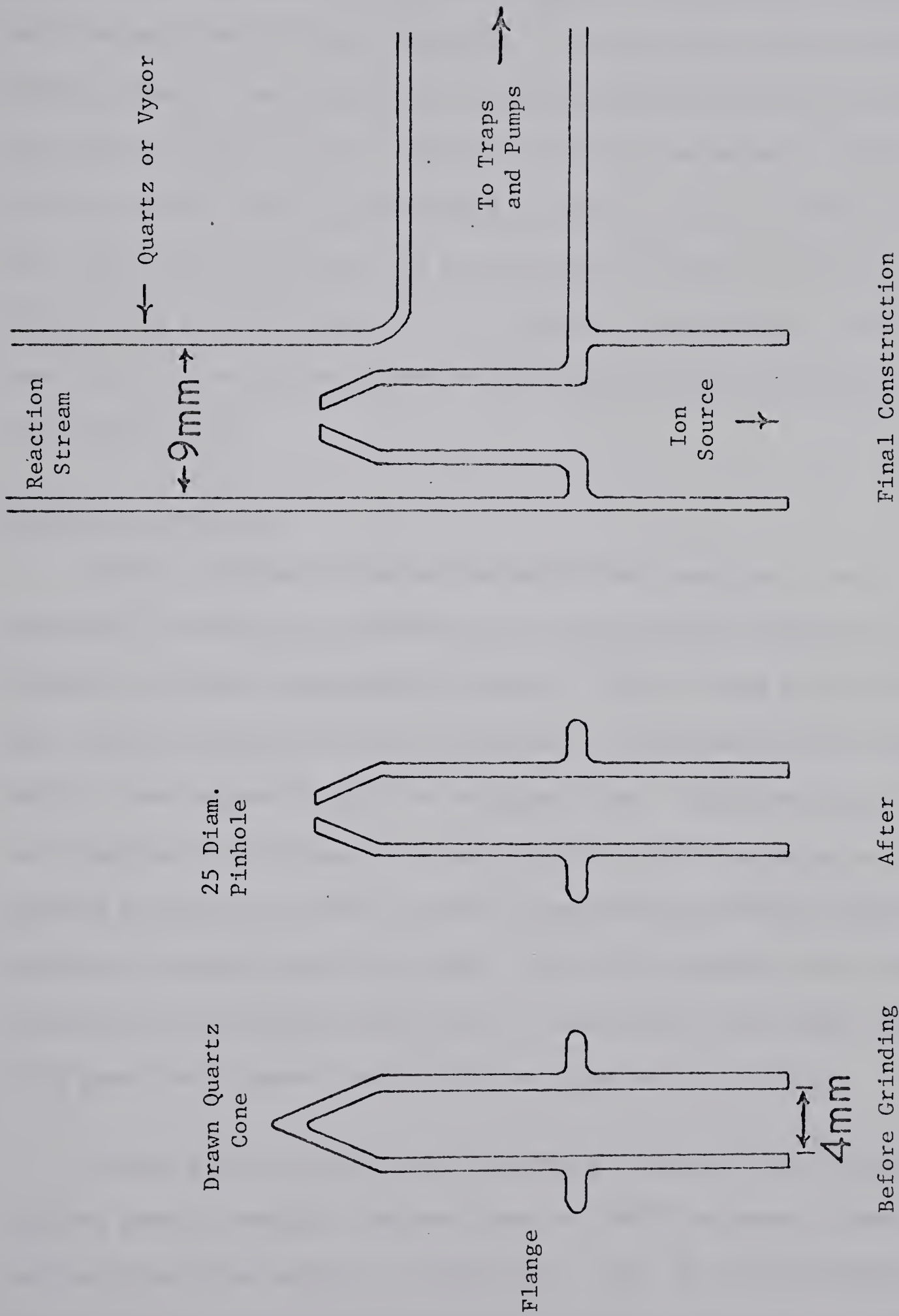


Figure 4. Construction of Sampling Leak and Reaction Zone.

was poured into the stem of the cone and another portion was mixed with the grinding compound. Leads from the dish containing the grinding compound and the stem of the quartz cone were connected to a voltmeter and the meter set to read resistance. The tip of the cone was then slowly ground. The appearance of the minutest hole in the tip caused the meter to fall from its reading of infinite resistance. The size of the aperture could be determined by comparison of the diameter of the hole against fine wires of known diameter under a microscope. In this manner a sampling leak of 25 μ diameter was prepared. The cone was then returned to the glassblowing shop for final construction of the reaction zone.

5) Operating procedure:

Before carrying out actual decomposition reactions it was necessary to measure the sensitivity of the mass spectrometer to each reactant in various pressures of helium. This was done by measuring out various pressures of the reactant into a calibrated dose volume of 8 cc and expanding into the storage volume. Helium was then added to bring the total pressure to the desired value. The gases were allowed to mix for at least 6 hours or preferably overnight before calibration measurements were made. The total storage volume during sensitivity measurements was 2700 cc. Measurements were made using a 50 μ -amp trap current and an electron beam energy of 70 ev.

During actual operation the following procedure was followed. Helium, passed through a charcoal trap at -196°C to remove traces of oxygen present, was used as a carrier gas. Most of the experiments were carried out at pressures of 10 torr carrier gas to which a few

mtorr of substrate gasses were added. The mixture was saturated with mercury vapor and passed through the reactor. A calibrated oil flow-meter was used to measure the gas flow and at a pressure of 10 torr helium, the flow through the reactor was 30 - 35 meters per second and the exposure time of the reactants to the radiation was 1.5 - 2.0 milliseconds.

Reactants were introduced into the helium flow stream by bleeding them through the reactant inlets. Reactants were kept in cylindrical pyrex tubes fitted with hi-vac stopcocks and 12/30 ground-glass-joints by which they could be attached to the reactant inlets. Bleeding of the reactants into the flow stream required that the reactants have a vapor pressure greater than that of the carrier. Liquids such as dimethyl mercury, phenylsilane, etc. which have a vapor pressure less than one atmosphere at room temperature were normally used with a constant room temperature water bath surrounding the lower part of the storage tube in which they were kept. Gases such as monosilane, propane, etc. were used with appropriate low-temperature slush baths to reduce their pressures below one atmosphere during operation. In high-pressure experiments where the pressure of the carrier gas was increased beyond the vapor pressure of the reactants, it was necessary to ballast the reactant volumes with helium in order to inject them into the flow stream.

The sampling leak located directly below the reaction zone allowed rapid sampling of the reaction mixture immediately after exposure to the radiation. The major portion of the mixture however, was pumped out directly or passed through 2 traps where the condensables

at -196°C could be collected for further analysis by gas-liquid chromatography (G.L.C.), etc.

STATIC SYSTEM

1) Vacuum system:

A conventional high-vacuum system (Fig. 5) evacuated to 10^{-6} torr by means of a two-stage mercury diffusion pump was used. The entire system was kept grease-free by using Delmar mercury float valves and helium-tested Hoke valves. A mercury manometer, McLeod gauge and Pirani gauge tubes (Consolidated Vacuum Corporation No. GP-001) were used to measure pressures. The main function of this part of the system was for the purification and storage of materials. The low temperature distillation train was also used to separate reaction products.

2) Analytical system:

Figure 6 is a diagram of the system used for the measurement, separation and collection of reaction products. A Toepler pump fitted with a calibrated gas burette was used for the measurement of products and calibration of the gas chromatograph. The gas chromatograph consisted of a thermal conductivity cell (Gow-Mac Model TR 111 B), a power supply (Gow-Mac Model 9999-C) and a Sargent recorder. The thermal conductivity cell was heated to 250°F and the detector current was kept constant at 250 milliampere. Helium, which was passed through a column containing silica gel, Linde type 4A molecular sieves and drierite to remove traces of water, was used as the carrier gas. Flow rates were measured using an oil manometer calibrated with a soap bubble flow meter. The injection unit consisted of two 3-way switch

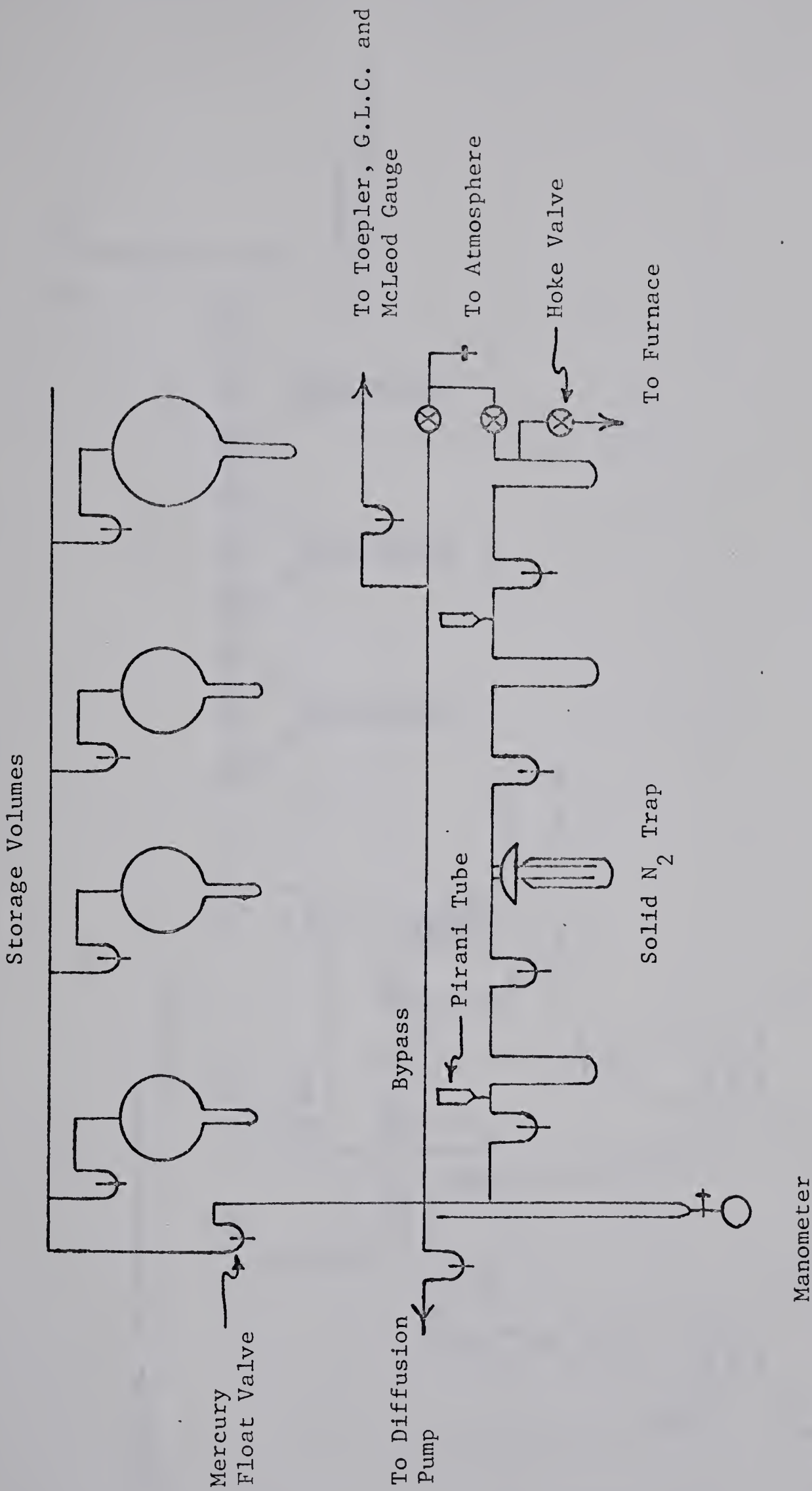


Figure 5. High Vacuum System.

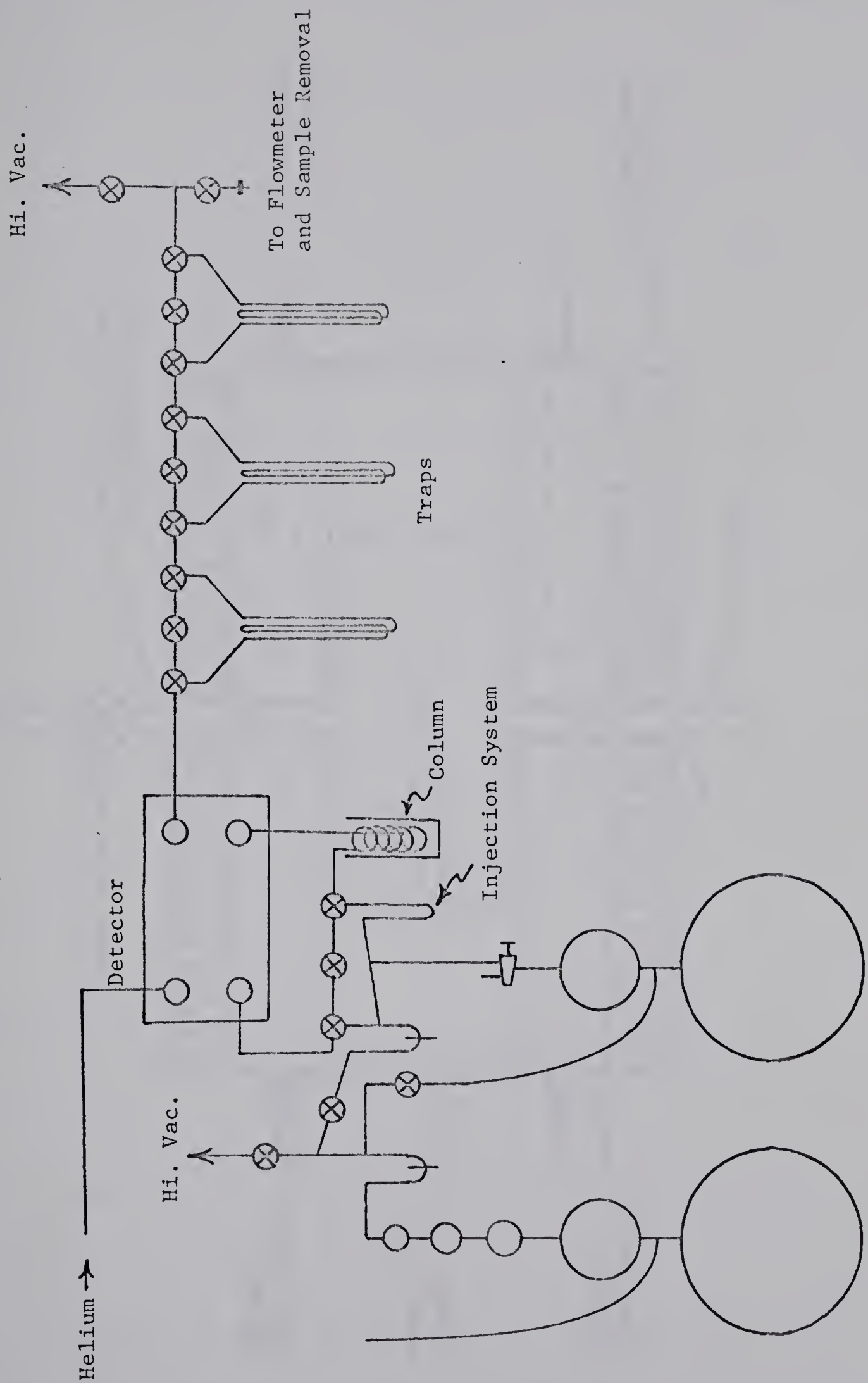


Figure 6. Analytical System.

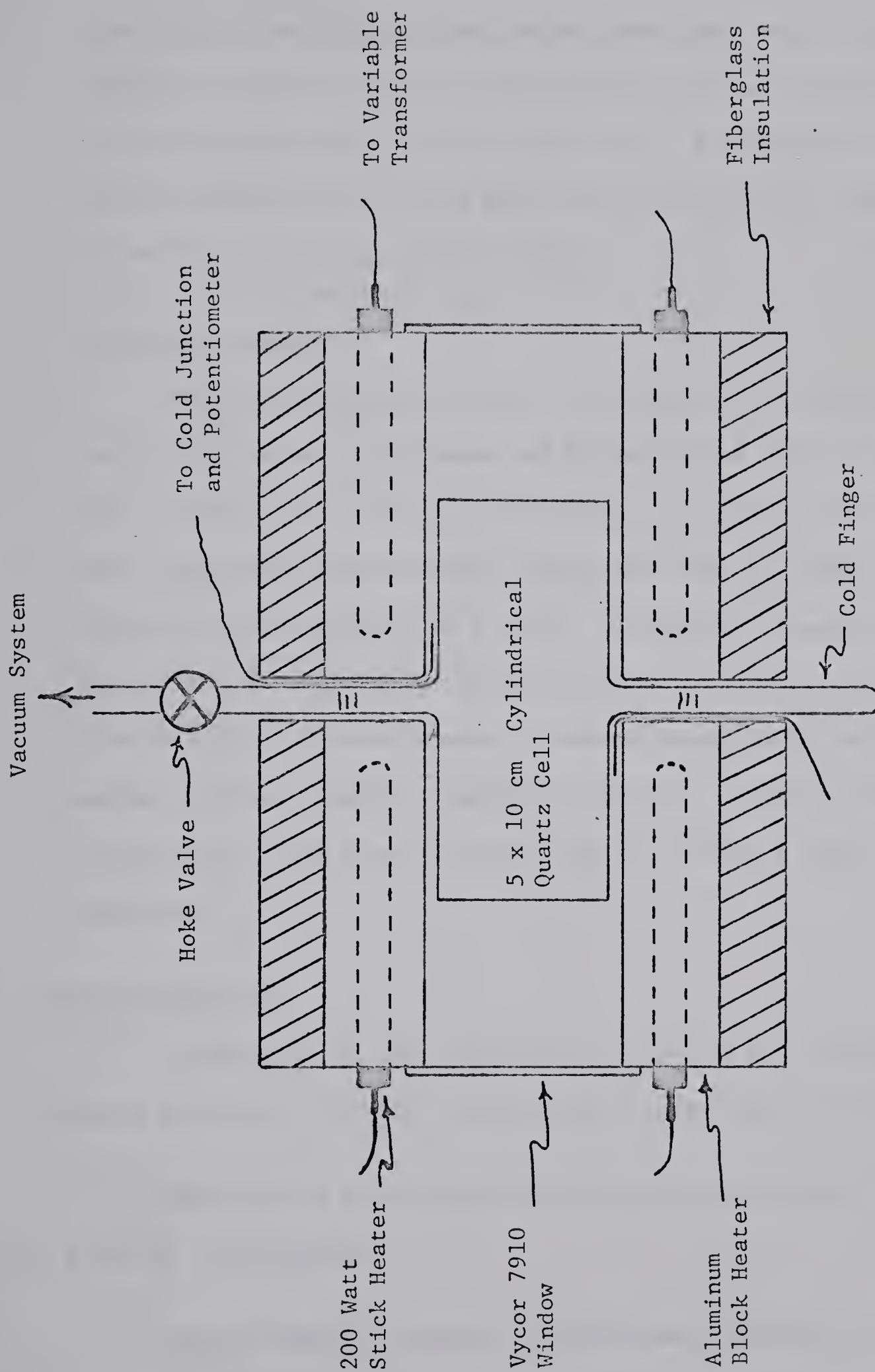


Figure 7. Static Photolysis System.

type Hoke valves and one 2-way switch type Hoke valve. Glass coil columns of 6 mm o.d. pyrex filled with the desired stationary phase on solid support were used for separation. A grease-free trapping system employing switch type Hoke valves was used for sample collection. All samples were collected at -196°C .

3) Photolytic system:

The photolysis system (Fig. 7) consisted of a cylindrical quartz cell with attached cold finger and helium-tested Hoke valve (total vol. 217 cc). The cell was surrounded by an aluminum block furnace. The illuminated volume of this reactor was 196 cc. Power for heating the furnace was supplied by a variac. Temperature measurements were made with iron-constantine thermocouples. Potentials were read on a Wheelco Model 310 potentiometer. Hanovia Model 30620 medium-pressure mercury arcs were used as radiation sources. Suitable filters could be attached to the face of these lamps to eliminate light of undesirable wavelength.

AUXILIARY EQUIPMENT

In addition to the apparatus described in the foregoing, the following equipment available in the chemistry building was also used.

Mass spectra were obtained on Associated Electrical Industries MS 2 and MS 9 instruments.

Nuclear magnetic resonance spectra were obtained on a Varian 100 Mc spectrometer.

Optical density measurements for the u. v. filter solutions were made on a Cary Model 14 M recording spectrophotometer using quartz cells with a 5 mm path length.

Light intensity measurements were obtained with a Photovolt Model 501 M photometer.

Filter solutions used (aqueous).

- (a) Concentrated $\text{NiSO}_4\text{-CoSO}_4$ solution.
- (b) "u. v. dye" 2,7-dimethyl-3,6-diazacyclohepta-1,6-diene perchlorate 200 mg/liter. For preparation and characteristics of these solutions consult reference (30).

TABLE II

G.L.C. Operating Conditions and Relative Retention Data.

Column	Length ft.	Temperature °C	Flow cc min ⁻¹	Compounds Analyzed and Relative Retention Times
Alumina 60/80	10	90	80	ethane 0.35
mesh deactivated				ethylene 0.51
with 2.5%				propane 2.25 min. 1.00
Silicone 550.				propylene 1.84
				isobutane 2.10
				n-butane 3.18
Silicone Gum	20	125	80	benzene 0.52
Rubber Se-30				dimethyl mercury 0.64
on Diataport-S				toluene 0.93
60/80 mesh.				phenylsilane 11 min. 1.00
				methylphenylsilane 1.51
				phenyldisilane 1.51
				dimethylphenylsilane 2.04
				methylphenyldisilane 3.15

TABLE II
(Continued)

Column	Length ft.	Temperature °C	Flow min^{-1} cc min^{-1}	Compounds Analyzed and Relative Retention Times
Silica gel, medium activity 30/60 mesh.	15	65	75	ethane <u>2.25 min.</u> <u>1.00</u> methylsilane 2.00 trimethylsilane 5.33
Silica gel, medium activity 30/60 mesh.	15	0	60	monosilane <u>7.0 min.</u> <u>1.00</u> ethane 1.79
Molecular Sieves (13X), 30/60 mesh.	10	0	60	nitrogen <u>7.5 min.</u> <u>1.00</u> methane 1.95

TABLE II

(Continued)

Column	Length ft.	Temperature °C	Flow -1 cc min	Compounds Analyzed and Relative Retention Times
8% diethyl adipate				ethane <u>8.0 min.</u> <u>1.00</u>
on Diataport -S 20				propane 1.22
60/80 mesh				ethylene 1.43
+		0	90	propylene 1.51
30% glutaronitrile -				
propylene 20				
carbonate				Cyclopropane 2.25
(30:70) on				<u>l</u> -butene 2.61
Diataport-S				isobutene 2.78
60/80 mesh.				allene 3.01
				<u>trans</u> -butene 3.16
				methylcyclopropane 3.28
				<u>cis</u> -butene 3.69

TABLE III

Materials Used.

Material	Source	Grade and Purity	Purification
nitrogen	Airco	Assayed reagent grade	None
carbon monoxide	"	"	"
carbon dioxide	"	"	"
hydrogen	"	"	"
neon	"	"	"
oxygen	"	"	"
allene	Chemical Procurement Laboratories	Research	"
isobutane	Phillips	Research 99.96 mole %	"
n-butane	"	Research 99.98	"
l-butene	"	Research 99.82	"
cis-butene	"	Research 99.82	"
trans-butene	"	Research 99.26	"
isobutene	"	Research 99.56	"

TABLE III

(Continued)

Material	Source	Grade and Purity	Purification
cyclopropane	Ohio Chemical of Canada	Anesthetic	Bubbled through alkaline KMnO_4 , dried, distilled at -112°C and collected at -196°C.
ethane	Phillips	Research 99.92 mole %	None
ethylene	"	Research 99.99	"
propane	"	Research 99.99 ⁺	"
propylene	"	Research 99.70	"
methane	"	Research 99.58	"
methane-d ₁	Merck	Research 98% deuteration	"
propane-d ₈	"	Research 98%	"
propane-2,2-d ₂	"	Research 98%	"
propane-1,1,1, 3,3,3-d ₆	"	Research 98%	"
monosilane	"	Research	Distilled at -159°C, collected at -196°C.
monosilane-d ₄	"	Research >96% deuteration	"

TABLE III
(Continued)

Material	Source	Grade and Purity	Purification
disilane	Merck	Research	Distilled at -126°C, collected at -159°C.
disilane-d ₆	"	" >96% deuteration	"
phenylsilane-d ₃	"	" >99% Si-D	Preparative gas chromatography.
dimethyl-d ₆ -mercury	"	" 98% deuteration	Degassed and collected at -98°C.
methylsilane	"	Research	None
axomethane	"	"	Distilled at -98°C, collected at -130°C.
methylcyclopropane	American Petroleum Institute	99.95 mole %	None
1-chloropropane	Eastman Organic	Technical	Preparative gas chromatography.
2-chloropropane	"	"	"
3-pentanone	"	"	"

TABLE III

(Continued)

Material	Source	Grade and Purity	Purification
dimethyl mercury	Eastman Organic	Highest purity	Degassed and collected at -98°C .
cyclopropyl bromide	Aldrich	Technical	Preparative gas chromatography.
benzene	Fisher	"	"
toluene	"	"	"
acetone	Shawinigan	"	"
helium	Canadian Helium Co.	"	Passed through drying tube.

CHAPTER III

THE Hg 6(3P_1) PHOTSENSITIZATION OF PROPANE

RESULTS

- 1) Decomposition of Chloropropanes.
- 2) Decomposition of Propane.
- 3) Deuterated Propanes.
- 4) The Role of H-atoms.

DISCUSSION

- 1) Trapping of the Propyl Radicals.
- 2) Photosensitization of Propane.
- 3) Light Intensity.
- 4) Secondary Decomposition of Primary Radicals.
- 5) The Role of H-atoms.
- 6) Primary Radical Distribution.

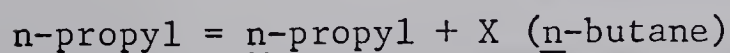
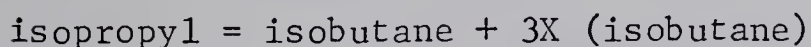
1) Decomposition of chloropropanes:

The determination of the primary processes involved in the Hg-photosensitized decomposition of propane and deuterated propanes rests solely upon the technique of scavenging the n- and isopropyl radicals via combination with methyl radicals as n- and isobutane respectively. The reliability of this technique was examined in a series of experiments carried out with 1- and 2- chloropropanes. The mercury sensitization of these compounds should be clean sources of the corresponding radicals, n-propyl and isopropyl. The mercury sensitized decomposition of dimethyl mercury served as a source of methyl radicals (29).

Typical reaction conditions were 0.35 mtorr of chloropropane and 15 mtorr of $\text{Hg}(\text{CH}_3)_2$ in 10 torr of He carrier. The products detected were ethane, from the recombination of methyl radicals; propylene from the disproportionation of propyl with methyl; n-butane from 1-chloropropane and isobutane from 2- chloropropane through the combinations of propyls with methyl; and small amounts of propane. The absence of higher than C_4 products indicated efficient scavenging of propyl radicals by methyl. In chloropropane, $\text{Hg}(\text{CD}_3)_2$ mixtures the propane was found to be over 90% perdeuterated indicating that it arose primarily from the decomposition of dimethyl mercury. The propylene however, was almost completely undeuterated indicating it to be a

product of the chloropropane decomposition. The butanes were found to have the composition $C_3H_7CD_3$. No isomerization of the propyl radicals ($\underline{i}\text{-}C_3H_7 \leftrightarrow \underline{n}\text{-}C_3H_7$) was detected. The initial experiments at high light intensities indicated abnormally high propylene to butane product ratios. Later experiments showed this ratio to be dependant upon light intensity. Table IV and Figure 8 illustrate this dependance.

Mixtures of 1- and 2-chloropropane (1:1) in the presence of excess dimethyl mercury were also sensitized. Reaction conditions and results of these experiments are given in Table V. The quenching cross sections of the two chloropropanes for Hg $6(^3P_1)$ atoms are essentially the same (Appendix A), and under identical conditions the extent of their decomposition when mercury sensitized separately is also equal. Therefore, the mercury sensitization of their 1:1 mixture should produce equal amounts of \underline{n} -propyl and isopropyl radicals. The primary yield was estimated from the butanes and propylene formed. The last column of Table V gives the corrected isopropyl/ \underline{n} -propyl ratios. The mean value of the four experiments is 1.05. The ratios were calculated using the following scheme to account for the excess propylene. Since the propylene yield from the 2-chloropropane is three times as great as from the 1-chloropropane (as indicated by their separate decompositions with excess dimethyl mercury),



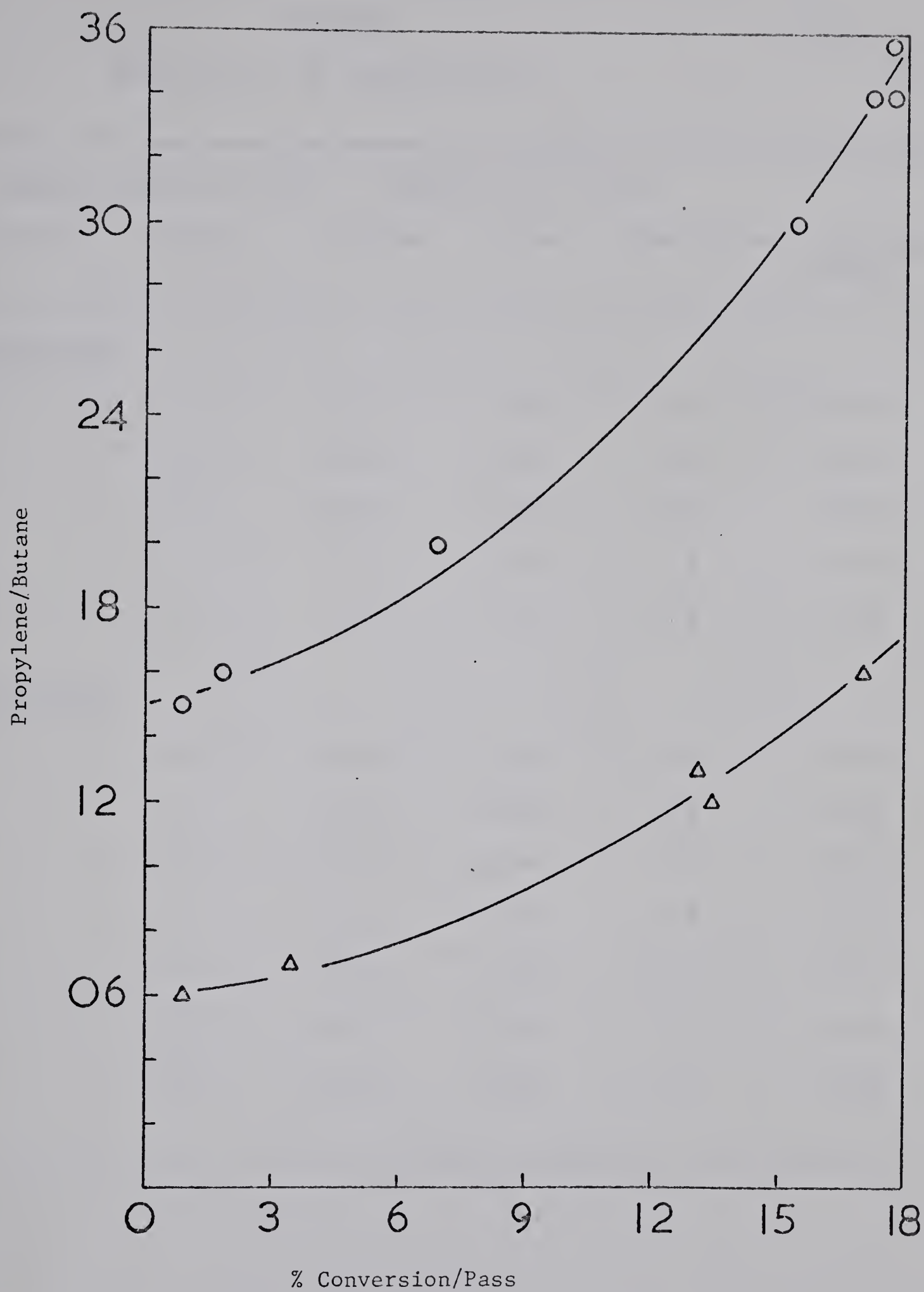


Figure 8. Propylene/Butane as a function of % Conversion/Pass:

(Δ) 1-chloropropane; (O) 2-chloropropane.

Decomposition of chloropropanes.

Reactant pressure (mtorr)		Products (10^{-6} mole)			
chloropropane	Hg(CH ₃) ₂	propylene	butane	%conversion	<u>propylene</u> <u>butane</u>
<u>1-chloropropane</u>					
0.35	12	0.01	0.16	0.9	0.06
0.33	12	0.03	0.41	3.5	0.07
0.35	12	0.12	0.87	13.0	0.13
0.30	13	0.33	2.80	13.4	0.12
0.35	12	0.37	2.26	17.1	0.16
<u>2-chloropropane</u>					
0.30	12	0.02	0.13	0.9	0.15
0.35	11	0.05	0.31	1.8	0.16
0.35	13	0.13	0.64	6.9	0.20
0.35	11	0.37	1.14	15.8	0.33
0.35	12	0.49	1.42	17.3	0.35
0.30	13	0.43	1.22	17.7	0.35
0.30	12	0.36	1.02	17.7	0.36

Product yields from the decomposition of a 1:1 mixture of 1- and 2-chloropropane with excess $\text{Hg}(\text{CH}_3)_2$.

$\frac{\% \text{ decomposition}}{\text{unit time}}$	isobutane	<u>n</u> -butane	propylene	$\frac{\text{isopropyl}}{\text{n-propyl}}$
6.7	0.60	0.62	0.26	1.15
16.0	2.31	2.75	1.59	1.08
9.5	0.55	0.71	0.32	0.96
17.0	0.57	0.83	0.74	1.00

Products are in μmoles with collection times ranging between 17 min. and 25 min. and reactant pressures varying between 0.4 millitorr and 1.3 millitorr of each chloropropane.

* Corrected for propylene formation.

where

$$X = \frac{\text{propylene}}{3 (\text{isobutane}) + \text{n-butane}}$$

2) Decomposition of propane:

Propane was decomposed in the presence of excess mercury dimethyl. The conditions and results of these reactions are given in Table VI and Figure 9. The products of this reaction were ethane, propylene, isobutane and n-butane. A search for higher than C₄ products showed they were absent.

The initial series of experiments at high light intensities gave results in good agreement with those of Kebarle and Avrahami (4), indicating a ca. 1:1 cleavage of the primary and secondary C-H bonds. However, even with the large values for the propylene to butane ratios obtained from the chloropropane experiments, it was not possible to account for all the propylene produced. This suggested that reactions other than disproportionation of methyl with propyl radicals were occurring.

A phenomenon common to reaction systems of this type is the build-up of solid material on the inner walls of the reactor. When the polymer results from hydrocarbon systems, it can be removed by flushing the reaction system with a few torr of oxygen while heating the reactor with a torch. This polymer buildup, along with a decreased transparency of the lamp after repeated use, causes an attenuation of the light intensity reaching the reaction zone. It was noticed that this had

TABLE VI

Decomposition of propane and dimethyl mercury mixtures.

C ₃ H ₈	Reactant pressure (mtorr)	Product ratios		% Conversion pass	Comments
		propylene butanes	isobutane n-butane		
		(10 torr helium carrier pressure)			
4.0	15	0.51	0.28	4.4	New Vycor reaction zone
1.5	15	0.62	0.44	2.5	New Vycor reaction zone lamp, Filter (a).
2.0	20	0.53	0.44	2.4	Filter (b).
2.0	12	0.52	0.31	2.3	Reaction zone cleaned.
6.5	20	0.38	0.66	2.2	
2.0	10	0.44	0.42	2.0	
5.6	20	0.50	0.37	1.8	
1.5	20	0.52	0.68	1.8	Filter (a).
1.0	10	0.38	0.72	1.5	
2.5	11	0.34	0.69	1.3	
2.0	11	0.33	0.71	1.2	
2.0	10	0.29	0.72	1.2	

TABLE VI

(Continued)

Reactant pressures (mtorr)		Product ratios		% Conversion	Comments
C_3H_8	$Hg(CH_3)_2$	$\frac{\text{propylene}}{\text{butanes}}$	$\frac{\text{isobutane}}{\text{n-butane}}$	pass	
3.0	20	0.51	1.38	0.8	Mixture of (a and b) filter solution.
3.0	25	0.42	1.29	0.8	Filter (a).
3.4	25	0.29	1.57	0.7	
2.3	25	0.35	1.00	0.6	
2.5	25	0.33	1.03	0.6	
2.1	25	0.35	1.22	0.5	
2.5	25	0.32	1.25	0.5	
2.3	20	0.24	2.33	0.4	Filter (a).
2.0	25	0.28	1.32	0.4	
1.2	20	0.15	3.99	0.4	Filter (a).
6.2	20	0.23	3.10	0.3	
4.3	25	0.22	3.06	0.3	100 mesh screen.

TABLE VI

(Continued)

Reactant pressures (mtorr)		Product ratios		% Conversion pass	Comments
C_3H_8	$Hg(CH_3)_2$	$\frac{\text{propylene}}{\text{butanes}}$	$\frac{\text{isobutane}}{\text{n-butane}}$		
2.5	25	0.28	1.61	0.3	
1.7	11	0.30	3.56	0.3	2 Hanovia Hg-arcs used.
4.4	20	0.24	3.85	0.3	100 mesh screen.
3.0	20	0.19	2.00	0.2	100 mesh screen.
1.8	11	0.24	5.33	0.2	Hanovia Hg-arc used.
1.7	12	0.23	7.56	0.2	Hanovia Hg-arc used.
3.0	20	0.23	5.14	0.1	100 mesh screen + filter (a).
3.4	20	0.16	4.55	0.1	100 mesh screen + filter (a).
		(100 torr helium carrier pressure)			
1.0	20	0.30	0.38	2.4	
2.0	15	0.32	0.59	1.3	
2.0	20	0.26	1.48	0.9	
2.0	15	0.35	1.26	0.8	Hg(CD ₃) ₂ used.

TABLE VI

(Continued)

Reactant pressures (mtorr)		Product ratios		Comments
C_3H_8	$Hg(CH_3)_2$	$\frac{\text{propylene}}{\text{butanes}}$	$\frac{\text{isobutane}}{\text{n-butane}}$	
2.0	15	0.46	1.27	$Hg(CD_3)_2$ used.
		(100 torr helium carrier pressure)		
			0.7	
		(10 torr helium + 3 torr propane + 6 torr $Hg(CH_3)_2$)		
3 torr	6 torr	0.12	8.33	0.10
3 torr	6 torr	0.11	8.48	0.06

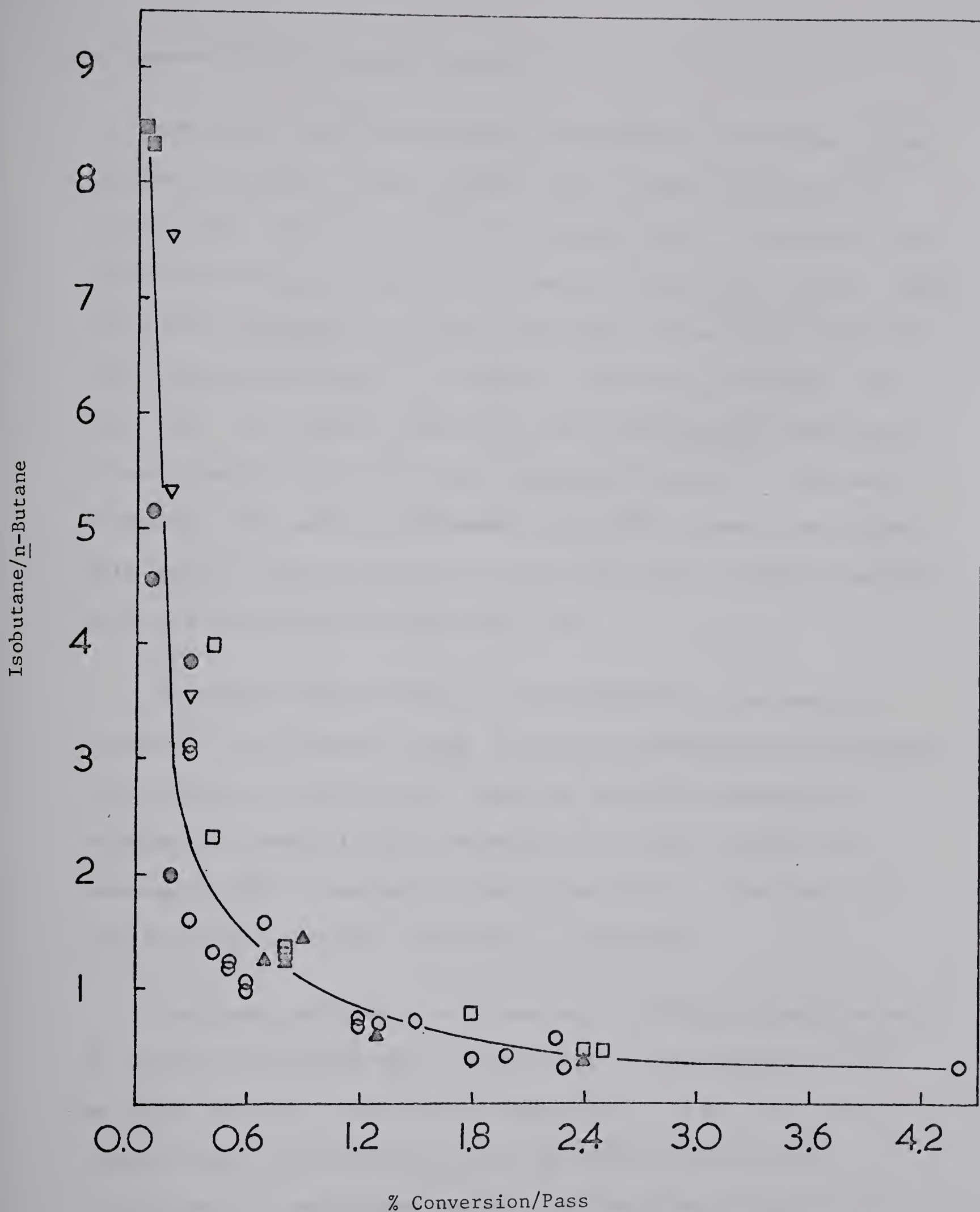


Figure 9. Isobutane/n-Butane as a function of % Conversion/Pass:

(○) normal run; (□) filter solution; (●) wire mesh screen;

(▲) 100 torr helium; (▽) Hanovia resonance lamp; (■) high pressure.

an apparent effect on product ratios.

Previously, in an investigation of the mercury sensitized decomposition of biacetyl, using a similar type of reactor, Harrison and Lossing (31), seriously considered the possibility of involvement of a higher excited state of mercury such as Hg $7(^3S_1)$ in the reaction. This state may be populated by stepwise excitation, either by absorption of 4358 Å radiation by Hg $6(^3P_1)$ or 4047 Å radiation by Hg $6(^3P_0)$ atoms (Fig. 10). The original system used in our investigation consisted of a quartz reaction zone and a lamp constructed of quartz. This led us to consider the possible involvement of Hg $6(^1P_1)$ atoms in our system. This species could be generated by direct absorption of 1850 Å radiation by ground state Hg $6(^1S_1)$ atoms (Fig. 10).

To examine the possibility of participation by more energetic species of excited mercury atoms, a series of experiments was performed using various optical filters. Radiation of 1850 Å wavelength was eliminated by installing a vycor reaction zone which limited transmission to light of wavelength greater than 2200 Å. This step proved that Hg $6(^1P_1)$ atoms were unimportant in the system.

The longer wavelength radiations were eliminated through the use of various filter solutions. A lamp having an inner diameter of 25 mm (Fig. 3A), and a reaction zone consisting of 11 mm o.d. vycor tubing allowed for circulation of a 7 mm thick filter solution. Circulation of a concentrated solution of $\text{NiSO}_4\text{-CoSO}_4$, which in a 5 mm path had a transmission at 4358 Å of 3% and less than 1% at 4047 Å, increased the ratio of isobutane to n-butane from the initial value of

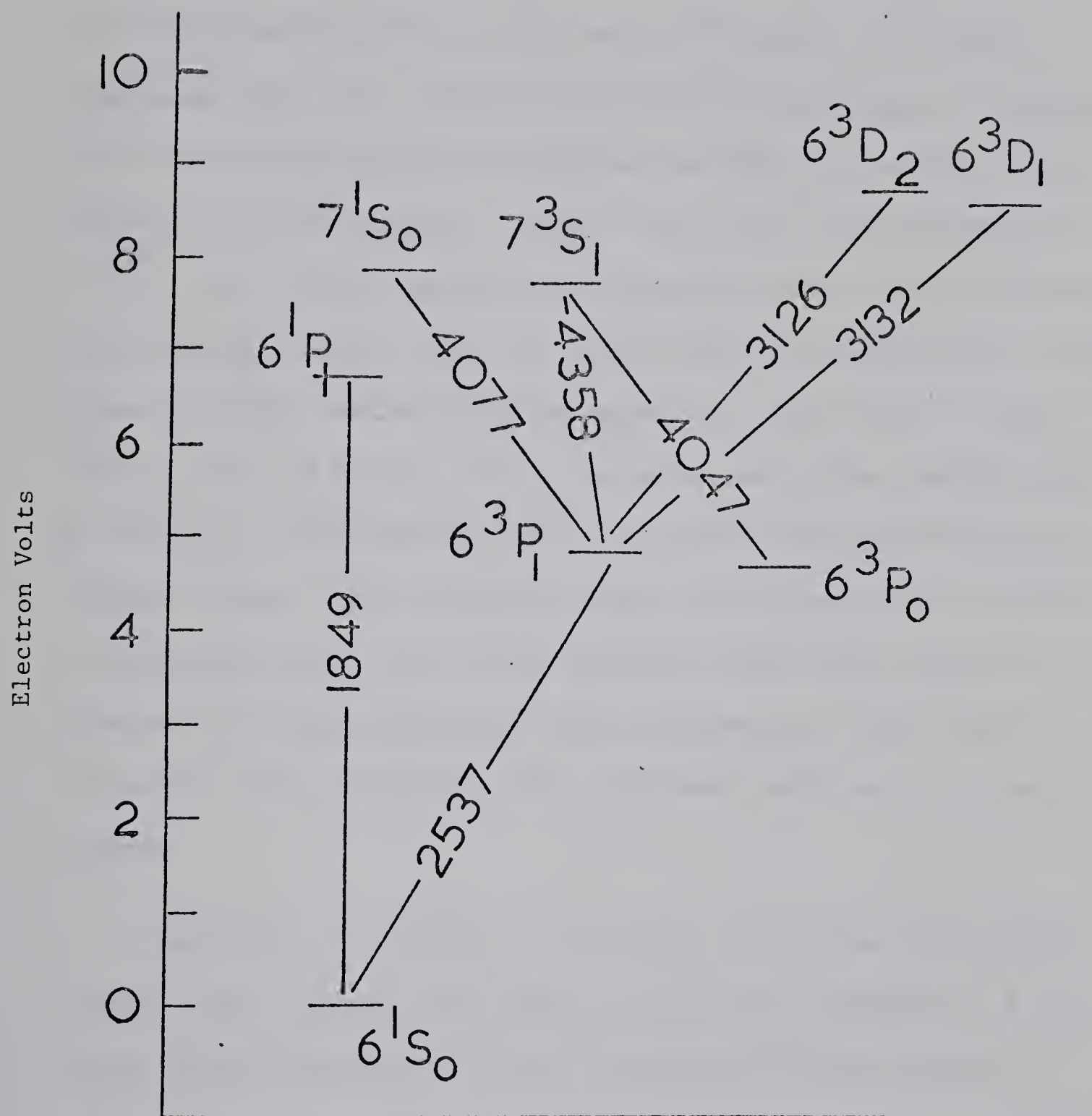


Figure 10. Energy levels of mercury.

0.7 to 1.3 ($7^1\text{So} + 7^3\text{S}_1$ levels eliminated, Fig. 10). Elimination of the 3125 Å and 3130 Å lines by the use of an "ultraviolet dye" (30), whose transmission at these wavelengths was less than 1% for a 5 mm path length had no effect on this ratio (6^3D_2 and 6^3D_1 levels eliminated, Fig. 10). Neutral density filters consisting of stainless steel wire mesh were used to determine the effect of incident light intensity upon the reaction. It was found that a ten-fold decrease in the light intensity caused the isobutane/n-butane ratio to increase approximately ten-fold (Fig. 9). These results indicated that a light intensity effect existed which was apparently independent of higher excited states of mercury. This conclusion was further substantiated by the use of low intensity commercial Hanovia low pressure mercury resonance lamps. These lamps are known to give very little radiation of wavelength other than the two resonance lines 1849 Å and 2537 Å. Irradiation by these lamps gave about the same as or even higher ratios than those obtained in the experiments using neutral density filters.

The effect of pressure on the product ratios was also studied. At high light intensity the propane pressure was increased to 3 torr and the mercury dimethyl to 6 torr, leaving the helium pressure at 10 torr. These experiments gave the highest values, 8.5 for isobutane/n-butane. Increasing the helium carrier pressure from 10 to 100 torr leaving the propane and dimethyl mercury pressures in the mtorr range had no effect on the product ratios.

It was recognized that the data, obtained from a large number of

experiments carried out under different experimental conditions, could be fitted to a relatively smooth curve when the isobutane/n-butane ratio is plotted against percentage conversion of propane to products per pass (Contact times were in the millisecond range for all experiments Fig. 9). The ratio is observed to increase from 0.3 to 8.5 with decreasing conversion and would extrapolate to over 9.0 at zero conversion. It is also noticed that when the reactants pressures are increased to a total of 9 torr with the ratio of mercury dimethyl to propane >2, the product ratio of isobutane to n-butane increases to a limiting high value of 8.5. Another feature of the reaction to be noted is the fact that generally when the isobutane to n-butane ratio is high, the relative propylene yield is low and can be readily accounted for using accepted literature values for the disproportionation to recombination ratios for methyl with propyl radicals

$$\{k_D/k_R = 0.16 \text{ for } \underline{i}\text{-C}_3\text{H}_7; k_D/k_R = 0.06 \text{ for } \underline{n}\text{-C}_3\text{H}_7\} \quad (32).$$

It was at this point that the chloropropanes were reinvestigated to see if the effect produced by light intensity was also evident here. The results of these experiments have already been mentioned in the previous section concerning the decomposition of chloropropanes (Table IV and Fig. 8).

3) Deuterated propanes:

Similar experiments were carried out with three deuterated propanes: 1, 1, -d₂(CH₃-CD₂-CH₃); 1,1,1,3,3,3,-d₆(CD₃-CH₂-CD₃); and perdeuterated propane (C₃D₈). Table VII and Figures 11, 12, 13, indicate the results of these experiments. Analogous light intensity and pressure

effects are evident in these cases. The highest isobutane to n-butane ratios are always obtained in experiments where the substrate pressures are the highest (3 torr propane and 6 torr dimethyl mercury in 10 torr helium). At these higher pressures the propylene formed is very small and can always be accounted for quite easily using the accepted disproportionation to recombination ratios for methyl with propyl radicals.

4) The role of H-atoms:

To examine the effect of H-atoms on the isomeric distribution of propyl radicals, the chloropropane - dimethyl mercury system was investigated with added hydrogen. Reaction conditions were, high light intensity, 2 mtorr of H_2 , 0.25 mtorr of chloropropane and 12 mtorr of $Hg(CD_3)_2$ in 10 torr of helium. The results are compiled in Table VIII.

Hydrogen was also added to systems in which mixtures of chloropropanes were decomposed. Table IX, gives the details of these experiments.

TABLE VII

Decomposition of deuterated propane plus dimethyl mercury mixtures.

<u>Reactant pressure (mtorr)</u>		<u>Product ratios</u>		<u>% Conversion</u> pass	Comments
propane	Hg(CH ₃) ₂	<u>propylene</u> butanes	<u>isobutane</u> n-butane		
<hr/>					
CH ₃ -CD ₂ -CH ₃	10 torr helium carrier pressure				
3.0	15	0.39	0.10	1.4	
1.0	10	0.38	0.10	0.9	
2.0	12	0.42	0.11	0.7	
2.7	15	0.34	0.17	0.4	
3 torr	6 torr	0.09	0.59	0.02	
<hr/>					
CD ₃ -CH ₂ -CD ₃					
3.0	15	0.56	7.0	1.1	
3.5	15	0.28	10.7	0.3	
3.2	15	0.24	12.6	0.3	
3.0	15	0.24	27.4	0.2	60 mesh screen

TABLE VII
(Continued)

Reactant	<u>pressures (mtorr)</u>		<u>Product ratios</u>		<u>% Conversion</u> pass	Comments
	propane	Hg (CH ₃) ₂	<u>propylene</u> <u>butanes</u>	<u>isobutane</u> <u>n-butane</u>		
3.2		15	0.11	>30.0	0.06	100 mesh screen
3 torr		6 torr	0.08	>30.0	0.10	
<u>C₃D₈</u>						
2.1		15	0.79	1.06	0.60	
4.0		15	0.46	1.33	0.12	
4.3		15	0.47	1.38	0.10	
2.0		15	0.35	1.55	0.06	60 mesh screen
3 torr		6 torr	0.16	5.97	0.04	

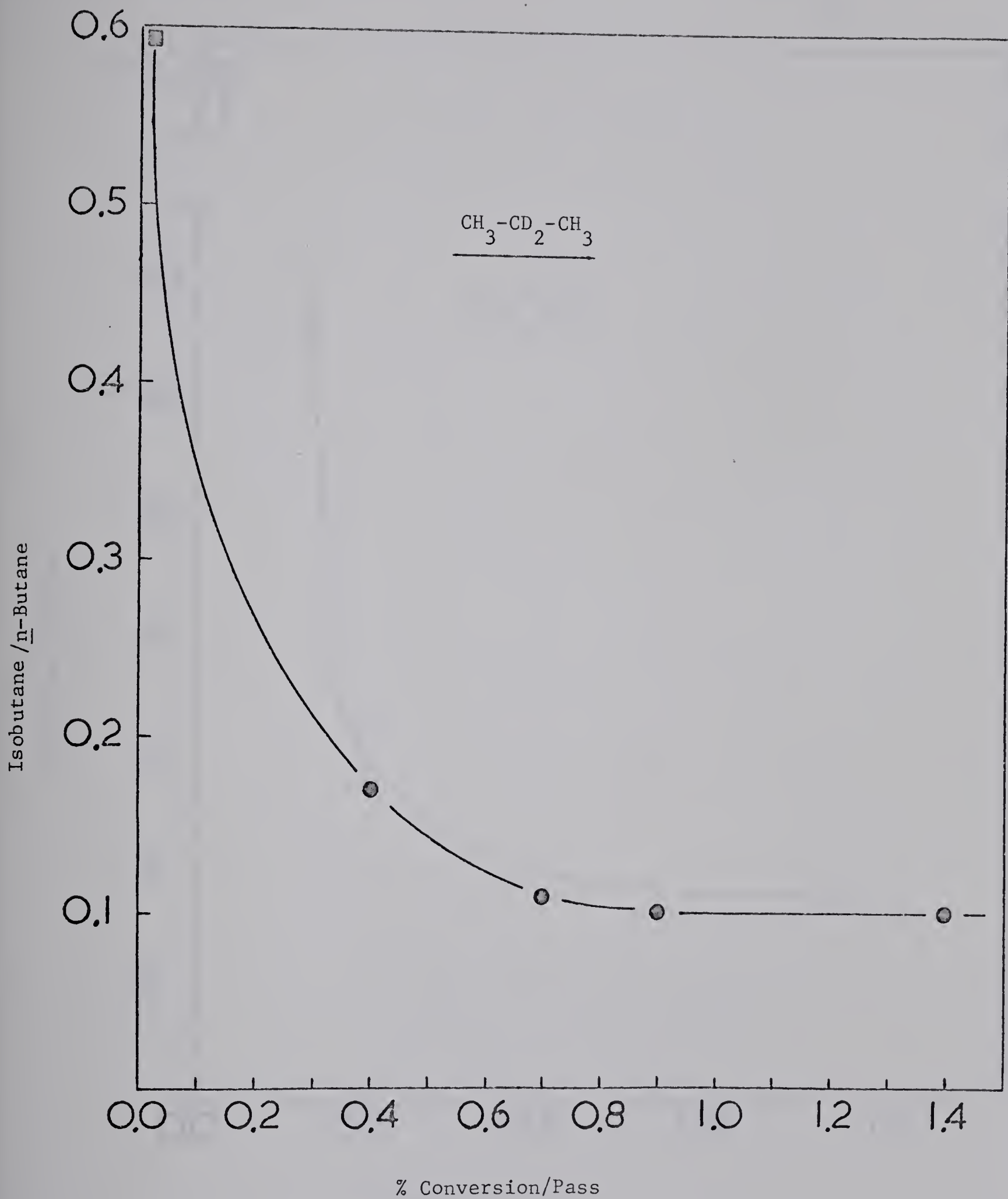


Figure 11. Isobutane/n-Butane as a function of % Conversion/Pass:

(●) normal run; (■) high pressure.

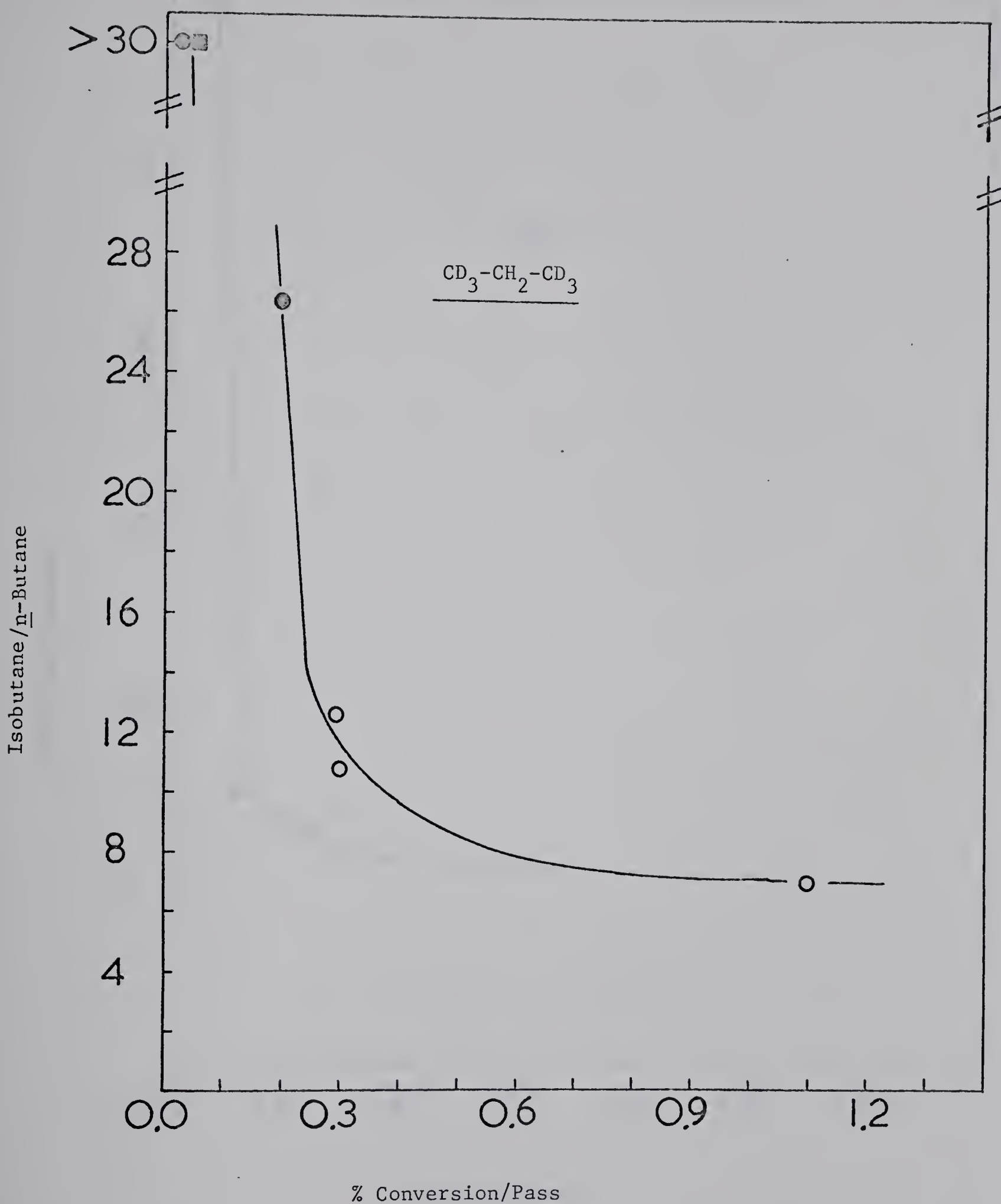


Figure 12. Isobutane/n-Butane as a function of % Conversion/Pass:

(O) normal run; (◐) wire mesh screen; (■) high pressure.

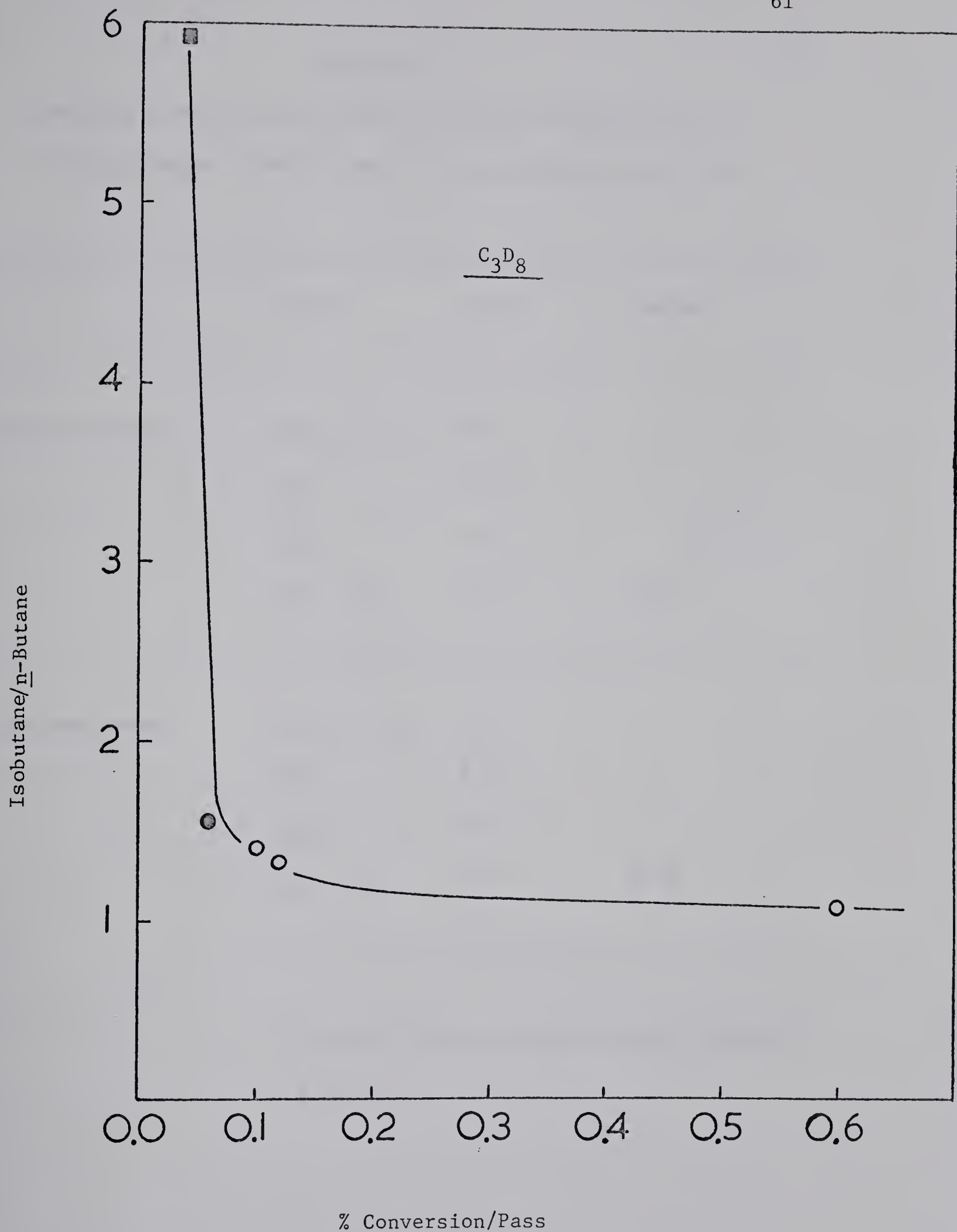


Figure 13. Isobutane/n-Butane as a function of % Conversion/Pass:

(O) normal run; (●) wire mesh screen; (■) high pressure.

TABLE VIII

Products from the mercury-photosensitized decomposition
of chloropropane, dimethyl mercury- d_6 and hydrogen mixtures.

	Product	μ moles	μ moles*
2-chloropropane	$i-C_3H_7 \cdot CD_3$	0.79	
	C_3H_6	1.24	
	C_3H_8	0.73	
	$C_2H_5 \cdot CD_3$	0.06	0.15
1-chloropropane	$n-C_3H_7 \cdot CD_3$	1.25	
	C_3H_6	0.53	
	C_3H_8	0.77	
	$C_2H_5 \cdot CD_3$	0.17	0.42

* Assuming 40% scavenging of ethyl radicals
with CH_3 .

TABLE IX

Butane ratios from the decomposition of 1- and 2-chloropropane mixtures with added dimethyl mercury and hydrogen.

Reactants

1:1 chloropropane mixture (0.2 mtorr each)

$\text{Hg}(\text{CH}_3)_2$ (12 mtorr)

H_2 (1 mtorr)

<u>Products</u>	<u>μ-moles</u>	$\frac{\text{i-C}_4\text{H}_{10}}{\text{n-C}_4\text{H}_{10}}$
$\text{i-C}_4\text{H}_{10}$	0.49	0.94
$\text{n-C}_4\text{H}_{10}$	0.52	

Reactants

7.2 :1 2-chloropropane/1-chloropropane mixture
(2.88 mtorr) (0.04 mtorr)

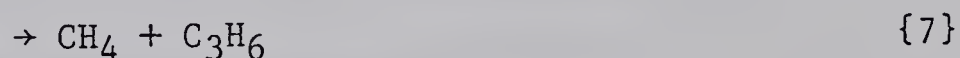
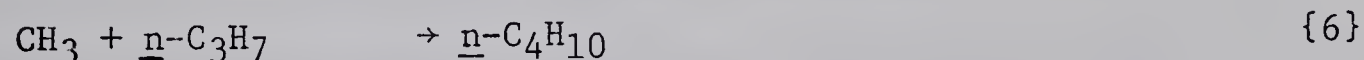
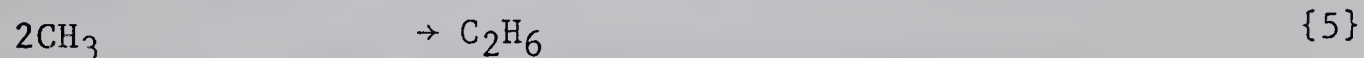
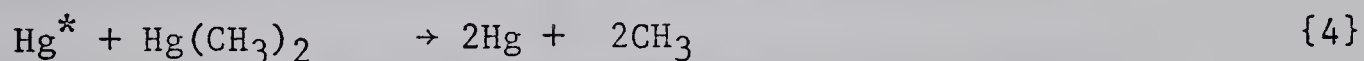
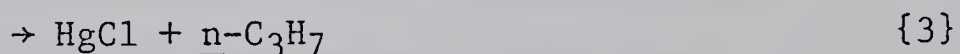
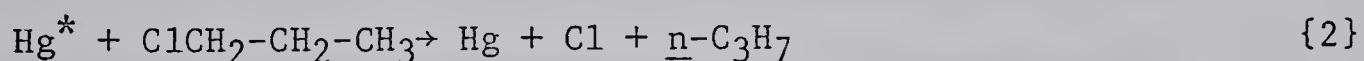
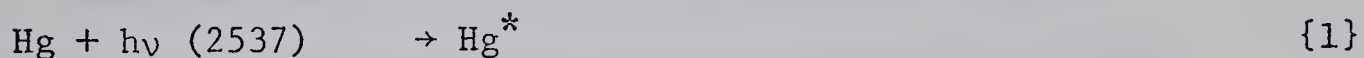
$\text{Hg}(\text{CH}_3)_2$ (12 mtorr)

H_2 (1 mtorr)

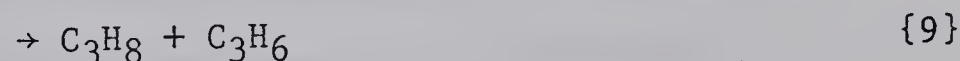
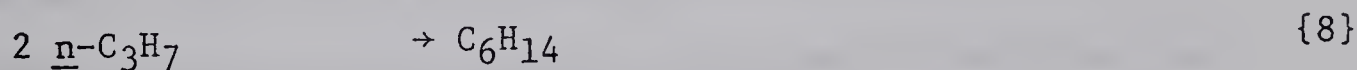
<u>Products</u>	<u>μ-moles</u>	$\frac{\text{i-C}_3\text{H}_7\cdot\text{CD}_3}{\text{n-C}_3\text{H}_7\cdot\text{CD}_3}$
$\text{i-C}_3\text{H}_7\cdot\text{CD}_3$	0.65	5.40
$\text{n-C}_3\text{H}_7\cdot\text{CD}_3$	0.12	

1) Trapping of the propyl radicals:

The technique of radical trapping has been tested using chloropropanes as propyl radical sources. The following reaction mechanism is proposed to account for the products observed. 1-Cl-propane is used in the discussion, if 2-Cl-propane were the propyl radical source reaction {2} or {3} would give isopropyl radicals and {6} would yield isobutane.



Saturation of the system with methyl radicals eliminates the importance of reactions involving the recombination and disproportionation of propyl radicals.



The high methyl radical concentration favors reactions of methyl with propyl radicals. The absence of higher than C_4 products indicates

that reactions such as {8} and {9} are minimized to the extent that they become undetectable.

These experiments also demonstrated that under the reaction conditions employed, the isomerization reaction,



was unimportant, as n-butane was the only C₄ from the decomposition of 1-chloropropane, dimethyl mercury mixtures, while isobutane was the only C₄ from the analogous reaction using 2-chloropropane as the propyl radical source.

Concerning the light intensity effect upon the propylene to butane ratios, it may be that the radicals formed have excess energy. There has been a report in the literature implying that "hot" ethyl radicals undergo disproportionation reactions more readily than thermalized radicals (34).[†] Decreasing the light intensity has the effect of lowering the radical concentrations. Due to their lower concentrations the lifetimes of the radicals increase, thus enhancing the probability of additional collisions with the carrier gas during which excess energy can be removed. At very low light intensities the radicals become thermalized before reacting.

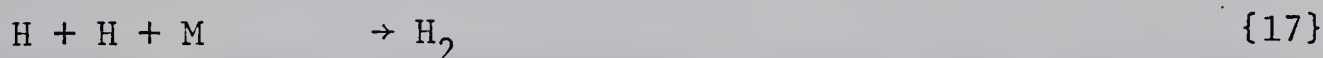
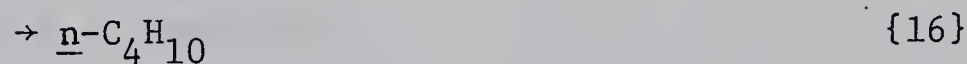
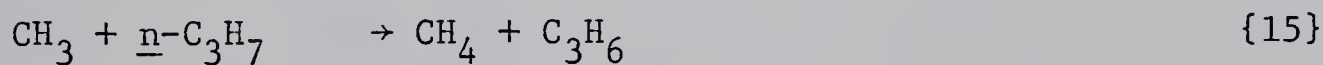
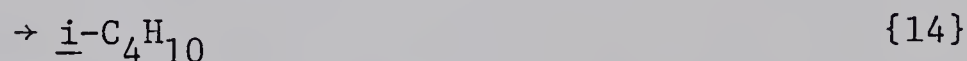
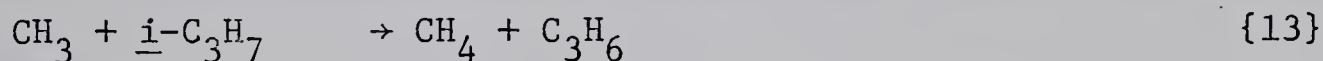
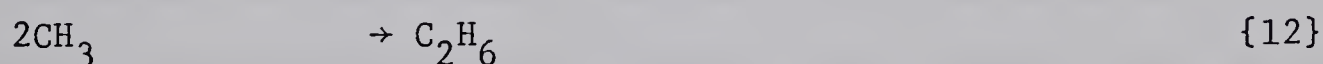
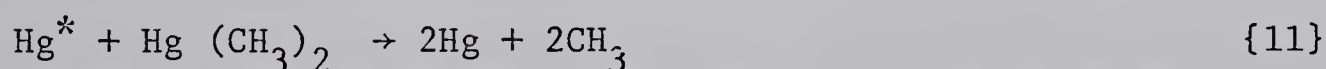
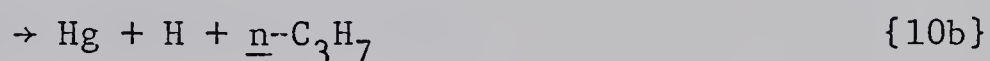
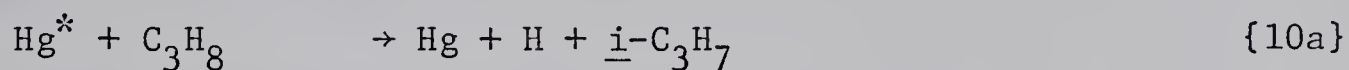
The technique was further tested with 1:1, 1- and 2-chloropro-

[†] Professor Rabinovitch has questioned the reliability of the results reported in this reference and does not believe that there is sufficient evidence to indicate abnormal disproportionation in the case of energy rich radicals.

pane mixtures. The results of these experiments as summarized in Table V clearly indicate that radicals are trapped giving product yields which, when disproportionation reactions are taken into consideration, reflect the relative concentrations of primary radicals in the system.

2) Photosensitization of propane:

The products from the photosensitized decomposition of propane, dimethyl mercury mixtures can be explained by the following reactions.



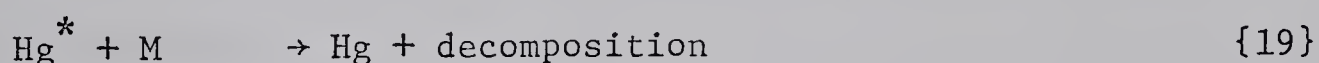
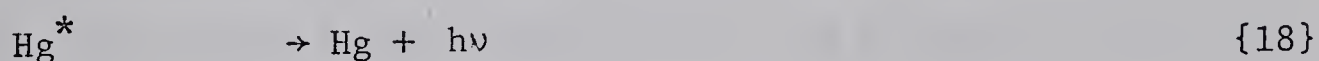
Although these reactions offer a general mechanism for the formation of the observed products, they cannot account for the observed increase of the isobutane to n-butane ratio with decreasing light intensity. Nor can they explain the lowering of the relative propylene yields as the incident light intensity is attenuated. In this respect other possible factors which could possibly explain the observed experimental results have been considered.

3) Light intensity:

It has been determined that the primary dissociation of propane by Hg $6(^1P_1)$ atoms, produced by the absorption of a photon of 1849 Å wavelength, yields 50% n-propyl and 50% isopropyl radicals (35). The results of the present study clearly indicate that this process is unimportant in the flow system and cannot be invoked to explain the variation in the isobutane/n-butane ratio. The experimental results also rule out the participation of higher excited states of mercury.

4) Secondary decomposition of primary radicals:

The extent of the secondary mercury sensitized decomposition of methyl and propyl radicals can be estimated from consideration of the reactions,



and {12-16}. Detailed calculations for the following discussion are given in Appendix C.

The value of k_{18} is given by Holstein's formula for the imprisonment lifetime (36, 37).

$$k_{18} = 1/\tau_i = (5/8 k_o R \{\pi \ln \frac{1}{2} k_o R\}^{\frac{1}{2}} \tau)^{-1}$$

where $k_o = 2.23 \times 10^{-12} \text{ N/T}^{\frac{1}{2}}$. The concentration of mercury, N, is $7.31 \times 10^{14} \text{ atoms cc}^{-1}$ and $T = 330^\circ\text{K}$.

The radius of the reaction vessel, R , is 0.45 cm and τ , the mean radiative lifetime of $6(^3P_1)$ atoms is 1.1×10^{-7} sec. Using these values $k_{18} = 1.18 \times 10^5 \text{ sec}^{-1}$.

For the decomposition reaction of dimethyl mercury the quenching cross section is 81 \AA^2 (Appendix A). The rate of quenching of Hg^* is given by,

$$k_{19}^M = k_{19}^*.$$

at 10 mtorr of dimethyl mercury

$$k_{19}^* = 1.9 \times 10^5 \text{ sec}^{-1}.$$

The decomposition of dimethyl mercury could be monitored directly by the mass spectrometer. At high light intensities and 10 mtorr pressure of dimethyl mercury it was observed to be 25%. For the flow rate and cell geometry involved a rate, R_d , of 4.9×10^{16} molecules $\text{cc}^{-1} \text{ sec}^{-1}$ can be calculated. The absorbed light intensity I_a , can be obtained from the following relationship.

$$I_a = R_d(k_{18} + k_{19}^*)/k_{19}^* = 8 \times 10^{16} \text{ quanta } \text{cc}^{-1} \text{ sec}^{-1}$$

Under steady-state conditions, which are reached at less than one tenth of the length of the reactor along the flow (29),

$$I_a = \{\text{Hg}^*\} (k_{18} + k_{19}^*)$$

and

$$\{\text{Hg}^*\} = I_a/(k_{18} + k_{19}^*) = 2.6 \times 10^{11} \text{ atoms } \text{cc}^{-1}.$$

The steady-state concentration of methyl radicals using Gomer

and Kistiakowsky's rate constant value of $k_r = 7.5 \times 10^{-11} \text{ cc molecule}^{-1} \text{ sec}^{-1}$ (38), for the second order recombination of methyl radicals, is

$$\{\text{CH}_3\} = (2R_d/k_r)^{1/2} = 3.6 \times 10^{13} \text{ radicals cc}^{-1}$$

Using the same rate constant for radical recombination and the assumption that propyl radicals are produced at a rate 100 times slower than methyl radicals a steady state concentration for propyl, $\{\text{C}_3\text{H}_7\} = 3.6 \times 10^{11} \text{ radicals cc}^{-1}$ can be calculated.

Quenching cross sections have not been measured for free radicals. If an effective quenching cross section of 40 \AA^2 is assumed for propyl and methyl radicals (NO which may be considered a stable free radical has $\sigma_Q^{2\dot{\text{A}}^2} = 43.2$ Appendix A), the rates of secondary reactions of these radicals with Hg^* can be estimated. They are,

$$R(\text{Hg}^*, \text{C}_3\text{H}_7) = 5.2 \times 10^{13} \text{ radicals cc}^{-1} \text{ sec}^{-1}$$

$$R(\text{Hg}^*, \text{CH}_3) = 8.3 \times 10^{15} \text{ radicals cc}^{-1} \text{ sec}^{-1}.$$

When these rates are compared with the rate of radical-radical reactions,

$$R(\text{CH}_3, \text{C}_3\text{H}_7) = k_r \{\text{CH}_3\} \{\text{C}_3\text{H}_7\} = 9.7 \times 10^{14} \text{ molecules cc}^{-1} \text{ sec}^{-1}$$

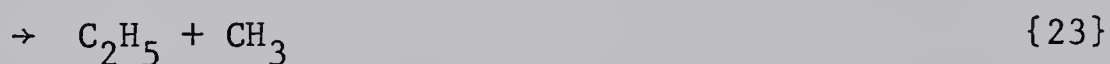
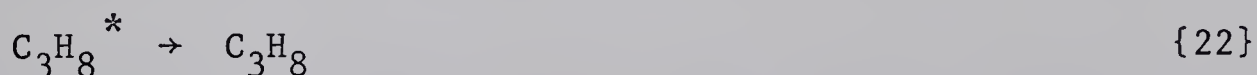
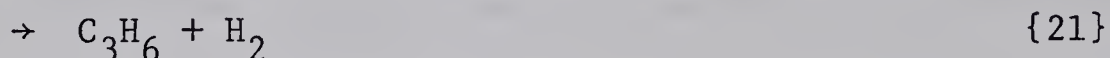
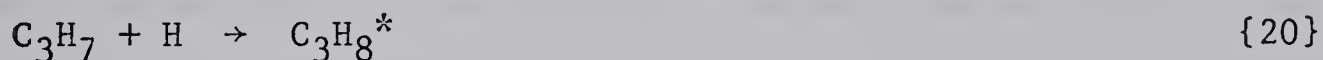
$$R(\text{CH}_3, \text{CH}_3) = k_r \{\text{CH}_3\}^2 = 9.7 \times 10^{16} \text{ molecules cc}^{-1} \text{ sec}^{-1}$$

it is seen that about 5% of the propyl radicals suffer secondary decomposition, while the decomposition of the methyl radicals is more extensive,

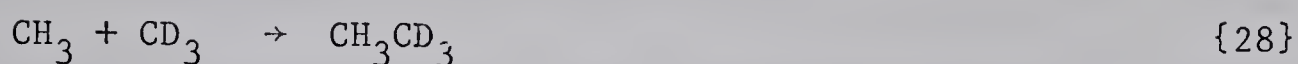
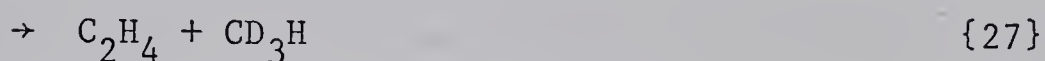
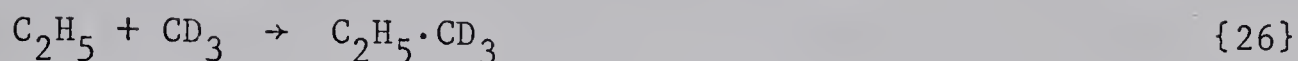
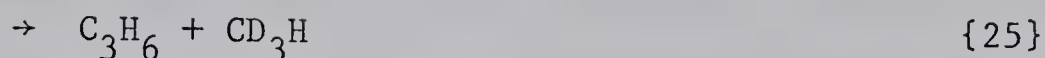
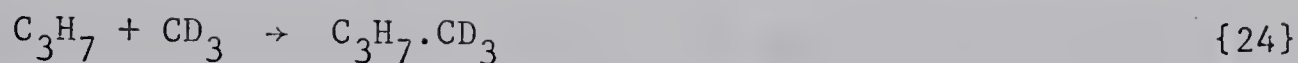
being about 8%.² The small yields of ethylene, propane, etc. from the mercury photosensitization of pure dimethyl mercury (29) most probably result from this secondary decomposition of methyl radicals. These results also clearly illustrate that the secondary decomposition of propyl radicals via collision with Hg^* cannot be responsible for the variation of butane product ratios with light intensity fluctuations.

5) The role of H-atoms:

The addition of hydrogen to the chloropropane-dimethyl mercury decomposition mixtures made it possible to examine the effects of H-atoms in the system to be observed. The results of these experiments are summarized in Table VIII. Appendix D contains the calculations mentioned. The products can be explained by the reactions:



² In a recent study of the pressure dependence of the methyl radical combination reaction (39), the authors suggest that the rate of combination of methyl radicals may have been overestimated. A smaller rate constant would result in larger steady-state radical concentrations and more secondary decomposition.



³ By taking the rate of {20} =

$$\{\text{C}_3\text{H}_6\} - \{\text{C}_3\text{H}_6\} \text{ from } \{25\} + \{\text{C}_3\text{H}_8\} + \{\text{C}_2\text{H}_5\cdot\text{CD}_3\}$$

and using 0.15 and 0.06 for the disproportionation to recombination ratios of methyl with iso- and n-propyl radicals respectively, it is found that about 55% of the n-propyl radicals and 69% of the isopropyl

3

The $\text{C}_2\text{H}_5\cdot\text{CD}_3$ yield was corrected for incomplete scavenging of ethyl by methyl, due to the competing reaction with H-atom. It was assumed that scavenging efficiency is 40% as with propyls.

radicals undergo reactions with H-atoms. H-atoms were also generated in the decomposition of mixtures of 1- and 2-chloropropane in the presence of excess dimethyl mercury. In spite of the extensive H-atom reactions the isomeric butane product ratios were only slightly altered (Table IX), indicating that the intensity effect of the propane reaction cannot be attributed to the presence of H-atoms in the system.

From the data in Table VIII it is possible to derive rate constant ratios of disproportionation to recombination, k_{25}/k_{24} , for the propyl + H reactions. The values are 1.4 for isopropyl and 0.6 for n-propyl. The reliability of these numbers are questionable as they are based upon single experiments. The value for isopropyl seriously conflicts with a value of 0.20 reported by Heller and Gordon (117).

Assuming identical rates for the propyl + H and ethyl + H reactions and a collision efficiency of helium of 0.25 in reaction {22}, a value of $k_{23} = 1.7 \times 10^7$ molecules $\text{cc}^{-1} \text{sec}^{-1}$ and 8.2×10^6 molecules $\text{cc}^{-1} \text{sec}^{-1}$ for the hot propane decomposition from n- and isopropyl radicals respectively. From the bond dissociation energies $D(\text{n-C}_3\text{H}_7 - \text{H}) = 98$, $D(\text{i-C}_3\text{H}_7 - \text{H}) = 94.5$, and $D(\text{C}_2\text{H}_5 - \text{CH}_3) = 85 \text{ kcal mole}^{-1}$ (Appendix B), 13 and 9.5 kcal mole^{-1} of excess energy is contained in the initially formed propane molecule via combination of H-atoms with n- and isopropyl radicals respectively. Because of its higher energy content, the species resulting from n-propyl radicals is expected to have a shorter lifetime. The ratio of the decomposition rate constants is 2. This is somewhat smaller than the ratio of 5 predicted theoretically by Marcus (40) or

6 predicted by Rabinovitch and Sester (41).

6) Primary radical distribution:

The nature of mercury sensitization processes dictates that the isomeric distribution of primary radicals is more closely approximated by the values obtained at milder reaction conditions. That is, at lower light intensities and higher substrate pressures. Under these conditions the interaction of excited mercury atoms with primary products is less important and the contribution of other possible secondary reactions is minimal. That this is indeed the case is suggested by the falloff of the relative propylene yields to the level obtained by other workers, corresponding to the disproportionation reactions of methyl with propyls. These considerations lead to the acceptance of the maximum values for the isopropyl/n-propyl ratios obtained in the high pressure experiments as good approximations of the true primary radical ratios. These data are summarized in Table X for the four propanes studied.

The earlier results of Avrahami and Kebarle were obtained at high light intensities and without the realization of the light intensity effect. Consequently, they are not representative of the primary radical yields and should be disregarded. The present results show good agreement with the ethylene scavenging values of Holroyd and Klein and very closely parallel the estimated quenching distribution of the Hg $6(3P_1)$ atom among the primary and secondary C-H and C-D bonds in the propane molecule.

The nitric oxide trapping technique of Woodall and Gunning has not

TABLE X

Propyl radical yields from the Hg $6(^3P_1)$ photosensitized decomposition of propane and deuterated propanes.

Propane decomposed	$\frac{\text{isopropyl}}{\text{n-propyl}}$
$\text{CH}_3\text{-CH}_2\text{-CH}_3$	9.1
$\text{CD}_3\text{-CH}_2\text{-CD}_3$	> 30.0
$\text{CH}_3\text{-CD}_2\text{-CH}_3$	0.6
$\text{CD}_3\text{-CD}_2\text{-CD}_3$	7.0

been reexamined. This system is very complex and relies heavily on various assumptions concerning rates and yields of the transformation of the nitroso propanes to the oximes and moreover, has not been "calibrated" with known mixtures of iso- and n-propyl radicals. The confidence in the results was greatly enhanced by the close coincidence with the mass spectrometric results, which now turn out to be fortuitous.

The discrepancy appears to be resolved in favor of the ethylene scavenging technique and of the linear form of the transition complex formed between the excited mercury atom and a paraffin molecule. The cyclic structure was invoked for the experimental data available at that time, which has now proved to be in error. The low quantum efficiency of the mercury sensitization of the neopentane molecule, which was also thought to lend support to the cyclic structure (vs. the linear one), has also turned out to be incorrect (42).

It has been conclusively shown that the effect of light intensity on the isomeric product ratios is not due to higher excited states of mercury formed in stepwise photon absorption. Neither can it be due in any large extent to hydrogen atom reactions.

CHAPTER IV

THE Hg 6(³P₁) PHOTSENSITIZED DECOMPOSITION OF CYCLOPROPANE

RESULTS

- 1) Decomposition of Cyclopropane.
- 2) Decomposition of Cyclopropyl Bromide.

DISCUSSION

THE PRIMARY PROCESSES IN THE Hg* + CYCLOPROPANE REACTION.

THE UNIMOLECULAR REACTIONS OF CHEMICALLY ACTIVATED METHYLCYCLOPROPANES.

- 1) Thermochemistry of the Methyl Plus Cyclopropyl Reaction.
- 2) Isomeric Distribution of Butene Products.
- 3) Miscellaneous Products.
- 4) Calculation of Rate Constants.
- 5) Evaluation of the Technique.

RESULTS

1) Decomposition of Cyclopropane:

Typical reaction conditions for the Hg (3P_1) photosensitized decomposition of cyclopropane were 0.5 - 1.0 mtorr of cyclopropane, 10 mtorr of dimethyl mercury and 10 torr helium carrier gas. The results of four experiments indicated that the detectable products of the reaction were; ethane and small amounts of propane, propylene and 1- butene. The ethane is a product of the dimethyl mercury decomposition. As the sensitization of pure dimethyl mercury and cyclopropane both yield propane and propylene as products, both these reactants contribute to their formation. No special attempt was made to assess the relative contribution from each reactant. Butene -1, is undoubtedly the recombination product of a C_3H_5 radical and a methyl radical. In this instance the C_3H_5 species was in all likelihood an allyl radical.

2) Decomposition of Cyclopropyl Bromide:

To obtain some knowledge of the possible reactions of cyclopropyl radicals with methyl radicals in the system, cyclopropyl bromide was decomposed in the reactor. Cyclopropyl bromide should decompose almost exclusively by elimination of a bromine atom to give a cyclopropyl radical. Table XI contains the conditions and results of these experiments. In addition to the products listed, trace amounts of another product possibly n-butane were observed.

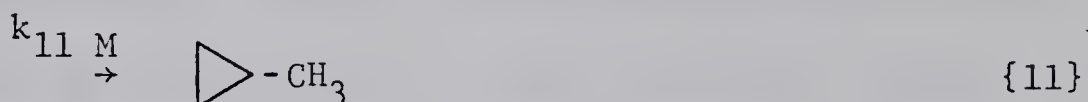
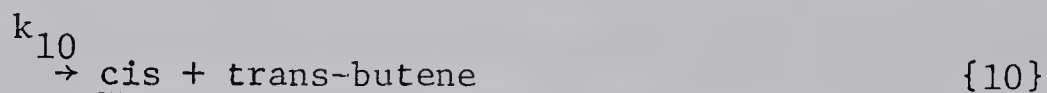
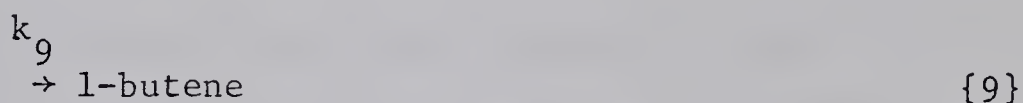
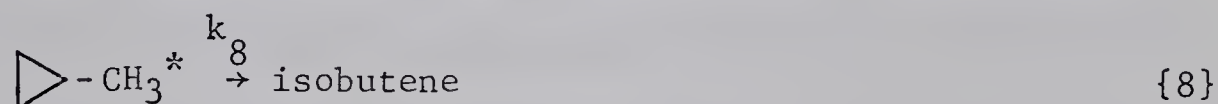
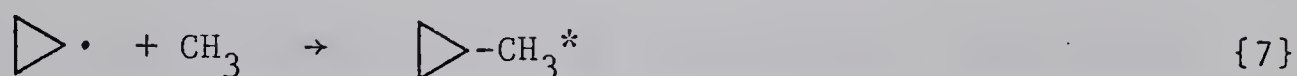
TABLE XI

Product yields from the photosensitized decomposition of
0.5 - 1.0 mtorr cyclopropyl bromide and 15 mtorr of dimethyl mercury

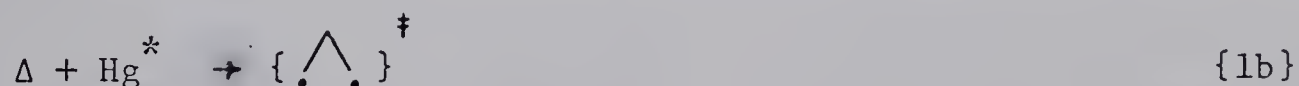
Helium pressure (torr)	4.5	13	14	19	21	40	72	110	145	190
<u>Products (10^{-6} moles)</u>										
<u>cis</u> -butene	0.18	0.29	2.22	0.19	0.11	0.44	0.66	1.25	0.85	0.51
<u>trans</u> -butene	0.25	0.38	3.00	0.25	0.13	0.44	0.57	1.16	0.74	0.41
isobutene	0.20	0.27	1.91	0.20	0.10	0.40	0.38	0.64	0.47	0.29
1-butene	0.86	1.10	8.36	0.74	0.45	2.00	2.38	3.70	2.28	2.00
methylcyclopropane	---	----	----	----	----	0.35	0.72	2.25	2.24	2.00
cyclopropane	0.16	0.21	1.58	0.49	0.20	1.51	0.70	1.64	1.35	1.21
propylene	0.35	0.28	1.25	0.32	0.16	0.74	0.29	0.62	0.52	0.49
allene	0.04	0.08	1.13	0.08	0.02	0.28	0.44	0.47	0.45	0.43
total C ₄	1.49	2.04	15.49	1.38	0.79	3.63	4.71	9.00	6.58	5.21
total butene	1.49	2.04	15.49	1.38	0.79	3.28	3.99	6.75	4.34	3.21
propane	0.12	0.15	0.40	0.09	0.04	0.06	0.20	0.28	0.18	0.03
ethylene	0.05	0.05	0.10	0.10	0.04	0.12	0.30	0.30	0.04	0.15

DISCUSSIONTHE PRIMARY PROCESSES IN THE $\text{Hg}^* + \text{CYCLOPROPANE}$ REACTION

The experimental results of the cyclopropyl bromide system (Table XI) indicate that when cyclopropyl radicals are generated in the presence of methyl radicals they will recombine to form a "hot" methylcyclopropane molecule which unless collisionally deactivated will isomerize to the isomeric butenes.

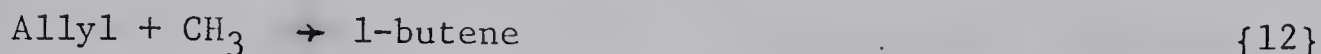


The detection of l-butene as the only butene product from the sensitized decomposition of cyclopropane under similar circumstances leads to the conclusion that reaction {1a}, the cyclopropyl plus H-atom split is unimportant in this system. The results of these experiments lend support to the proposal that the major quenching act in the $\text{Hg} (^3\text{P}_1)$ plus cyclopropane system results in the formation of a vibrationally excited trimethylene species.



This species is then either stabilized to reform cyclopropane, isomerizes

to propylene, or decomposes to give an allyl radical and a H-atom. In the presence of large amounts of methyl radicals, these allyl radicals are scavenged to give 1-butene.

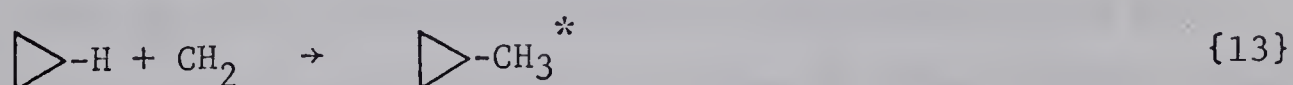


Except for its small quenching cross section, cyclopropane exhibits parallel features to propylene in its reaction with $\text{Hg } ({}^3\text{P}_1)$ atoms. Unlike paraffins which exhibit large differences in reactivity upon deuterium substitution, the quenching efficiencies of propylene and cyclopropane are essentially unaffected (Appendix A). This implies quenching into the C-C σ -bond of cyclopropane rather than the C-H bond.

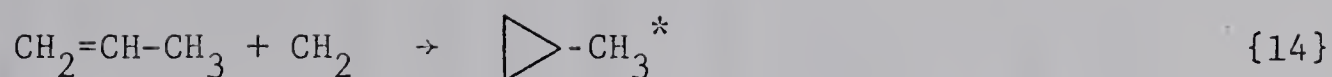
Avrahami and Kebarle, have studied the mercury sensitized decomposition of propylene in a similar reactor using methyl radicals as scavengers (43). The results of this study correlate quite closely with the present cyclopropane study, in that the major decomposition product is 1-butene formed by the recombination of allyl and methyl radicals. In addition to the allyl plus H-atom split (89%), a vinyl plus methyl split (11%) and a cyclization step (0.2%) giving cyclopropane were reported.

THE UNIMOLECULAR REACTIONS OF CHEMICALLY ACTIVATED METHYLCYCLOPROPANES

The unimolecular decomposition of chemically activated cyclopropane and methylcyclopropanes has been the subject of several studies (44-50). In these investigations the chemically activated species were produced by the insertion of methylene into the C-H bonds of cyclopropane;



or by addition across the double bond in olefins;



The exothermicity of reactions {13} and {14} are different and thus offer a means for producing excited cyclopropanes with different energy contents. The energy content can also be altered by choosing different methylene sources.

Although the apparatus was not specifically designed to study the kinetics of unimolecular reactions, an attempt was made to explore the chemical activation method using the mass spectrometric technique. The results of this endeavor are summarized in Table XI and Figures 13 - 16.

1) Thermochemistry of the methyl plus cyclopropyl reaction:

If the methyl and cyclopropyl radicals are assumed to possess only thermal energies, the excess energy residing in the methylcyclopropane molecule will be equal to the exothermicity of the reaction plus the small thermal contributions from the radicals. In the case of radical-radical recombinations, the exothermicity is equal to the strength of the bond being formed, which unfortunately for $\text{c-C}_3\text{H}_5-\text{CH}_3$ is not known. The C-H bond energies in ethane and cyclopropane are quite similar, if their C-C bond energies are also compatible, the exothermicity of reaction {7} should be $88 \text{ kcal mole}^{-1}$ (Appendix B). When the thermal contributions from the radicals are considered, the methylcyclopropane species should contain energy in excess of $90 \text{ kcal mole}^{-1}$. The over-all activation energy for isomerization has been reported as $\sim 64 \text{ kcal mole}^{-1}$ (51, 52). Unless at least $26 \text{ kcal mole}^{-1}$ of energy is removed by collisions, the energy rich methylcyclopropane

TABLE XII

Product ratios from methyl and cyclopropyl radical reaction as
a function of He carrier gas pressure.

P _{He} (torr)	4.5	13	14	19	21	40	72	110	145	190
$\omega \text{ sec}^{-1} \text{ (x } 10^{-8})$	0.9	2.6	2.8	3.8	4.2	8.0	14.4	22.0	29.0	38.0
$\omega^{-1} \text{ sec (x } 10^{10})$	110.0	38.5	35.7	26.3	23.8	12.5	6.9	4.6	3.5	2.6
isobutene/total C ₄	0.13	0.13	0.12	0.14	0.13	0.11	0.08	0.07	0.07	0.06
<u>cis</u> -butene/total C ₄	0.12	0.14	0.14	0.14	0.14	0.12	0.14	0.14	0.13	0.10
<u>trans</u> -butene/total C ₄	0.17	0.19	0.19	0.18	0.16	0.12	0.12	0.13	0.11	0.08
1-butene/total C ₄	0.58	0.54	0.54	0.54	0.57	0.55	0.51	0.41	0.35	0.38
methylcyclopropane/ total C ₄	-----	-----	-----	-----	-----	0.10	0.15	0.25	0.34	0.39
isobutene/total butene	0.13	0.13	0.12	0.14	0.13	0.12	0.10	0.09	0.11	0.09
<u>cis</u> -butene/total butene	0.12	0.14	0.14	0.14	0.14	0.13	0.17	0.19	0.20	0.16
<u>trans</u> -butene/total butene	0.17	0.19	0.19	0.18	0.16	0.13	0.14	0.17	0.17	0.13
1-butene/total butene	0.58	0.54	0.54	0.54	0.57	0.60	0.60	0.55	0.53	0.62

TABLE XII
(Continued)

P _{He} (torr)	4.5	13	14	19	21	40	72	110	145	190
<u>cis-butene/trans-</u> butene	0.72	0.76	0.75	0.76	0.85	1.00	1.16	1.09	1.15	1.24
cyclopropane/propylene	0.46	0.75	1.26	1.53	1.25	2.04	2.41	2.65	2.60	2.47
allene/total C ₄	0.03	0.04	0.07	0.06	0.03	0.08	0.09	0.05	0.07	0.08
butenes/methyl- cyclopropane	-----	-----	-----	-----	-----	9.37	5.54	3.00	1.94	1.61
<u>cis+trans</u> /total butene	0.29	0.33	0.33	0.32	0.30	0.27	0.31	0.36	0.37	0.29
										<u>ave=0.06</u>

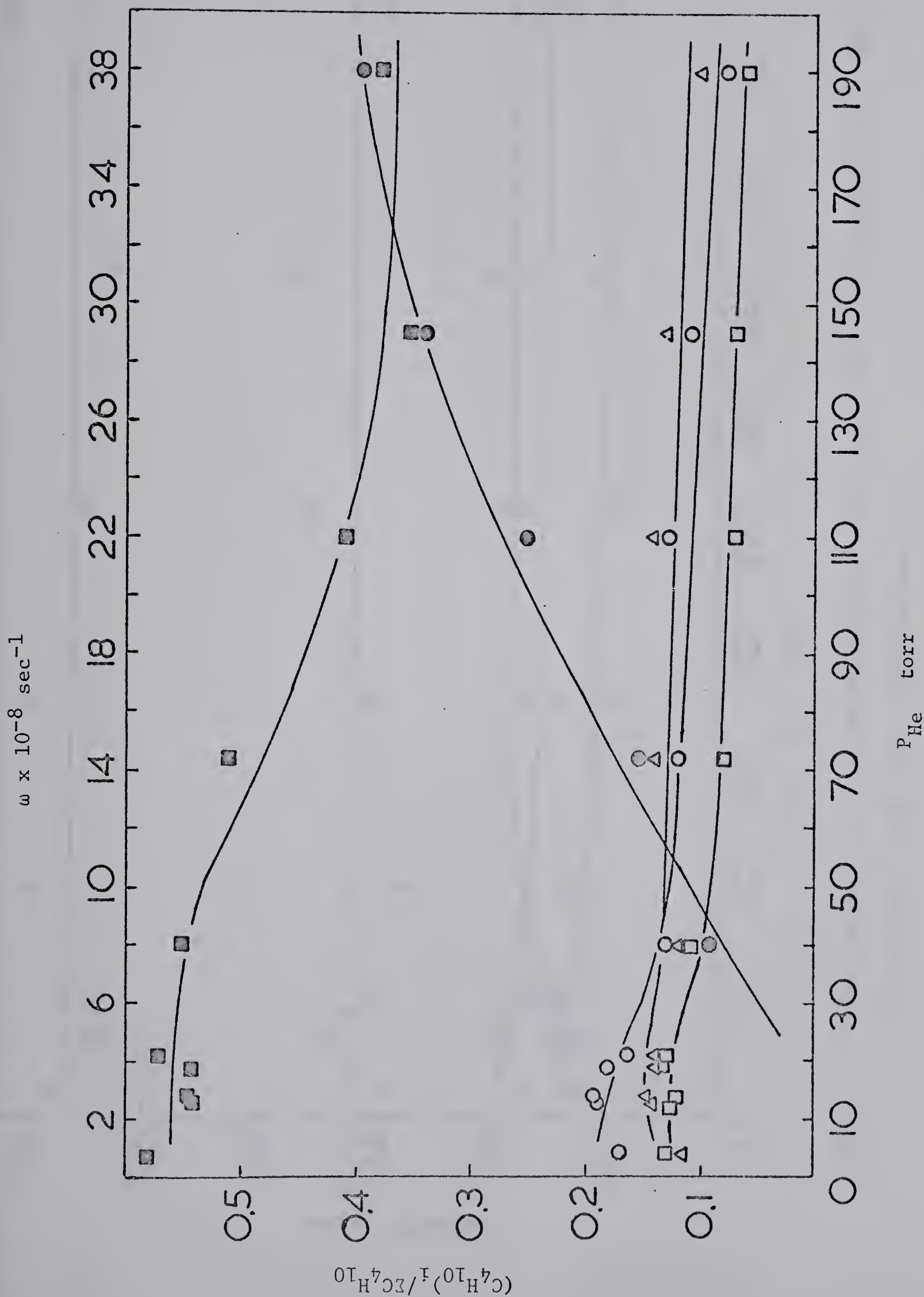


Figure 14. C_4H_{10} product ratios as a function of pressure: (\square) isobutene; (Δ) cis-butene; (\circ) trans-butene; (\blacksquare) 1-butene; (\bullet) methylcyclopropane.

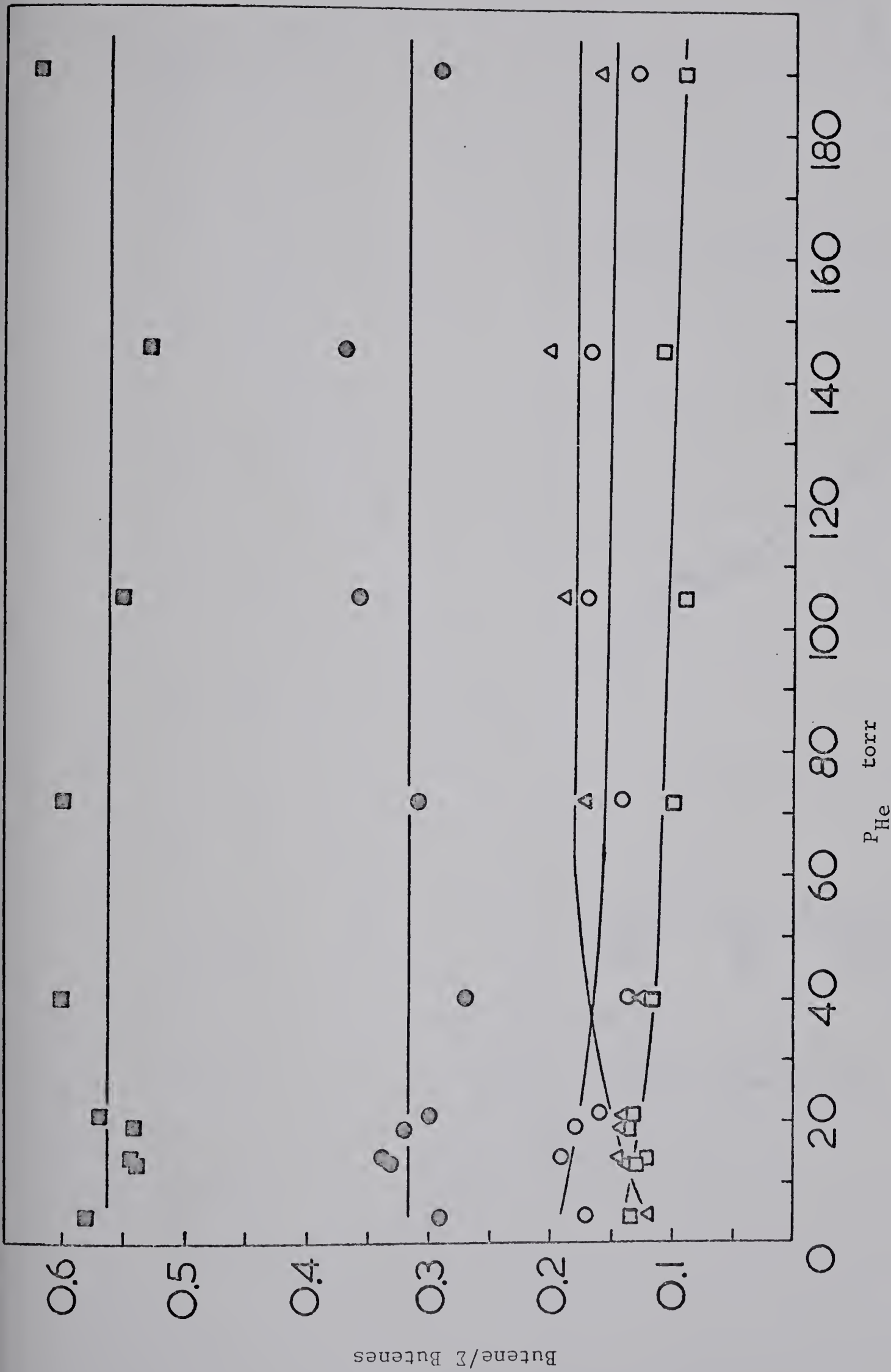


Figure 15. Butene ratios as a function of pressure: (Δ) cis-butene; (\circ) trans-butene; (\blacksquare) 1-butene; (\square) isobutene; (\bullet) cis + trans-butene.

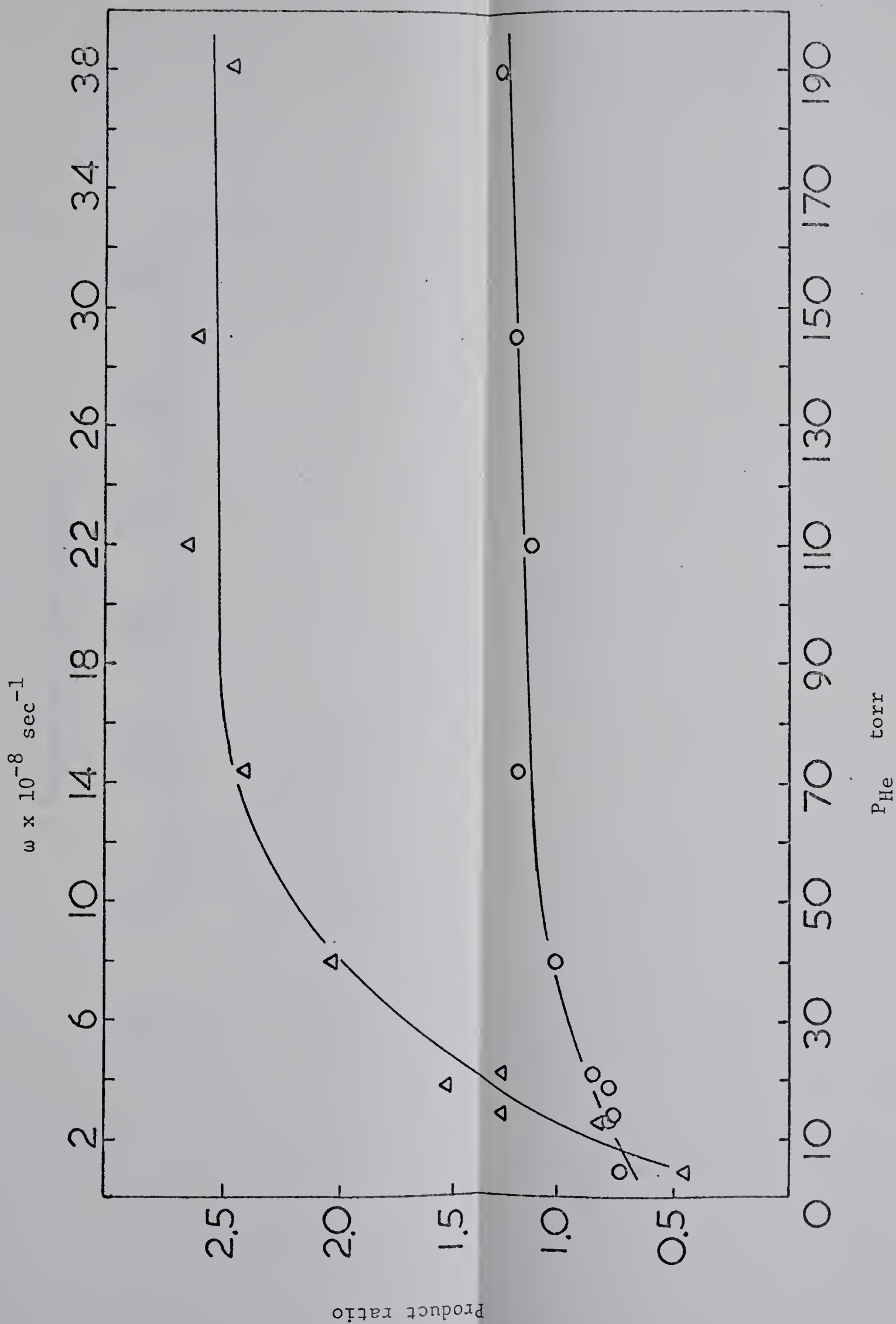


Figure 16. Product ratios as a function of pressure: (Δ) cyclopropane/propylene; (\circ) cis-butene/trans-butene.

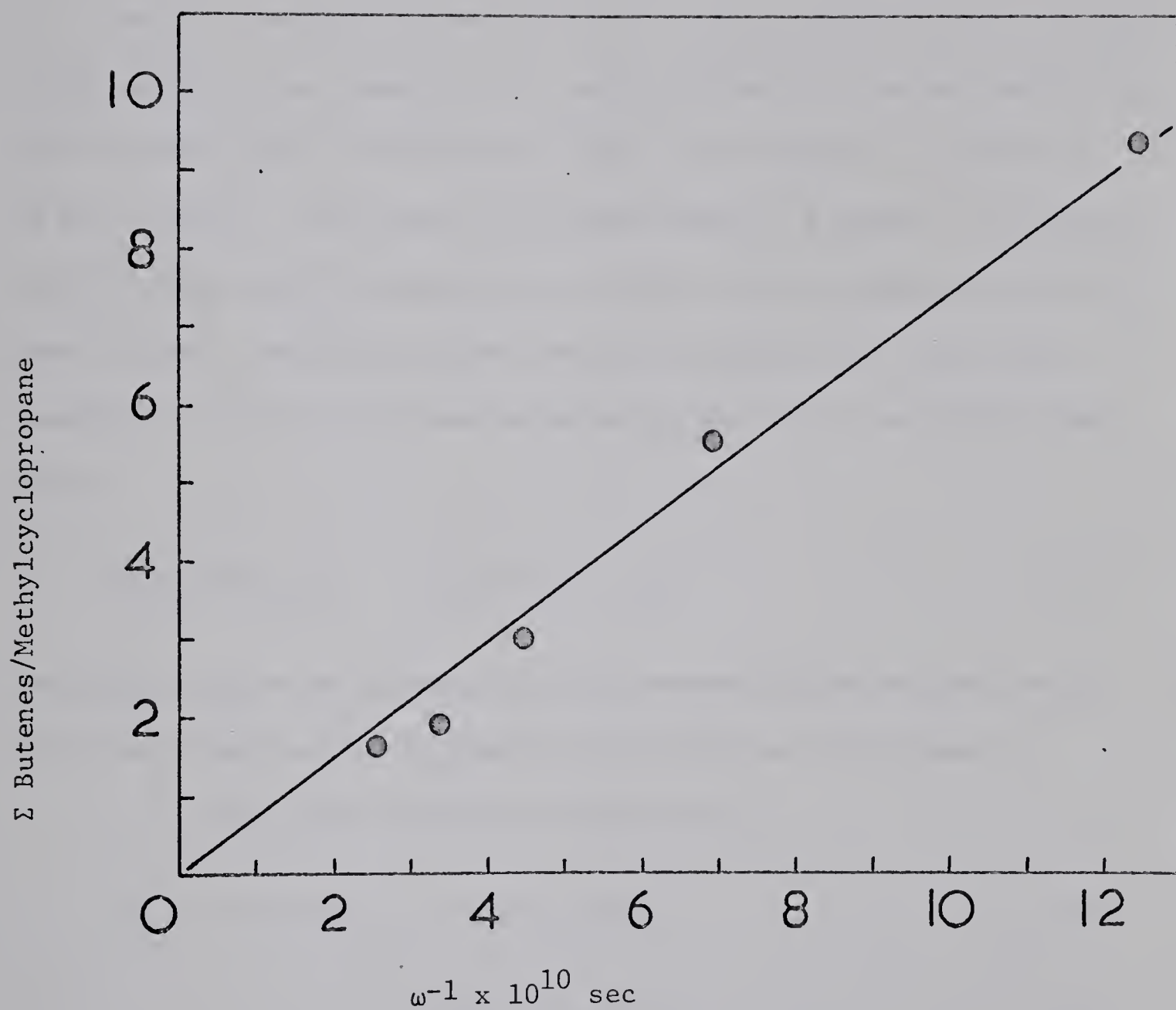
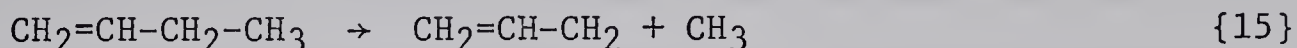


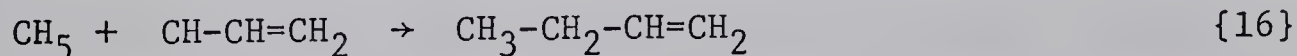
Figure 17. Butene/Methylcyclopropane ratios vs. ω^{-1} .

will be isomerized via reactions {8 - 10} to form isomeric butenes. Table XII and Figure 14 indicate the effect of pressure upon the product distribution.

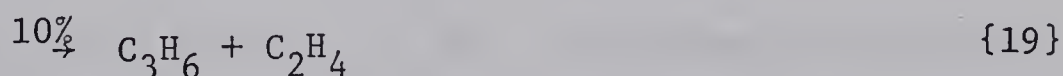
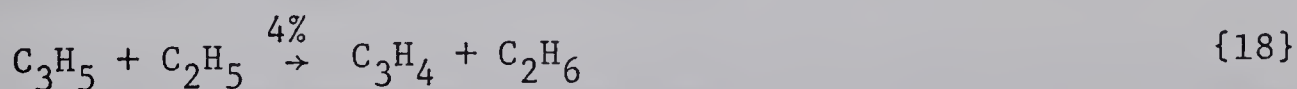
As the structural isomerization of methylcyclopropane to olefins is exothermic by at least 8 kcal mole⁻¹ depending upon the particular butene formed, the excited butenes will have energies in excess of 98 kcal mole⁻¹. The allylic C-C bond energy in 1-butene is reported to be 72 kcal mole⁻¹ (Appendix B). These factors indicate that unless ~26 kcal mole⁻¹ of excess energy is removed, the olefin can decompose by allylic C-C bond scission to give allyl and methyl radicals.



The disappearance of butene-1 by this process will be minimal as the allyl radicals produced by reaction {15} will be rescavenged as by the methyl radicals in the system.



A value for k_{17}/k_{16} has not been reported. A study of the allyl plus ethyl system yielded the following results (53).



Assuming a reaction of the following type does not occur,



a value of $k_{18}/k_{20} \sim 0.05$ should be quite close for the value of the disproportionation/recombination ratio of methyl with allyl radicals. In which case reaction {17} is unimportant.

Isobutene and cis- and trans-butene do not possess weak allylic C-C bonds thus their decomposition should be less important. Although, allylic C-H bonds are present in these molecules, they are ~ 10 kcal mole⁻¹ stronger than allylic C-C bonds and are less likely to break. Cleavage of these bonds would give a radical which if scavenged by methyl would be a C₅ olefin. The fact that pentenes were not detected indicates that this process is unimportant. Any decomposition products occurring by methyl cleavage would be rescavenged by methyl to give the original olefin.

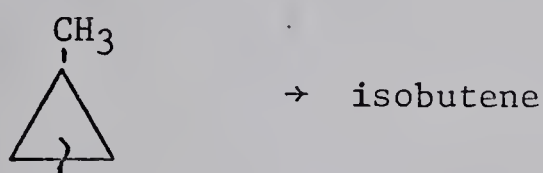
The assumption that the measured butene products are representative of the initially formed amounts seems to be valid. Figure 15 indicates that the relative amounts of 1-butene, cis- and trans-butene and isobutene are essentially constant over the pressure range studied.

2) Isomeric distribution of butene products:

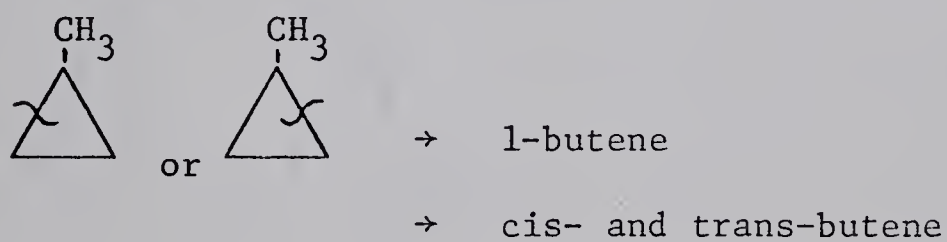
TableXIII contains the average values for the isomeric butene distribution relative to 1-butene as 100. Experimental data from several other investigations are also listed for comparison. All investigations indicate that isobutene is produced in significantly

smaller yields than either the 1- or 2-butenes. This is in agreement with the observation that the activation energy for the formation of isobutene is ~ 2 kcal mole⁻¹ higher than for the formation of the other butenes (51, 52).

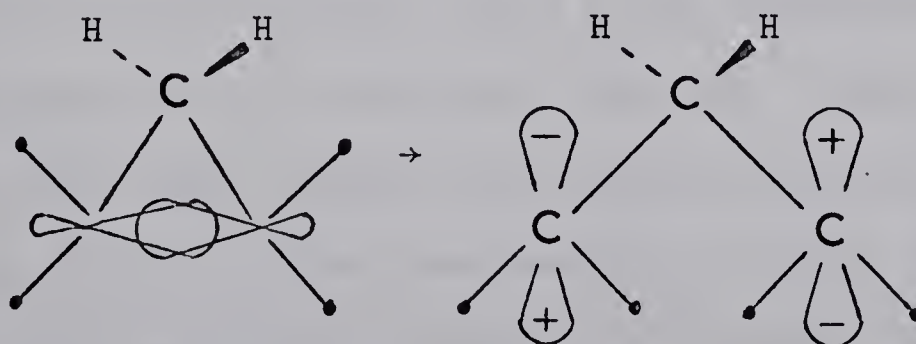
The formation of isobutene must arise from the rupture of the C-C bond directly opposite to the attached methyl group.



1-butene and the cis- and trans-butenes must result from cleavage of the C-C bond adjacent to the methyl group.

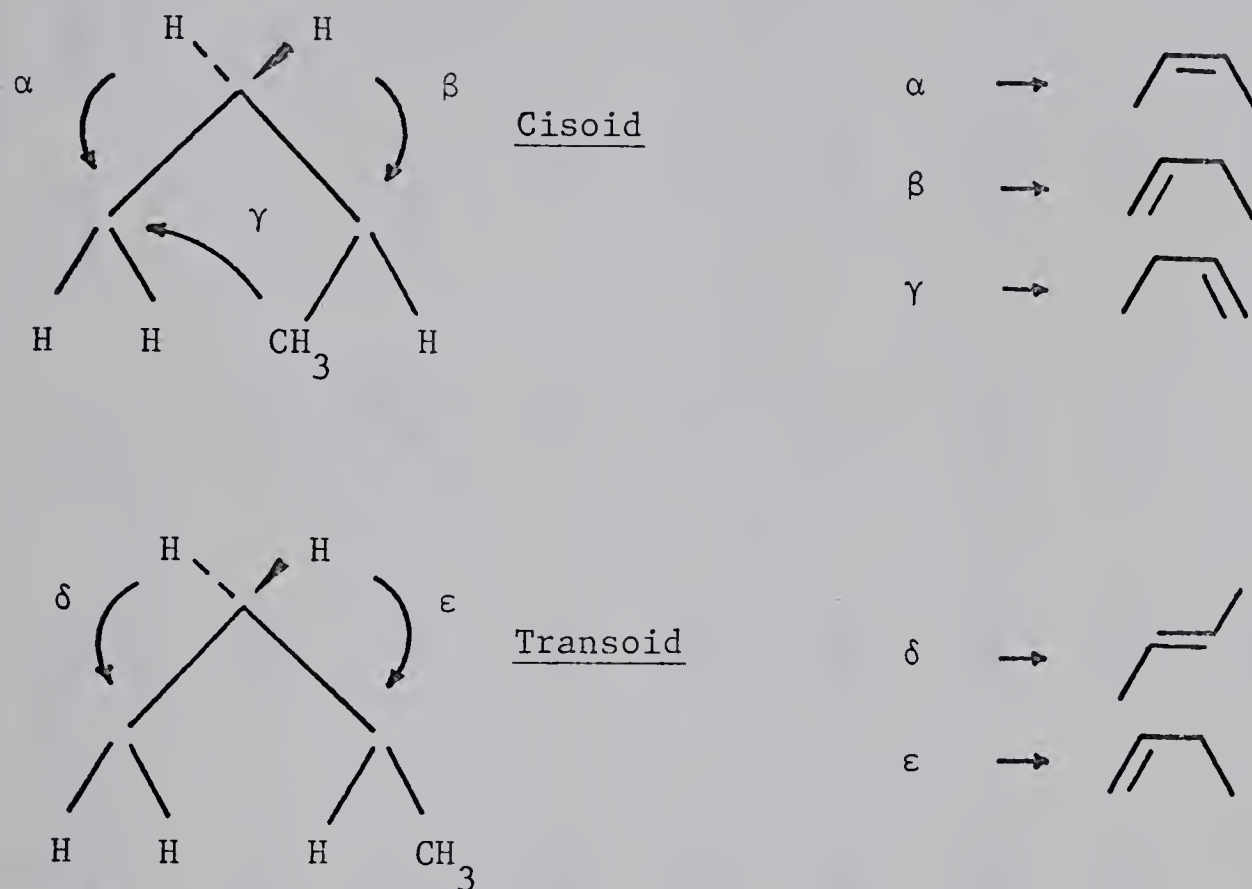


When the stereochemistry of the isomerization reaction is considered, an interesting feature arises. The ring opening step presumably takes place via a conrotatory mechanism in which an intermediate antisymmetric singlet state trimethylene species is formed (54, 55).



The present study cannot offer evidence to substantiate or disprove the conrotatory mechanism or the nature of the molecular orbitals

involved in the intermediate. Some information may be obtained about the position of the methyl group in the intermediate, however. The intermediate can have the following two structures each forming specific butenes upon hydrogen migration.



The cisoid structure gives only cis-butene and 1-butene as a result of H-atom migration, while the transoid structure gives trans-butene and 1-butene.

The results of the pressure study indicate that cis-butene is preferentially formed in the initial hydrogen transfer reaction. Unless collisional deactivation takes place, isomerization to the more stable trans- form will take place (Fig. 16). These results are in agreement with other studies which indicate a trend towards higher cis/trans ratios at higher pressures (44, 45, 51). On this basis, assuming equal probabilities for H-atom transfer via paths α , β , δ , and ϵ , the high pressure limit of the cis/trans ratio might appear to

TABLE XIII

Lifetime and energies of activated molecules and butene isomer distribution









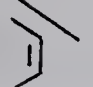
Source and Reference	Lifetime $1/k_t$ sec	E kcal/mole					$\sum \text{isomers} / \text{isoprene (ave.)}$
ΔCH_3 thermal (51)	8.3×10^{-7}	90	100	16	63	28	2.0
ΔCH_3 thermal (52)	-	-	100	18	72	30	2.4
$\text{CH}_2\text{N}_2 + \Delta$ (45)	2.3×10^{-10}	122	100	27	- 82 -	-	$1.05 \pm .21$
$\text{CH}_2\text{CO} + \Delta$ 3100 Å (45)	3.6×10^{-10}	119	100	31	- 116 -	-	$1.43 \pm .45$
$\text{CH}_2\text{CO} + \Delta$ 2600 Å (45)	4.9×10^{-10}	117	100	35	- 127 -	-	$1.22 \pm .35$
$\text{CH}_2\text{N}_2 + \text{C}_3\text{H}_6$ (45)	8.3×10^{-10}	115	100	42	- 122 -	-	$0.99 \pm .17$
$\text{CH}_2\text{CO} + \text{C}_3\text{H}_6$ 3100 Å (45)	1.7×10^{-9}	111	100	34	- 86 -	-	$1.20 \pm .22$
$\text{CH}_2\text{CO} + \text{C}_3\text{H}_6$ 2600 Å (45)	2.4×10^{-9}	109	100	21	- 72 -	-	$1.11 \pm .26$
ΔCF_3 thermal (56)	-	-	100	6.7	245	176	1.39

TABLE XIII

(Continued)

Source and Reference	Lifetime 1/k _t sec	E kcal /mole					 (ave.)
CH ₂ CO + CF ₃ -CH=CH ₂ 3200 Å (49, 50)	2.4 x 10 ⁻⁸	109	100	11	- 243	-	-
CH ₃ + Δ this work	2.3 x 10 ⁻⁹	97.8 a 110.4	100	20	32	27	1.2
		94.0 b 105.0					

(a) Calculated from equation {28} using E₀ = 61.4 kcal mole⁻¹ and A=10^{14.61} sec⁻¹ for s=15 and 18 respectively (52).

(b) Calculated from equation {28} using E₀ = 63.2 kcal mole⁻¹ and A=10^{15.45} sec⁻¹ for s=15 and 18 respectively (51).

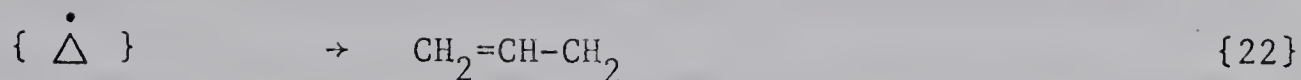
be a good approximation of the relative importance of the two intermediates. Unfortunately, hydrogen transfer from the methyl group complicates matters. An additional reaction producing 1-butene via γ , decreases the rate of butene production by α and β . Unless the importance of γ can be assessed, an estimate of the Cisoid/Transoid ratio cannot be made. It may be possible to obtain this information using CD_3 radicals as scavengers. 1-butene production via γ should then yield the isotopically labelled molecule $\text{CD}_2=\text{CH}-\text{CH}_2-\text{CH}_2\text{D}$. Formation of 1-butene by γ would not be a surprising reaction as hydrogen transfer here would proceed through a 5-membered ring mechanism. Investigations indicate that H-atom transfers are favored in the order 1, 4 > 1, 3 > 1, 2 (57 - 59). The results of the present study revealing a preponderance of 1-butene relative to 2-butene (cis & trans) suggests that an additional 1-butene forming step such as γ may be quite important.

When the results of the present study are compared with earlier studies (Table XIII), it is observed that 2-butene (cis & trans) is obtained in somewhat lesser relative amounts than previously measured.

There seems to be two possible explanations for the discrepancy.

- a) The mechanistic features and energetics of the reaction forming the excited methylcyclopropane via radical combination are such that the isomerization paths are altered.
- b) The experimental results are incorrect or not representative of the butene yields from the initial isomerization reaction.

For instance, if allyl radicals are formed as a result of excited cyclopropyl radical isomerization,



They would be scavenged as butene-1 by methyl radicals {16}.

An activation energy of $\sim 22 \text{ kcal mole}^{-1}$ has been estimated for reaction {22} (60). Carbon-bromine bonds are of the order of $\sim 70 \text{ kcal mole}^{-1}$ (33). Under the conditions of Hg $6(^3\text{P}_1)$ sensitization with the Hg^* atom possessing a total of $112 \text{ kcal mole}^{-1}$ electronic excitation energy, a reaction such as {22} may very well be possible. The fact that the relative butene ratios are reasonably constant over the entire pressure range studied (Fig. 15) seems to indicate that it is unimportant.

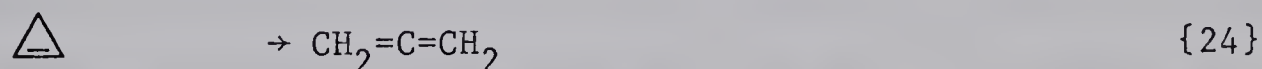
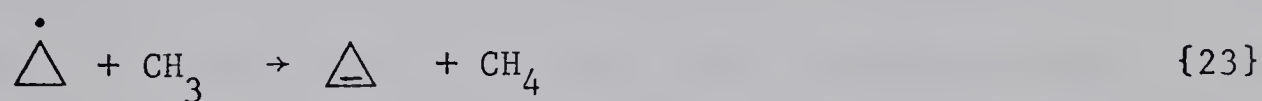
3) Miscellaneous products:

In addition to the methylcyclopropane and butenes discussed, the following products were detected, ethane, ethylene, propane, propylene, cyclopropane and allene. Trace quantities of an unidentified species were also detected.

Ethane can easily be explained as it undoubtedly arises from the recombination of two methyl radicals. The origin of the ethylene and propane is less certain. Ethylene and propane have been reported as products of the mercury sensitized decomposition of dimethyl mercury (29). These two products have also been reported in other cyclopropyl radical systems (60, 61) and until a more thorough investigation using $\text{Hg}(\text{CD}_3)_2$ as a source of methyl radicals is completed, the importance of these two products cannot be ascertained.

Figure 16 indicates that there is a relationship between the cyclopropane/propylene ratio and the pressure of the carrier gas. This ratio is observed to increase with increasing pressure. Propylene has been observed as a product of dimethyl mercury decomposition (29), cyclopropane is not. It should be mentioned here that acetylene, which is also reported to be a minor product of the decomposition of dimethyl mercury, has the same retention time as cyclopropane on the column used for separation. The product believed to be cyclopropane was trapped and analyzed by mass spectrometry. The results of this analysis showed that the major portion of the trapped sample was cyclopropane with a trace of acetylene. As each individual experiment was not analyzed separately for its cyclopropane and acetylene content the cyclopropane/propylene relationship cannot be considered definitely established and the trend illustrated in Figure 16 may only be fortuitous.

The detection of allene as one of the products was not surprising. Allene could conceivably come from the disproportionation reaction of methyl with cyclopropyl radicals.



If this assumption is correct, a value of 0.06 for the disproportionation to recombination ratio for methyl with cyclopropyl radicals via {23} can be obtained by taking the allene/C₄H₈ ratio (Table XII). The value of 0.06 seems to be reasonable and is identical to the measured value for methyl with n-propyl radicals.

4) Calculation of rate constants:

The rate constant for the total formation of butenes is $k_t = k_8 + k_9 + k_{10}$. The rate constant for collisional stabilization is $k_{11}M$. The following relationship can be used to account for the observed product ratios.

$$\frac{\text{butenes}}{\text{methylcyclopropane}} = \frac{k_t \{ \triangle - \text{CH}_3 \}^*}{k_{11}M \{ \triangle - \text{CH}_3 \}^*} \quad \{25\}$$

This expression simplifies to,

$$\frac{\text{butenes}}{\text{methylcyclopropane}} = \frac{k_t}{k_{11}M} = \frac{k_t}{\omega\lambda} \quad \{26\}$$

where ω is the gas kinetic collision frequency and λ is the efficiency of the deactivating gas. ω can be calculated using the gas kinetic expression (Appendix C). Values for the collision efficiency of helium are less certain however, the only relevant value being the one obtained by Chesick (51), indicating an efficiency of 0.07 - 0.05 relative to methylcyclopropane.

Figure 17 is a plot of butenes/methylcyclopropane vs. ω^{-1} . From expression {26} the slope of this line will be equal to k_t/λ . A least-mean-squares calculation with the origin weighted so that the straight line would pass through it gives a value of $k_t/\lambda = 7.4 \times 10^9 \text{ sec}^{-1}$. Using a value of 0.06 for λ , a value of $4.44 \times 10^8 \text{ sec}^{-1}$ is obtained for k_t . If the preceeding assumptions are correct, a lifetime, $1/k_t = 2.25 \times 10^{-9} \text{ sec}$ is obtained for the activated methylcyclopropane molecule. Rate constants for the specific butenes can be obtained from the following relationship.

$$\frac{(C_4H_8)_i}{\text{total butene}} = \frac{k_i}{k_t} \quad \{27\}$$

These values are,

$$k_8 = 0.50 \times 10^8 \text{ sec}^{-1}$$

$$k_9 = 2.48 \times 10^8 \text{ sec}^{-1}$$

$$k_{10} = 1.46 \times 10^8 \text{ sec}^{-1}$$

From the simplified Rice-Ramsperger-Kassel relation

$$k_t = A \left\{ 1 - \frac{E_0}{E} \right\}^s \quad \{28\}$$

where A is the frequency factor for isomerization, E_0 the critical energy necessary for isomerization, and s the number of effective oscillators, a value for E the excitation energy of the methylcyclopropane can be calculated. E_0 has been estimated as $\sim E_a - 1.8 \text{ kcal mole}^{-1}$. (56). The Arrhenius parameters from both studies of the thermal isomerization of methylcyclopropane (51, 52) were used to calculate E and the results are tabulated in Table XIII.

As a comparison, the excess energy can be calculated in another manner using the following relationship.

$$E = \Delta H_7 + E_{\text{ex}} + sRT \quad \{29\}$$

ΔH_7 is the exothermicity of the reaction ($88 \text{ kcal mole}^{-1}$), E_{ex} is the excess energy of the radicals (assumed = 0) and sRT is the thermal energy.

For $s = 15$ and $T = 330^\circ \text{ K}$

$$E_{(s=15)} = 97.9 \text{ kcal mole}^{-1}$$

$$\text{For } s = 18, E_{(s=18)} = 99.9 \text{ kcal mole}^{-1}$$

Considering the approximate nature of the calculations, the agreement between the two methods {28} and {29} is quite reasonable.

5) Evaluation of the technique:

The preliminary results of the study of the unimolecular decomposition of excited methylcyclopropane are encouraging. With refinements in the technique and apparatus the study of chemically activated species using the mass spectrometric method should yield valuable and interesting data.

The use of CD_3 radicals as scavengers could yield data concerning the secondary deuterium isotope effect, as well as establish the origin of some of the miscellaneous products observed. An investigation using perdeuterated methyl radicals could also offer some evidence concerning the nature of the transition complex (Cisoid or Transoid). This study could also yield some information about the effect of isotopic substitution on the reaction.

The study of the unimolecular decomposition of trifluoromethylcyclopropane could be studied in a similar manner by simply employing CF_3 radicals as scavengers (perfluoro acetone or perfluoro azomethane). Using suitable radical sources the reactions of a series of chemically activated species could be investigated.

CHAPTER V

THE PHOTOCHEMISTRY OF SILICON COMPOUNDS

RESULTS

- 1) Flow System (Hg $6(^3P_1)$ photosensitization).
- 2) Static Photolysis.

DISCUSSION

Hg $6(^3P_1)$ PHOTSENSITIZATION.

- 1) The Decomposition of Benzene, Toluene and Phenylsilane- d_3 .
- 2) Secondary Reactions.

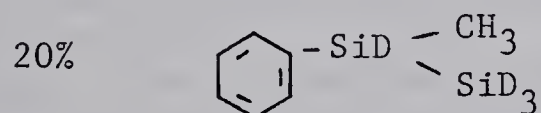
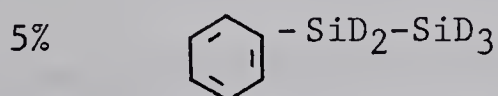
THE PHOTOLYSIS OF PHENYLSILANE- d_3 .

- 1) 2700 Å Photolysis.
- 2) Summary and Comparison with Benzene and Toluene.
- 3) The Reactions of Silicon Containing Free Radicals.

RESULTS1) Flow system (Hg $6(^3P_1)$ photosensitization):

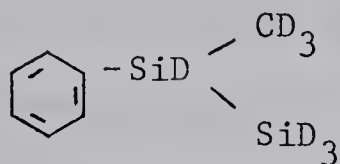
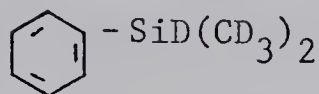
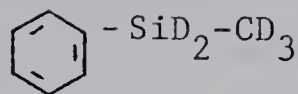
Phenylsilane- d_3 was decomposed in the fast-flow system at low reactant pressures with the aim of determining the primary processes involved in the Hg-sensitization reaction. The majority of these experiments were carried out using an excess of methyl radicals generated from the photosensitized decomposition of dimethyl mercury. The purpose of these experiments was to trap the intermediate silicon containing free radicals with methyl radicals.

Four products having a greater molecular weight than phenylsilane- d_3 were detected. A rough estimation of their importance is.



Typical reaction conditions were 0.25 to 1.0 mtorr of phenylsilane- d_3 , and 12 to 25 mtorr of Hg(CH₃)₂ in 10 torr of He carrier gas.

These products were identified by trapping out the desired products after separation by gas chromatography and submitting the samples for analysis by mass spectrometry. The use of dimethyl mercury- d_6 as a source of methyl- d_3 radicals was also employed. This technique also helped with the analysis of the products of the reaction, giving the analogous products.



Toluene was also detected but due to interference from the phenylsilane- d_3 an estimation of its importance could not be made by G.L.C. . A direct mass spectrometric measurement of the toluene formed in the reaction was made by sampling the reaction mixture after exposure to the radiation. The result of this measurement indicated that a maximum of 30% of the decomposition products terminated as toluene. Small quantities of benzene were also detected.

A surprising feature of the reaction was the absence of methylsilane. Although a thorough investigation was carried out with the specific purpose of detecting methylsilane, none could be found. The only appreciable non-aromatic silicon containing product observed was trimethylsilane. Trace quantities of di- and tetramethylsilane were detected.

Experiments were also carried out in the flow system using phenylsilane- d_3 as the only reactant. The main products detected under these conditions were $\text{C}_6\text{H}_5\text{D}$ and $\text{C}_6\text{H}_5\cdot\text{Si}_2\text{D}_5$. Of these two products, $\text{C}_6\text{H}_5\text{D}$ was the larger by a factor of about four. A small amount of product distilling at -98°C was collected and a very weak mass spectrum indicated that SiD_4 and Si_2D_6 may have been present. Disilane, if present is a very

minor product and the majority of the silyl radicals must end up as monosilane, $C_6H_5Si_2D_5$ or polymer. An estimate of monosilane could not be made by G.L.C. as the vapor pressure of the monosilane at liquid nitrogen temperature is greater than that existing under the reaction conditions employed. The D_2 from the reaction could not be measured due to the helium used as the carrier gas. An attempt to measure the D_2 with the mass spectrometer, using 20 ev as the electron accelerating voltage so as not to ionize the helium, was unsuccessful due to the loss of sensitivity at this lower energy. The only other deuterium containing products observed in the reaction were small amounts of HD and CH_3D . In all of these experiments a polymer film was deposited on the wall of the reactor. The polymer buildup was reduced in experiments using methyl radicals as scavengers as compared to the decomposition of the phenylsilane- d_3 alone. It was found that as in the study by Niki and Mains (17), some of the polymer could be removed by generating hydrogen atoms in the reaction zone.

2) Static photolysis:

Phenylsilane- d_3 was photolyzed at $150^\circ C$ and 42 ± 2 torr in the reactor shown in Figure 7. Light intensity measurements were made by 3-pentanone actinometry at 40 torr and $150^\circ C$ (62). The light source was equipped with a filter (Baird-Atomic 2850 Å interference filter) which transmitted radiation of wavelength between 2650 and 3100 Å.

The products detected from the photolysis reaction were, monosilane- d_4 , benzene (C_6H_6 , C_6H_5D), phenyldisilane- d_5 and small amounts of isotopic hydrogens (H_2 , HD, D_2). The hydrogen appears to arise from a dark reaction. Phenylsilane- d_3 decomposes slowly at room temperature the only

detectable product being hydrogen. A dark reaction was in fact carried out and the hydrogen yield as well as the isotopic distribution support this assumption.

Disilane was specifically looked for in all of the experiments. It appeared to be absent from all runs except for one (Run No. 5) in which a very small amount of product was isolated which gave a mass spectrum indicative of Si_2D_6 . This was detected in one of the reactions in which the total decomposition was the highest and may be a product of the secondary photolysis of phenyldisilane $-\text{d}_5$.

Table XIV summarizes the results of experiments in which quantum yield measurements were carried out. The quantum yield of phenyldisilane $-\text{d}_5$ is not included in the table for two reasons. First of all a standard sample of the material was not available for calibration purposes and secondly, in all experiments it was detected only in trace quantities as a shoulder on the phenylsilane $-\text{d}_3$ tail of the G.L.C. spectrum.

In addition to the experiments described in Table XIV the following two were carried out. Reaction conditions were the same (150°C ; 42 ± 2 torr phenylsilane $-\text{d}_3$) except for the addition of mono- and disilane.

Monosilane (150 torr SiH_4) was added to one of the photolysis experiments. Careful analysis of the products from this run revealed a small but easily detectable amount of disilane product which appeared to have the composition $\text{Si}_2\text{H}_4\text{D}_2$.

Disilane (50 torr Si_2H_6) was also added to the photolysis system. Four main products were detected. Monosilane (mostly SiD_3H , also SiD_4

and SiH_3D) benzene (almost exclusively C_6H_6), trisilane (Si_3H_8) and some phenyldisilane ($\text{C}_6\text{H}_5\cdot\text{Si}_2\text{H}_5$). The benzene/monosilane ratio measured for this experiment was 0.30. This is several times higher than that measured in the pure phenylsilane- d_3 system (Table XIV) and indicates that in the presence of a readily abstractable hydrogen source a larger portion of the phenyl radicals will terminate as benzene.

TABLE XIV

Photolysis of phenylsilane -d₃.

Run	Irradiation time (min.)	Φ_{SiD_4}	Φ^* benzene
1	240	0.83	0.03
2	232	0.79	0.07
3	300	0.71	0.06 300 torr N ₂ added.
4	275	0.73	--- 284 torr CO ₂ added.
5	275	0.71	--- 1039 torr CO ₂ added.
6	275	0.73	---
		ave. = 0.75	

Photolysis conditions were 150° C and 42 ± 2 torr of phenylsilane -d₃.

* Benzene fraction consisted of C₆H₆ and C₆H₅D.

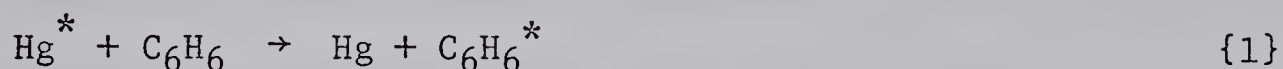
DISCUSSION

Hg 6(³P₁) PHOTSENSITIZATION

1) The decomposition of benzene, toluene and phenylsilane -d₃:

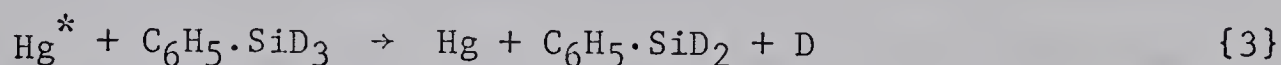
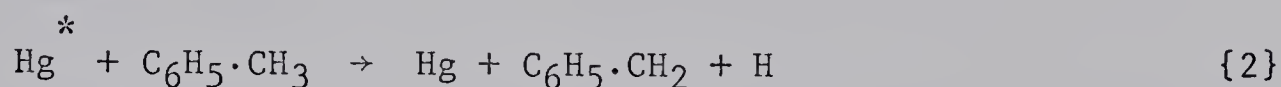
Mercury 6(³P₁) atoms are known to be electrophilic reagents in their reactions. The large quenching cross sections for benzene and toluene (Appendix A) offer proof that the aromatic ring with its large density of π -electrons is quite efficient in quenching electronically excited Hg 6(³P₁) atoms.

Quenching into this system should give an electronically excited triplet species with an excess energy content of 112 kcal mole⁻¹ (63).



For benzene this species will be the first excited triplet state with ~29 kcal mole⁻¹ of translational, rotational and vibrational energy (64). Although the 112 kcal mole⁻¹ obtained in the transfer reaction is probably not sufficient to rupture the carbon-carbon bonds in the resonance stabilized aromatic ring, it is more than the 103 kcal mole⁻¹ required to break the C-H bonds (Appendix B). In substituted benzenes such as toluene, C-C bonds are available with even lower bond strengths; D(C₆H₅-CH₃) = 93 kcal mole⁻¹; {Appendix B}. Unless this energy is dissipated through some type of radiative or nonradiative photophysical process or processes (processes which do not lead to chemical change) photochemical reactions should occur (bond rupture, isomerization, etc.).

In the mercury sensitized reactions of substituted benzenes such as toluene and phenylsilane -d₃ a second primary process is possible, that of reaction with the C-H or Si-D bonds of the side chain.



Quenching at this site should result in immediate C-H or Si-D cleavage.

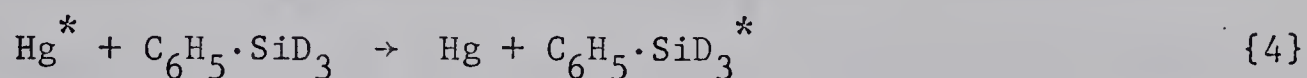
The results of this study point out some of the substantial differences between the mercury sensitized reactions of alkyl and silyl substituted aromatic compounds.

Very little decomposition is observed in the mercury sensitized reaction of benzene at 2537 Å (65 - 67). Practically no reaction is detected at 25° C. At 400° C the disappearance of benzene is more pronounced with the appearance of biphenyl as the major product, its quantum yield being $\phi_{\text{biphenyl}} = 0.1$ (67). Other, more volatile products observed are H₂, CH₄, C₂H₆, C₂H₄, C₃H₆ and C₃H₈. The latter study also offers some evidence for an excited molecule mechanism in that an increase in pressure caused a decrease in product yields.

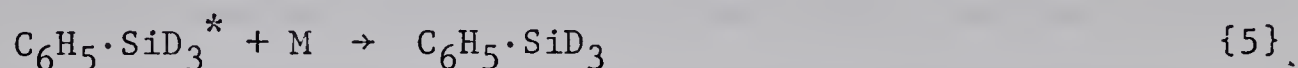
Toluene also appears to be stable at ordinary temperatures (68). At 150° C $\phi_{\text{H}_2} = 5 \times 10^{-4}$, but at 400° C $\phi_{\text{H}_2} \approx 0.1$. Other products include CH₄ and C₂H₆. The pressure dependence of the product yields in this case also suggests that an excited molecule is formed in the primary quenching act with a Hg 6(³P₁) atom.

In this study, phenylsilane -d₃ was observed to undergo extensive decomposition in its reactions with Hg 6(³P₁) atoms. The extent of decomposition as measured directly by the mass spectrometer ranged from 4.5 to 25% per single pass, depending upon the condition of the reaction zone.

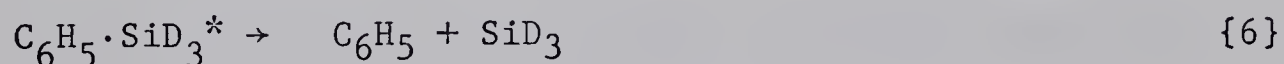
The two primary processes occurring in the initial quenching act appear to be quenching into the Si-D bonds of the side chain {3} and interaction with the aromatic ring.



Reaction {3} should lead to immediate Si-D bond cleavage, while the excited species produced by reaction {4} should have alternative possibilities. For example, it may be collisionally deactivated,



or it may decompose.



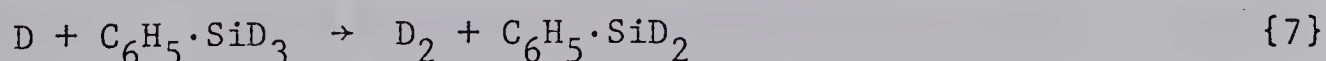
In this instance decomposition should occur via rupture of the C-Si bond. The reason for this being that it is probably the weakest bond in the molecule.

The quenching cross section of phenylsilane -d₃ has not been measured. An intuitive estimation of the relative quenching by the silyl and phenyl groups in the molecule can be made using the quenching cross sections for SiD₄ and benzene of 46.7 and 73.3 Å² respectively (Appendix A). From these values one would expect a 2 to 1

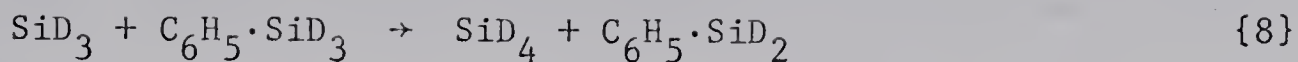
ratio in favor of reaction with the aromatic ring. Other factors should be taken into account however. Although carbon is more electronegative than silicon and should withdraw electrons into the ring, evidence for d-orbital participation in which the π -electron density in the benzene ring is withdrawn into empty d-orbitals of silicon has been found. A spectroscopic experiment has definitely confirmed that the $-\text{SiH}_3$ group withdraws electron density into the 3d-orbitals of silicon from the benzene ring (27). These factors should increase the quenching at the $-\text{SiD}_3$ site. This effect is quite small however, and the major reaction should still occur at the aromatic site.

The results of the flow-system using methyl radicals as scavengers indicate that the major portion of the recoverable products require Si-D cleavage. This, plus the fact that a maximum of 30% of the decomposition products terminated as toluene, suggests that the major reaction occurs at the Si-D position.

At the time of this study however, a parallel investigation of the sensitization reaction at 110°C was conducted in a static system (69). The results of this study indicated a quantum yield of decomposition near unity with $\Phi_{\text{D}_2} \approx 0.30$ and $\Phi_{\text{SiD}_4} \approx 0.70$. Assuming that the deuterium yield reflects the quenching at the Si-D site; reaction {3} followed by



and the SiD_4 represents the extent of reaction with the aromatic system; reaction {6} followed by

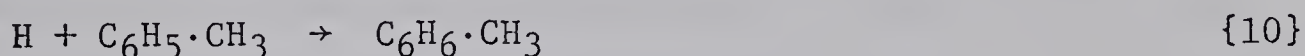
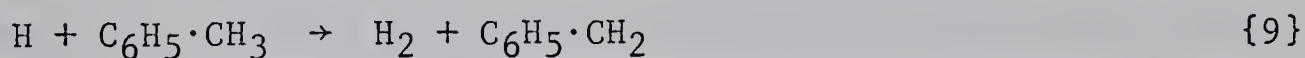


A ratio of ~ 2:1 in favor of quenching at the aromatic site results. This is consistent with the expected results based upon relative quenching abilities. In view of the poor mass balance achieved in the flow system experiments, the data obtained from the static system is probably more reliable in this respect. In addition to the above mentioned products, small amounts of benzene and phenyldisilane -d₅ were also detected. In no instance was disilane detected as a product. A pressure study was also carried out in this investigation. It was found that increasing the total pressure of the substrate to 160 torr had no effect on the quantum yield of decomposition.

The most obvious difference between the reaction of Hg 6(³P₁) atoms with the silyl substituted benzene and benzene and toluene is the greater efficiency of decomposition in the first system. A reason for the apparent high stability of benzene and toluene has not been offered. Radiative decay by phosphorescence from the first triplet state to the ground state singlet ($T_1 \rightarrow S_0 + h\nu$) does not appear to be an important process as attempts to observe phosphorescence from the triplet state of benzene in the gas phase have not been successful. It seems likely that the energy is dissipated through collisional deactivation or perhaps the energy rich molecules undergo geometrical isomerization reverting to the original compounds upon deactivation. Delayed fluorescence resulting from triplet - triplet annihilation ($T_1 + T_1 \rightarrow S_1 + S_0$; $S_1 \rightarrow S_0 + h\nu$) has been reported to appear from the vapors of anthracene, perylene, phenanthrene and

pyrene (70). Similar evidence for benzene and toluene has not been reported.

In toluene the strength of the β -hydrogen of the side chain $D(C_6H_5 \cdot CH_2 - H) = 85 \text{ kcal mole}^{-1}$ while $D(C_6H_5 - CH_3) = 93 \text{ kcal mole}^{-1}$ (71). The weakening of the β C-H bond and the strengthening of the C-C bond apparently results from the resonance stabilization of the benzyl radical. In this respect it seems strange that an electronically excited triplet toluene molecule does not undergo more efficient cleavage at the β -hydrogen or C-C phenyl-methyl bond. The 112 kcal mole^{-1} transferred in the reaction by quenching at the aromatic group is more than sufficient to cause bond cleavage. Although some hydrogen is reported to be formed in the reaction, it may arise from quenching at the side chain {2}. The fact that greater yields of hydrogen are observed at higher temperatures may very well be due to more effective competition of the abstraction reaction {9} with the addition reaction {10} at higher temperatures.



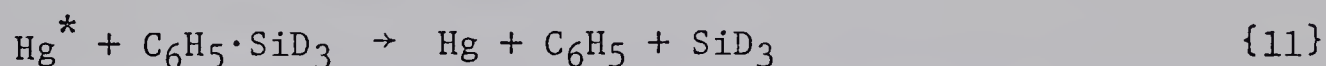
Bond energy data is not available for phenylsilane at the present time. The C-Si bonds for a series of methylsilanes have been measured and are reported to be between 77 and 79 kcal mole^{-1} (72). Using these values as a rough guide to the C-Si bond strength in phenylsilane, with the realization that the reported d-orbital participation should cause a slight strengthening, a bond energy of about 80 kcal mole^{-1} is estimated. The bond strength in monosilane is

reported to be 95.2 kcal mole⁻¹ (73). Taking this as the Si-D bond strength in phenylsilane-d₃ with the realization that d-orbital participation should weaken this bond while deuterium substitution should strengthen it, it is observed that the C-Si and not the β-hydrogen bond is the weakest in the molecule.

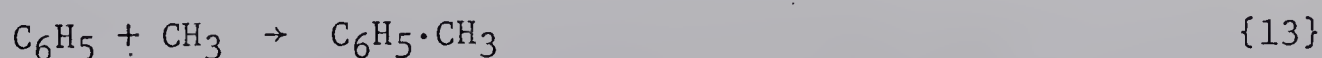
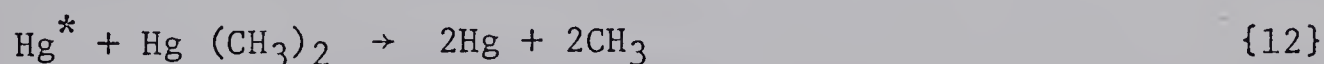
The presence of this relatively weak bond (~80 kcal mole⁻¹) at this position in the molecule seems to be responsible for the great difference in stability between toluene and phenylsilane -d₃ towards Hg 6(³P₁) sensitization. Although the β-hydrogen in toluene is also relatively weak, its position appears to be sufficiently remote from the quenching site to allow deactivation before decomposition occurs.

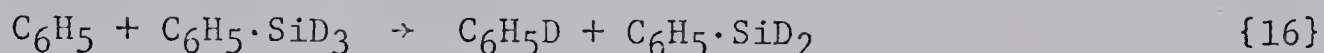
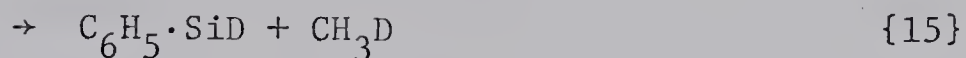
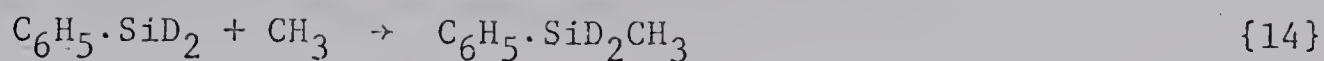
2) Secondary reaction:

Assuming that reactions {3} and {6} are the processes leading to decomposition of the phenylsilane-d₃ molecule, analysis of the final products should yield some information about the reactivity of silicon containing free radicals. It should be mentioned here that in the absence of evidence for an excited molecule in the phenylsilane -d₃ reaction the primary decomposition may be better written as;

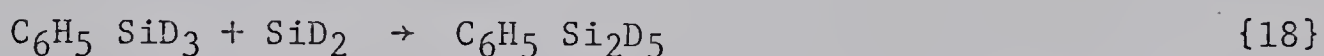
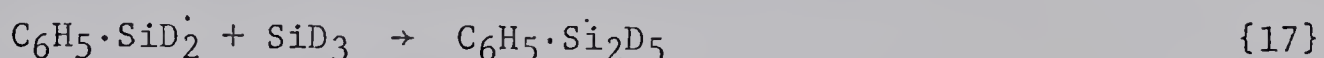


Some of the products are readily explained while only speculation can be offered for the formation of others. The following reactions are proposed for the formation of the observed products.

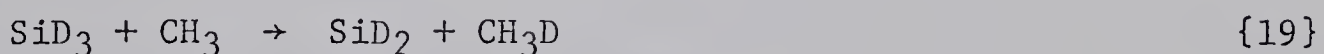




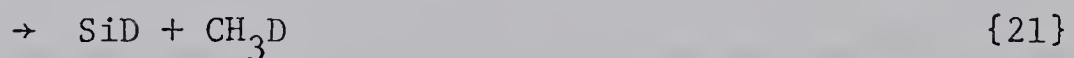
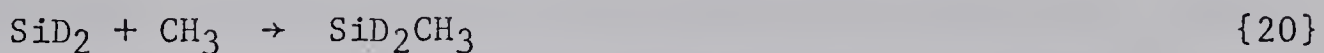
Phenyldisilane-d₅ can be formed by two processes.



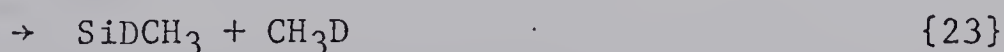
Methylsilane -d₃ was not detected as a reaction product. It appears that silyl radicals disproportionate rather than combine with methyl radicals.



The formation of small amounts of dimethyl- and trimethylsilane is difficult to explain. The SiD₂ radical formed via {19} may combine or disproportionate with another methyl radical;

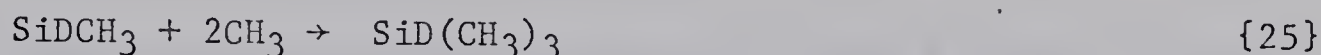


The radical formed by {20} can again recombine or disproportionate with additional methyl radicals;

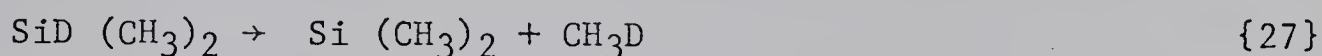


Trimethylsilane -d₁ could then be formed by methyl recombination

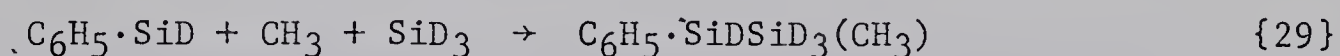
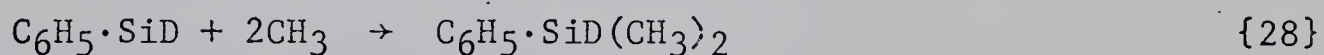
with the radicals formed in reactions {21} and {23}.



A trace quantity of tetramethylsilane was detected, indicating that removal of the last deuterium probably occurs also;



The formation of dimethylphenylsilane -d₁ and 1,1-methylphenyldisilane -d₄ cannot be readily explained and only the two general reactions are offered.

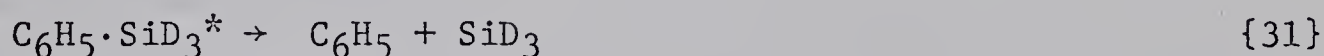
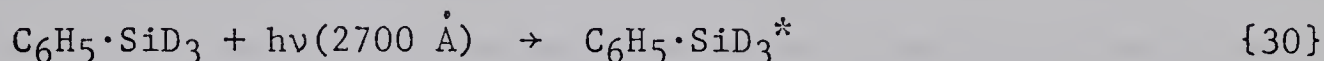


The large number of di-, tri- and tetramethyl silicon containing compounds observed indicate that silicon containing free radicals disproportionate to a much greater extent than alkyl radicals. When alkyl radicals disproportionate two stable molecules are produced, an alkane and an olefin. The inability of silicon to form double bonds produces a situation in which a stable molecule and a radical species are produced. It appears that this radical species is capable of undergoing further disproportionation in reactions of the type proposed in {21, 23 and 26}.

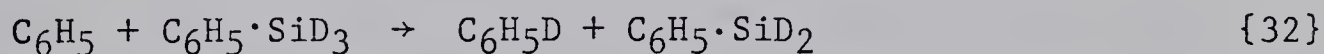
THE PHOTOLYSIS OF PHENYLSILANE -d₃1) 2700 Å photolysis:

The photolysis of phenylsilane -d₃ at 2700 Å offers a system in which the reactions of this molecule in its first excited singlet state can be studied. Unlike benzene and toluene, which reportedly do not undergo visible decomposition from their first excited singlet state when photolyzed at 2537 Å (66, 74), phenylsilane -d₃ decomposes readily.

The photolytic decomposition of phenylsilane -d₃ should take place via the following scheme.

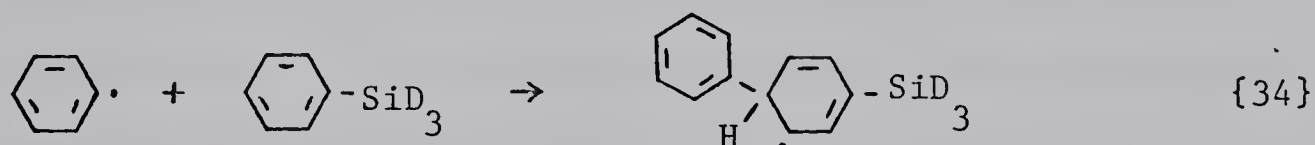


The radicals formed by reaction {31} should abstract a hydrogen or deuterium from the substrate to give benzene and mono-silane, in which case their yields should be equal.



From the data in Table XIV an average value of $\phi_{\text{SiD}_4} = 0.75$ is obtained. If the phenyldisilane -d₅ contribution, and the loss due to disproportionation and polymer formation were taken into account ϕ_{decomp} would most probably be unity.

Examination of Table XIV indicates that ϕ_{benzene} is very low and is not even remotely comparable to ϕ_{SiD_4} . This is rather disturbing and no satisfactory explanation can be given for this observation at the present time. In the presence of a readily abstractable hydrogen source such as disilane, a noticeable increase in the benzene/monosilane ratio was observed. This indicates that if conditions favorable for hydrogen atom abstraction are employed, the competitive reaction for phenyl radical disappearance can be minimized. The C-H bond in benzene is reported to be 103 kcal mole⁻¹. At 150° C and the low light intensity conditions employed ($I_0 \sim 1.7 \times 10^{-10}$ einsteins cm⁻²) abstraction from the -SiD₃ group should be the dominant reaction. The experimental results indicate that the competitive reaction is ~ 20 times faster. The only reaction which could offer competition of such magnitude would be addition to the aromatic ring.

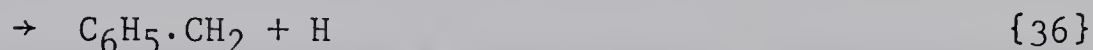
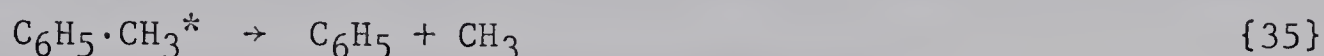


This reaction would give a cyclohexadienyl radical which would then abstract hydrogen or deuterium or recombine or disproportionate with other radicals. There is some evidence for reaction with the ring in that the benzene detected consisted of C₆H₅D and C₆H₆.

2) Summary and Comparison with benzene and toluene:

As mentioned previously, benzene and toluene do not undergo significant decomposition when irradiated in the first singlet absorption band at 2537 Å. When photolyzed in their second and third absorption bands at ~ 2000 and 1850 Å respectively, photochemical reactions occur with a quantum yield of decomposition approaching unity (74,75).

Two of the primary steps proposed (74,76) in the decomposition of toluene at the shorter wavelengths ($\lambda < 2200 \text{ \AA}$) are,



Phenylsilane $-\text{d}_3$ undoubtedly decomposes in a reaction analogous to {35} when irradiated at 2700 \AA . There does not appear to be any evidence for β -hydrogen fission in a reaction parallel to {36}. Although small amounts of isotopic hydrogens are observed, they most likely originate from a dark reaction. From bond energy estimations made earlier in this chapter the Si-D bond in this molecule is probably stronger than the C-Si bond making deuterium elimination less likely.

For benzene and toluene, emission is not observed in the gas phase when excitation to the second or third singlet states occurs (77). Fluorescence has been observed from benzene when irradiated in its first absorption band (63,78).

The results of this study indicate that emission from the first excited singlet state of phenylsilane $-\text{d}_3$ will not be observed. The first excited singlet state of this molecule must be very short lived with respect to decomposition as inert gas pressures up to 1039 torr failed to decrease the quantum yield of SiD_4 significantly (Table XIV).

3) The reactions of silicon containing free radicals:

The following phenomena are features distinguishing the reactions of silyl radicals from alkyl radicals.

a) Methylsilane is not observed as a product from the mercury

sensitized co-decomposition of dimethyl mercury and phenylsilane -d₃.

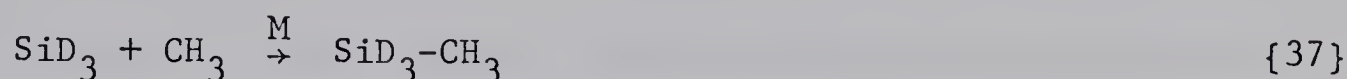
- b) Disilane is not a final product of the mercury sensitized decomposition of phenylsilane -d₃ in a static system (69).
- c) Disilane is not observed in the 2700 Å photolysis of phenylsilane -d₃.

At the present time, insufficient data is available to explain these observations. It seems likely, however, that bond energy considerations may be important.

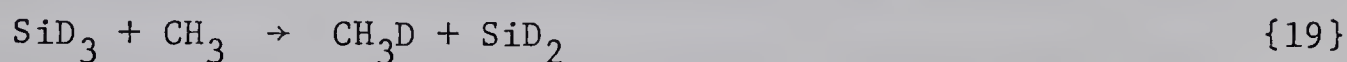
Bond energy data for monosilane is incomplete and discrepancies exist for that which is available. Reported values for the average Si-H bond energy in monosilane range from 72.6 to 79 kcal mole⁻¹ (79 - 81). The latest values for ΔH_f and the average Si-H bond energy in SiH₄ are 7.8 and 72.6 kcal mole⁻¹ respectively (81). The latest value for D(SiH₃-H) is 95.2 kcal mole⁻¹ (73) and D(Si-H) is reported to be 74.6 kcal mole⁻¹ (82). This leaves 120.6 kcal mole⁻¹ for the second and third Si-H bond energy. At the present time these last two mentioned bond strengths are not known. The only guide to these values is given in a theoretical paper by Jordan (83), in which the lower electronic levels of the SiH, SiH₂ and SiH₃ radicals and their mean bond energies are calculated. This treatment proposes that the mean bond energy in SiH₂ is the greatest, while those in SiH₄ and SiH are only slightly lower. If this is the case, D(SiH-H) would have to be at least 74.6 kcal mole⁻¹ leaving a maximum D(SiH₂-H) = 46 kcal mole⁻¹. This implies that SiH₂ is very easily formed.

A bond energy scheme of this nature could explain the failure to detect methylsilane as a reaction product. For example, if a silyl

and a methyl radical were to collide with each other, the possibility of combining to form methylsilane if collisionally stabilized should exist.

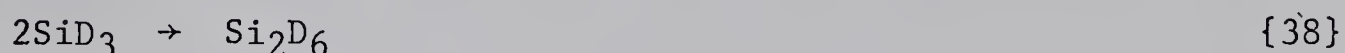


The bonding scheme previously mentioned however, suggests that the exothermicity of the disproportionation reaction



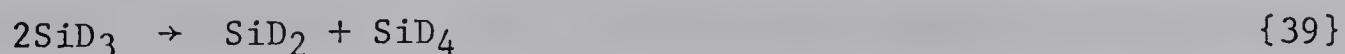
would be at least 58 kcal mole⁻¹. In view of the low pressures used in the experiments with the flow system and the predicted stability of the SiH₂ radical, reaction {19} may be favored as the major process under the conditions employed.

The absence of disilane as a product of the static photolysis and sensitization reactions imply that silyl radicals do not recombine.



It should be mentioned here that the slow generation of silyl radicals in the photolysis system would favor reaction with the substrate via abstraction to give SiD₄. The non-occurrence of disilane in this instance is not conclusive proof that silyl radicals do not recombine. The radical concentrations in the sensitized reaction should be much higher and the fact that disilane is absent here as well, offers proof that reaction {38} does not occur.

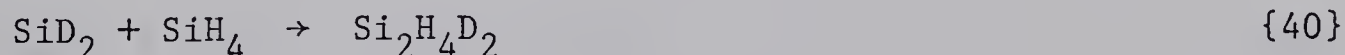
If the bond energy estimates are correct, the exothermicity of a disproportionation of the type



would be at least 39 kcal mole⁻¹. Under these circumstances, disproportionation reactions such as {39} may be the major processes.

Because of their hydridic character, Si-H bonds appear to be much more susceptible towards insertion reactions than C-H bonds. Dimethylsilene $\{:\text{Si}(\text{CH}_3)_2\}$ has been postulated to show a preference for Si-H bond insertion (84). A study of methylene insertion into the Si-H bonds of phenylsilane in diethyl ether solution indicates that Si-H insertion is very rapid compared to C-H insertion (85). Methylene has also been found to insert readily into the Si-H bonds of monosilane (86) and methylsilane (87). Singlet-D sulfur also inserts preferentially into Si-H bonds (88). Other species of carbenes such as CBrCl and CBr₂ have also been reported to insert readily into Si-H bonds (89). The vacuum u. v. photolysis of methylsilane has been done recently and evidence obtained here indicates that SiH₂ and CH₃SiH insert predominantly into Si-H bonds (20).

The isolation of a small amount of disilane product which appeared to have the composition Si₂H₄D₂ from the photolysis of phenylsilane -d₃ in the presence of 150 torr of SiH₄ suggests that a reaction such as the following may be occurring.



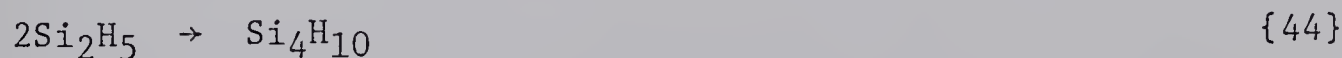
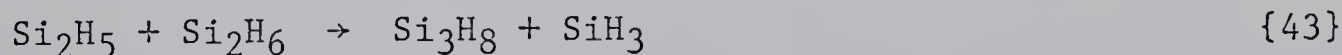
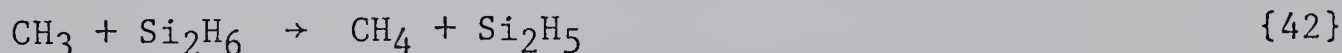
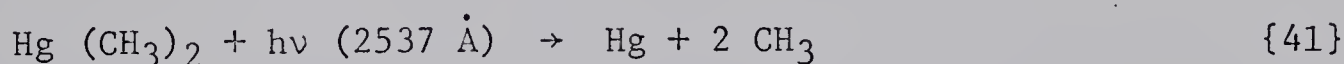
The results of this experiment are in excellent agreement with results involving the reactions of recoil silicon atoms with phosphine (90). These authors report that recoil silicon atoms react with gaseous phosphine to give SiH₄ as the sole product. The addition of SiH₄ to the gaseous phosphine gave Si₂H₆ as well as SiH₄. The authors suggested SiH₂ as the

disilane precursor.

The reports that SiH_2 radicals readily undergo insertion reactions indicate that they must be in their singlet states. This is in agreement with the prediction by Jordan that the ground state of SiH_2 is a singlet.

The photolysis of phenylsilane $-d_3$ in the presence of 50 torr Si_2H_6 offers some interesting information concerning the reactivity of Si_2H_5 radicals. Trisilane (Si_3H_8) was observed as the only straight-chain silicon compound higher than disilane. Tetrasilane was not detected.

Unfortunately, insufficient data are available to explain this phenomenon. This observation is however in accordance with the results obtained from experiments in which $\text{Hg}(\text{CH}_3)_2$ was photolyzed in the presence of Si_2H_6 (91). The results obtained in the latter case infer that unless Si_2H_5 radicals are produced in sufficiently high concentrations they will react with Si_2H_6 molecules in some manner to produce trisilane.



The photolysis of phenylsilane $-d_3$ in the presence of Si_2H_6 produces Si_2H_5 radicals at a much slower rate and reaction {43} would be favored under these circumstances. The proposed reactions of Si_2H_5

{43, 44} are only speculative as only preliminary experiments were carried out using the $\text{Hg}(\text{CH}_3)_2$, Si_2H_6 system. The results obtained from this system are promising and a thorough study should yield information relevant to the reactions of Si_2H_5 radicals.

CHAPTER VI

THE REACTIONS OF METHYL RADICALS WITH SILANES.

RESULTS

- 1) SiH_4 and SiD_4 .
- 2) Si_2H_6 and Si_2D_6 .
- 3) $\text{C}_6\text{H}_5\cdot\text{SiD}_3$.

DISCUSSION

- 1) SiH_4 and SiD_4 .
- 2) Si_2H_6 and Si_2D_6 .
- 3) Phenylsilane- d_3 .
- 4) Calculated and Observed Activation Energies.
- 5) Primary Kinetic Isotope Effect.

RESULTS1) SiH_4 and SiD_4 :

Monosilane is transparent to wavelengths greater than 1850 Å (92). In the absence of a catalyst (such as nickel) monosilane is stable up to 350°C (93). This is in agreement with the observations of this study in that at all the temperatures studied, hydrogen was not a reaction product. Azomethane has been used as a photolytic source of methyl radicals up to a temperature of 205°C (21). During the present study azomethane was allowed to stand in the reactor for 3 hours at a temperature of 215°C, the highest temperature used in the rate measurements. At the end of this period the non-condensables at -196°C were measured and found to be almost undetectable indicating that the decomposition of azomethane at this temperature is very slow and should not interfere with the experiments.

The perdeuterated silane was the first compound investigated. During its study various reaction and analytical conditions were tested. The conditions and results of this study are summarized in Table XV. The initial experiments were conducted under low light intensity conditions using a single lamp and a Kodak Wratten NO. 18A filter to eliminate wavelengths below 3150 Å. These conditions required long exposure times. The abstraction reaction was found to proceed at a high rate and in order to facilitate ethane analysis a high light intensity system was adopted and used for the remainder of the measurements. This system employed two light sources equipped with

pyrex windows which filtered out light of wavelength below 2800 Å. The increased light intensity also necessitated shorter photolysis times and eliminated the possibility of significant temperature fluctuations during the experiment.

2) Si_2H_6 and Si_2D_6 :

Disilane does not absorb in the u. v. region above 2100 Å (94). Thermal decomposition is reported to take place at about 300°C (92, 95). During the product analysis a careful search was conducted for SiH_4 and H_2 which would arise from decomposition of the disilane. Only trace amounts were found. Table XVI contains the relative data for the disilane experiments.

3) $\text{C}_6\text{H}_5\cdot\text{SiD}_3$:

Phenylsilane does not absorb u. v. radiation of wavelength greater than 2800 Å (27), and is not decomposed by the light transmitted by the pyrex filter. At room temperature phenylsilane- d_3 decomposes very slowly, the only gaseous products being isotopically mixed hydrogens. The thermal stability of phenylsilane- d_3 at 215°C was tested by placing a sample of the compound in the reactor and heating for 5 hours. At the end of this period the sample was removed and analyzed. The only products non-condensable at -98°C were isotopic hydrogens and a trace amount of SiD_4 . Decomposition was very small amounting to 0.2% with the hydrogens accounting for more than 90% of the decomposition products. The methane product from the reaction was analyzed isotopically for its CH_4 and CH_3D content using a MS 10 mass spectrometer in order to determine the rate constants

for ring and side chain abstraction. TableXVII outlines the conditions and results of this investigation.

TABLE XV

The reactions of methyl radicals with monosilane.

Temp. (°C)	Time (sec)	{AZO} (10 ⁻⁶ moles cc ⁻¹)	{SiD ₄ }	Products (10 ⁻⁶ moles)					N ₂	k ₅ /k ₂ ^{1/2}	
				CH ₄ {4}	CH ₃ D{5}	C ₂ H ₆	C ₂ H ₆ [*]				
Single lamp & Wratten 18A filter.											
30	7200	1.199	3.310	0.18	4.48	12.50	11.33		23.70	0.339	
75	6000	3.619	1.609	4.03	13.52	26.50	26.11		55.35	1.516	
117	6000	1.735	2.276	1.55	23.85	1.62	1.43		27.20	7.942	
167	5400	2.656	3.177	4.64	45.96	0.92	0.64		39.32	16.600	
215	3600	3.880	0.655	13.30	22.34	0.92	0.63		41.49	51.176	
Two lamps & pyrex filters.											
54	186	0.252	3.569	0.01	0.38	0.80	0.79		1.20	0.624	
65†	270	1.289	1.953	0.46	0.96	7.50	7.43		10.12	0.745	
70	360	0.273	2.474	0.02	0.94	1.62	1.60		2.88	1.136	

* Corrected for reaction {1b}.

† CH₃D determined by mass spectrometry.

TABLE XV

(Continued)

Temp. (°C)	Time (sec)	{AZO} (10 ⁻⁶ moles cc ⁻¹)	{SiD ₄ }	Products (10 ⁻⁶ moles)					N ₂	k ₅ /k ₂ ^{1/2}	
				CH ₄ {4}	CH ₃ D{5}	C ₂ H ₆	C ₂ H ₆ [*]				
Two lamps & pyrex filters.											
113	510	0.199	2.280	0.03	2.73	0.73	0.70		3.20	4.513	
158	300	0.173	1.395	0.03	1.86	0.23	0.21		1.57	11.857	
215†	300	1.614	2.324	2.54	14.51	0.51	0.42		12.81	39.970	
		<u>{AZO}</u>	<u>{SiH₄}</u>	<u>CH₄{4}</u>	<u>CH₄{5}</u>					<u>k₅/k₂^{1/2}</u>	
29	240	0.298	1.362	0.01	0.45	1.67	1.65		1.99	1.191	
68	243	0.541	1.612	0.03	2.11	1.96	1.93		3.76	4.302	
108	240	1.099	0.921	0.20	4.56	2.60	2.55		6.80	14.287	
150	270	1.035	2.509	0.20	10.53	0.39	0.34		7.61	31.387	
160	300	1.879	0.973	1.11	14.67	1.90	1.79		15.68	46.485	

* Corrected for reaction {1b}.

† CH₃D determined by mass spectrometry.

TABLE XV

(Continued)

Temp. (°C)	Time (sec)	{AZO} (10 ⁻⁶ moles cc ⁻¹)	{SiD ₄ }	Products (10 ⁻⁶ moles)					N ₂	k ₅ /k ₂ ^{1/2}
				CH ₄ {4}	CH ₃ D{5}	C ₂ H ₆	C ₂ H ₆ [*]			
		<u>{AZO}</u>	<u>{SiH₄}</u>	<u>CH₄{4}</u>	<u>CH₄{5}</u>					<u>k₅/k₂^{1/2}</u>
187	240	0.335	1.466	0.06	4.12	0.23	0.19		6.12	49.890
213	240	0.798	0.766	0.37	8.09	0.09	0.07		2.65	112.614

* Corrected for reaction {1b}.

† CH₃D determined by mass spectrometry.

TABLE XVI

The reaction of methyl radicals with disilane.

Temp. (°C)	Time (sec)	{AZO} (10 ⁻⁶ moles cc ⁻¹)	{Si ₂ H ₆ }	Products (10 ⁻⁶ moles)					N ₂	k ₅ /k ₂ ^{1/2}
				CH ₄ {4}	CH ₄ {5}	C ₂ H ₆	C ₂ H ₆ *			
33	240	0.420	0.561	0.01	2.19	0.96	0.94		2.60	18.564
53	240	0.364	0.588	0.01	2.66	0.44	0.42		2.61	32.274
89	240	0.869	0.907	0.03	8.13	0.39	0.35		5.82	69.755
114	300	0.549	0.661	0.03	8.04	0.20	0.16		4.93	125.348
138	240	0.804	0.748	0.06	9.32	0.12	0.08		5.80	204.682
139	240	0.445	1.073	0.01	5.97	0.04	0.01		3.42	222.510
192	240	1.296	0.483	0.40	14.77	0.24	0.17		9.81	345.600
202	300	0.418	0.344	0.07	7.08	0.06	0.03		4.21	498.370
		{AZO}	{Si ₂ D ₆ }	CH ₄ {4}	CH ₃ D{5}					k ₅ /k ₂ ^{1/2}
37†	300	0.420	2.015	0.24	2.42	1.38	1.36		3.45	4.254
54	270	0.237	1.228	0.01	1.44	0.57	0.56		2.08	6.832

* Corrected for reaction {1b}.

† CH₃D measured by mass spectrometry.

TABLE XVI
(Continued)

Temp.	Time	{AZO} (10 ⁻⁶ moles cc ⁻¹)	{Si ₂ H ₆ }	Products (10 ⁻⁶ moles)					N ₂	k ₅ /k ₂ ^{1/2}
				CH ₄ {4}	CH ₄ {5}	C ₂ H ₆	C ₂ H ₆ [*]			
		<u>{AZO}</u>	<u>{Si₂D₆}</u>	<u>CH₄{4}</u>	<u>CH₃D {5}</u>					<u>k₅/k₂^{1/2}</u>
90	270	0.646	1.129	0.04	5.69	0.88	0.75	4.88		23.292
115	270	0.252	1.003	0.16	2.97	0.13	0.11	2.36		38.214
147	270	0.986	1.107	0.28	11.10	0.40	0.35	7.76		74.090
189	300	0.318	0.245	0.11	4.72	0.23	0.20	3.90		176.254

* Corrected for reaction {1b}.

† CH₃D measured by mass spectrometry.

The reactions of methyl radicals with phenylsilane-d₃.

Temp.	Time	{AZO} (10 ⁻⁶ moles cc ⁻¹)	{C ₆ H ₅ ·SiD ₃ }	Products (10 ⁻⁶ moles)							N ₂	k _{5H} /k ₂ ^{1/2}	k _{5D} /k ₂ ^{1/2}
				CH ₄ {4}	CH ₄ {5}	CH ₃ D{5}	C ₂ H ₆	C ₂ H ₆ *	C ₂ H ₆				
37	300	0.530	1.362	0.01	0.13	0.29	3.55	3.52	4.91	0.203			0.458
55	300	0.272	1.236	0.01	0.07	0.33	1.62	1.60	2.45	0.189			0.871
83	300	0.450	0.981	0.05	0.18	1.03	2.65	2.62	4.14	0.473			2.668
105	300	0.708	1.095	0.15	0.76	2.43	3.35	3.30	6.90	1.521			4.856
141	300	0.550	1.008	0.17	0.56	3.59	1.20	1.16	5.18	2.114			13.610
167	270	0.492	1.372	0.16	0.54	4.19	0.47	0.44	4.34	2.612			20.129
197	300	0.527	1.268	0.24	0.57	5.90	0.30	0.26	5.29	3.600			37.415

* Corrected for reaction {1b}.

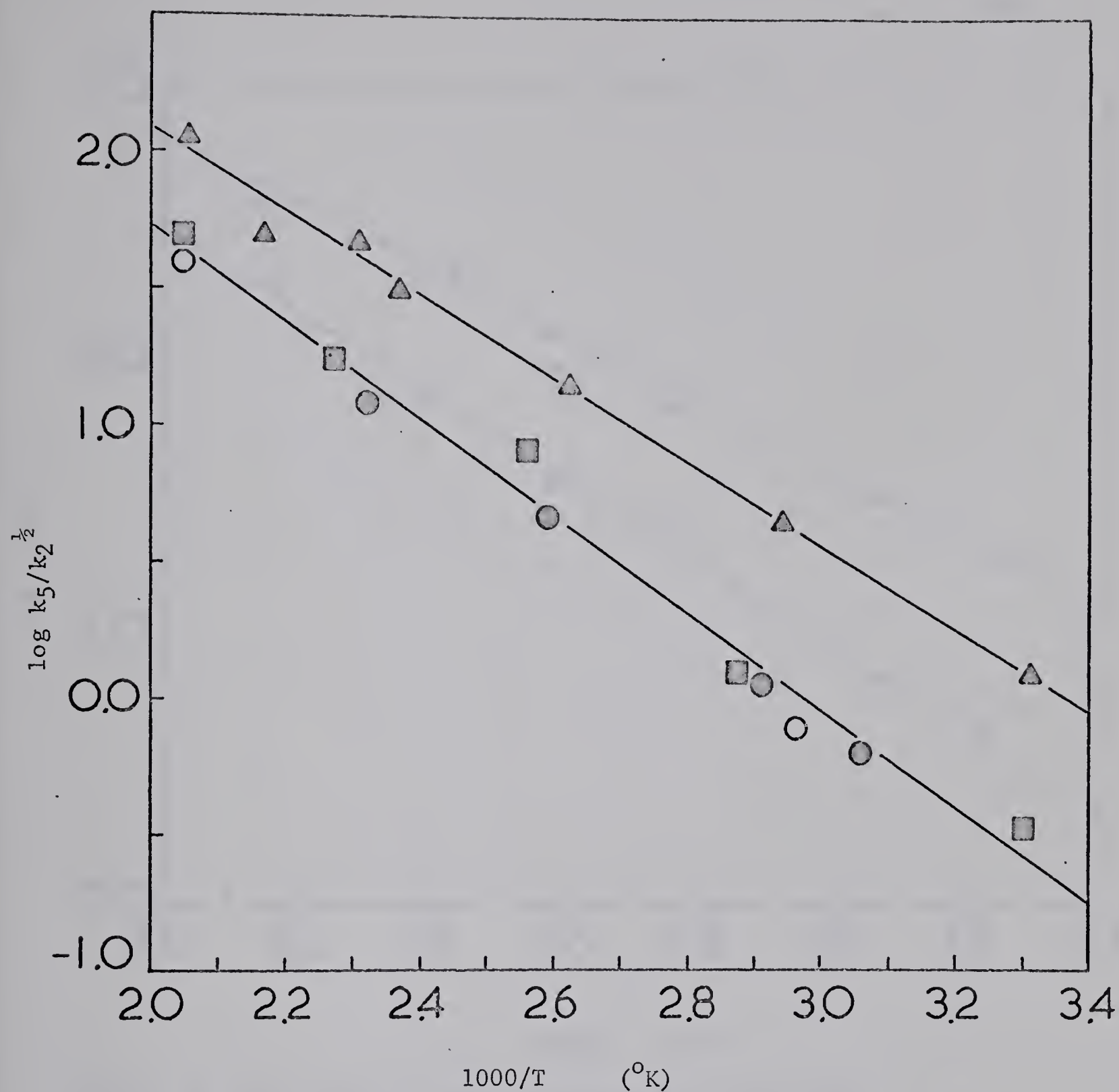


Figure 18. Reactions of methyl radicals with monosilanes: (■) monosilane-d₄ with single lamp and Wratten 18A filter; (●) monosilane-d₄ with 2 lamps and pyrex filter; (○) monosilane-d₄ with 2 lamps and pyrex filter with CH₃D determined by mass spectrometry; (▲) monosilane.

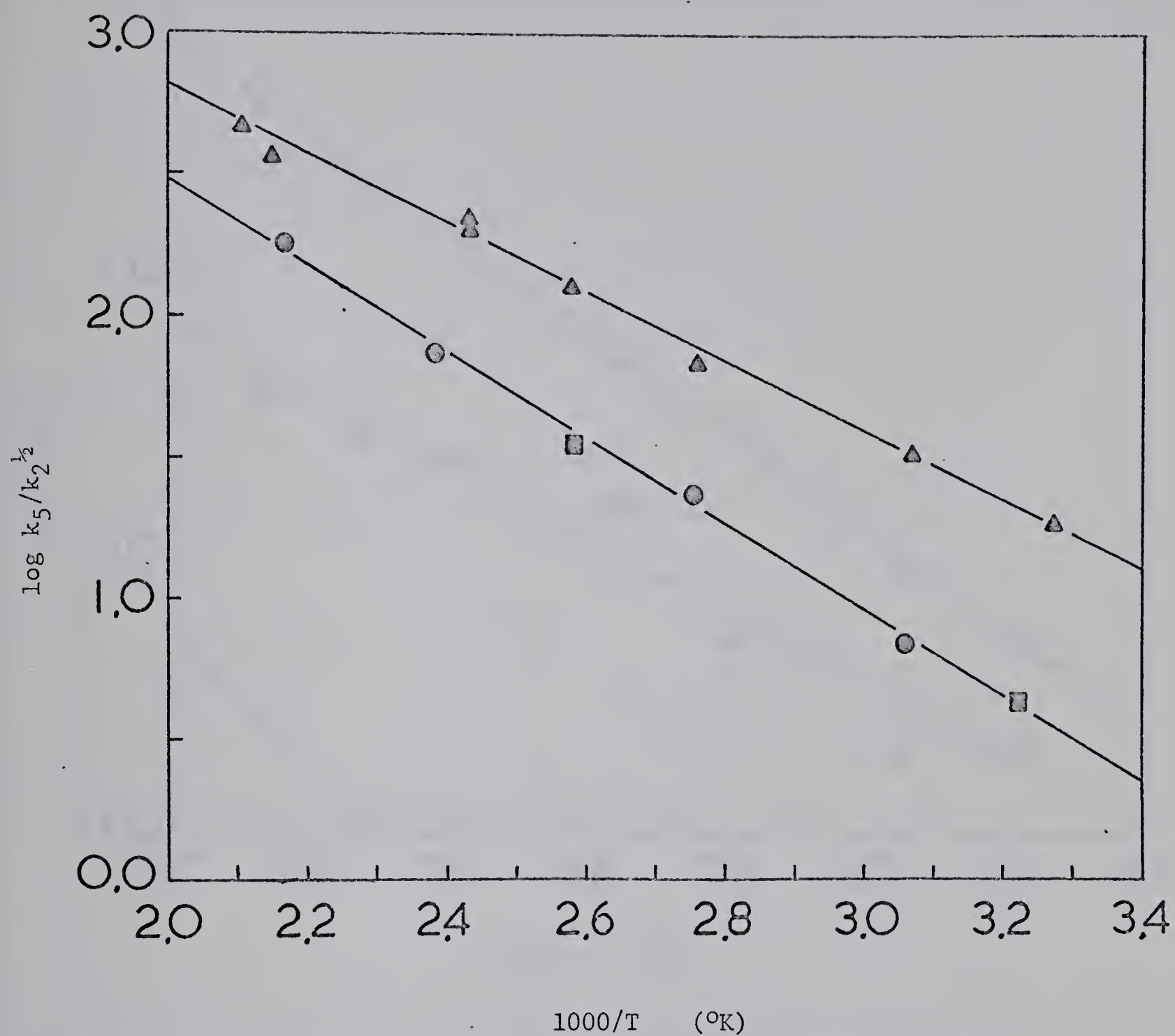


Figure 19. Reactions of methyl radicals with disilanes;
 (Δ) disilane; (\circ) disilane-d₆; (\blacksquare) disilane-d₆,
 CH₃D determined by mass spectrometry.

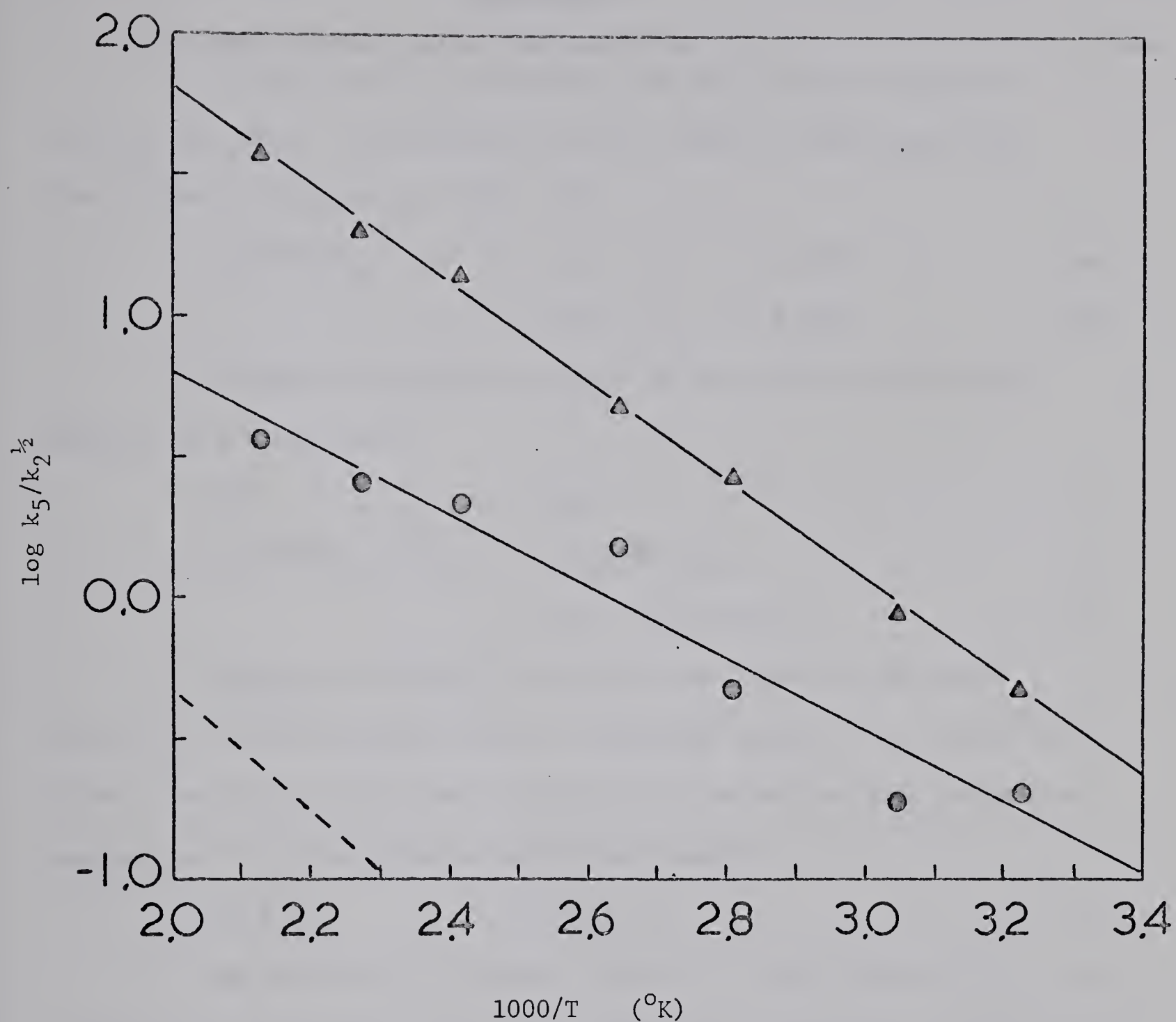


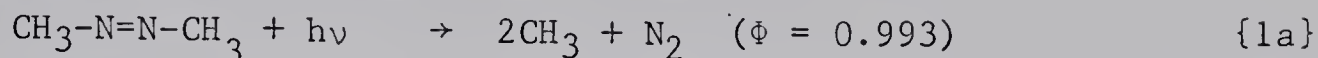
Figure 20. Reactions of methyl radicals with phenylsilane- d_3 :

(Δ) reaction with side chain; (\circ) reaction with ring;

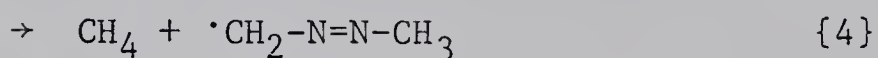
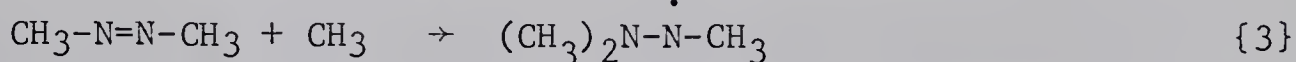
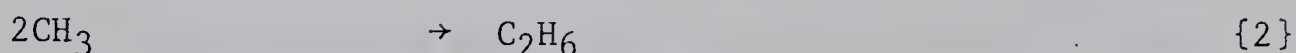
(-- --) direct abstraction from ring in toluene, Ref. (102).

DISCUSSION

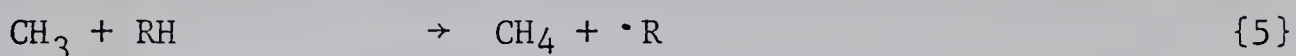
The photolysis of azomethane has been studied extensively (21, 95, 100). Decomposition has been found to take place via the following two processes (99, 100).



Secondary processes are those of free radical combination, addition and abstraction.



Reactions {1b} and {2} are the sole producers of ethane, while {4} is the exclusive reaction producing methane. If another substance containing abstractable hydrogens is introduced into the system, methane can be produced by an additional reaction.



The combination of methyl radicals to form ethane {2} has been studied very thoroughly (38, 101). The value of the rate constant from the more recent study is, $\log k_2 \text{ (cc mole}^{-1} \text{ sec}^{-1}) = 13.34 \text{ (101).}^4$ The

⁴ See footnote p.70 . In the present case an overestimation of the rate of methyl radical recombination would have the effect of making the pre-exponential factors too large by a constant factor. As the activation energy for methyl radical recombination is assumed to be zero, the measured activation energies would be unaffected.

rate of abstraction of hydrogen from azomethane by methyl radicals is $\log k_4(\text{cc mole}^{-1} \text{ sec}^{-1}) = 10.93 \pm 0.11 - (7,800 \pm 200/2.303RT)$ (21, 96). The rate of formation of methane and ethane can be measured and the following kinetic expression can be used to calculate the rate constant ratio for reactions {2} and {5}.

$$k_5/k_2^{1/2} = \left[\frac{R_{\text{CH}_4}}{R_2^{1/2}} - \frac{k_4}{k_2^{1/2}} \{(\text{CH}_3\text{N})_2\} \right] \{\text{RH}\}^{-1} \quad \{6\}$$

In reactions where deuterium is abstracted and the CH_3D is measured by mass spectrometry, the expression simplifies to,

$$k_5/k_2^{1/2} = \left[\frac{R_{\text{CH}_3\text{D}}}{R_2^{1/2}} \right] \{\text{RH}\}^{-1} \quad \{7\}$$

Figures 18-20 are Arrhenius plots of $\log k_5/k_2^{1/2}$ vs. $1000/T$ for the reactions studied using the data from Tables XV, XVI and XVII. A least-mean-squares treatment of the data was used to obtain the best straight lines which fit the experimental results. Arrhenius parameters for the reaction of methyl radicals with the silanes studied in the present investigation are summarized in Table XVIII. For comparison some of the data available for the reactions of methyl radicals with the analogous hydrocarbons are included.

1) SiH_4 and SiD_4 :

The pre-exponential factors for the reactions of methyl radicals with monosilane and its deuterated counterpart are almost identical. The difference may well be due to experimental error. These values are very close to those measured for reactions of methyl radicals with

methane (Table XVIII). The bond dissociation energy of methane, $D(\text{CH}_3\text{-H}) = 104 \text{ kcal mole}^{-1}$ (33). The latest value for $D(\text{SiH}_3\text{-H})$ is $95.2 \text{ kcal mole}^{-1}$ (73). The lower bond energy in silane appears to be reflected in the lower activation energy required in its metathetical reaction with methyl radicals.

2) Si_2H_6 and Si_2D_6 :

Disilane and perdeuterated disilane have A-factors which are the same within experimental accuracy. These pre-exponential factors are very similar to those quoted for the reactions of methyl radicals with ethane (Table XVIII). A noticeable difference again appears in the activation energies of the silane and alkane reactions. For ethane $D(\text{C}_2\text{H}_5\text{-H}) = 98 \text{ kcal mole}^{-1}$ (33). Data for $D(\text{Si}_2\text{H}_5\text{-H})$ is not available. If silanes follow a similar trend as the alkanes, this value must be lower than $95 \text{ kcal mole}^{-1}$. There is evidence for this trend in that the activation energy for abstraction from disilanes is lower than for monosilanes.

3) Phenylsilane - d_3 :

This study offers information concerning the effect of aromatic substitution upon the abstraction reaction. Abstraction of a β -hydrogen from toluene by a methyl radical requires a lower activation energy than is usually necessary to remove hydrogen from methyl groups. This is attributed to resonance stabilization of the benzyl radical.

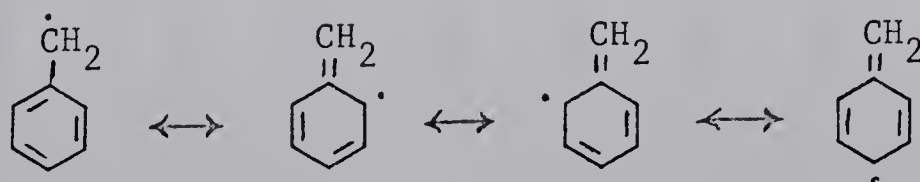


TABLE XVIII

Reactions of methyl radicals.

Reaction	log A cc mole ⁻¹ sec. ⁻¹	E _a kcal mole ⁻¹	Ref.
CH ₃ + C ¹⁴ H ₄ → CH ₄ + C ¹⁴ H ₃	11.83	14.65	107
CD ₃ + C ¹⁴ D ₄ → CD ₄ + C ¹⁴ D ₃	12.60	17.80	106
CD ₃ + C ₂ H ₆ → CD ₃ H + C ₂ H ₅	12.21	11.8	108
CD ₃ + C ₂ D ₆ → CD ₄ + C ₂ D ₅	12.21	13.3	108
CH ₃ + C ₆ H ₅ ·CD ₃ → CH ₃ D + C ₆ H ₅ ·CD ₂	11.60	11.3	102
CH ₃ + C ₆ H ₅ ·CD ₃ → CH ₄ + C ₆ H ₄ ·CD ₃	10.70	10.0	102
CH ₃ + C ₆ H ₅ ·CD ₃ → CH ₄ + C ₆ H ₄ ·CD ₃	~7.0	~ 4.0	102
This work *			
CH ₃ + SiH ₄ → CH ₄ + SiH ₃	11.80 ± .07	6.99 ± .56	

* Errors quoted here are statistical with activation energy errors based on a 90% confidence limit.

TABLE XVIII

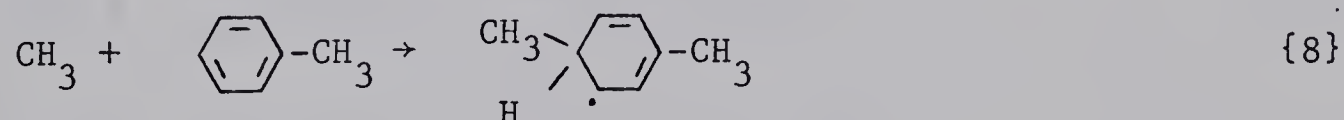
(Continued)

Reaction	log A cc mole ⁻¹ sec. ⁻¹	E _a kcal mole ⁻¹	Ref.
	This work *		
CH ₃ + SiD ₄ → CH ₃ D + SiD ₃	11.98 ± .10	8.19 ± .65	
CH ₃ + Si ₂ H ₆ → CH ₄ + Si ₂ H ₅	11.96 ± .04	5.63 ± .32	
CH ₃ + Si ₂ D ₆ → CH ₃ D + Si ₂ D ₅	12.19 ± .03	6.96 ± .35	
CH ₃ + C ₆ H ₅ ·SiD ₃ → CH ₃ D + C ₆ H ₅ ·SiD ₂	11.99 ± .03	8.03 ± .31	
CH ₃ + C ₆ H ₅ ·SiD ₃ → CH ₄ + C ₆ H ₄ ·SiD ₃	10.03 ± .13	5.87 ± 1.32	

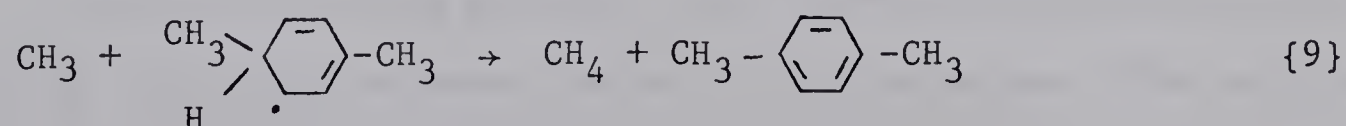
* Errors quoted here are statistical with activation energy errors based on a 90% confidence limit.

The inability of silicon to form double bonds eliminates stabilization of this type for the phenylsilyl radical. The absence of this effect manifests itself in the activation energy required to remove a deuterium from phenylsilane- -d_3 . There does not appear to be a weakening of the Si-D bond by attachment of the aromatic group to the silicon atom. In this case the Si-D bonds on the side chain behave like primary bonds.

The results of the reaction of methyl radicals with the aromatic ring are less convincing. Figure 19 illustrates the scatter in the experimental data. One would expect the C-H bonds of the aromatic ring to be significantly stronger than the Si-D bonds on the side chain. These bond energy considerations require a higher activation energy for ring abstraction. Although the data are poor, they clearly indicate a lower activation energy for the mechanism producing methane via reaction with the ring. A study of the reaction of methyl radicals with toluene in the 100 to 300° C temperature range, revealed a complex mechanism for reaction of methyl radicals with the aromatic ring (102). These authors proposed two mechanisms operating simultaneously. One of the mechanisms, supposedly predominant at lower temperatures, involved preliminary addition of methyl to the ring to form a cyclohexadienyl radical.



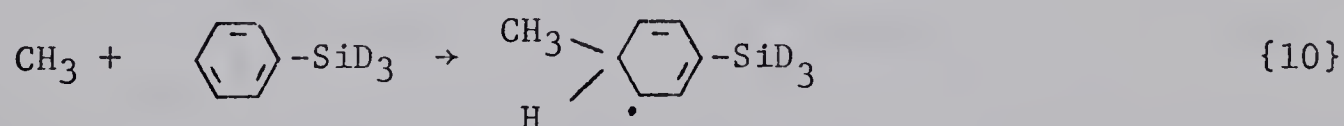
The radical thus formed subsequently disproportionates with another methyl radical.



The estimated Arrhenius parameters for this mechanism are given in Table XVIII. Assuming that the disproportionation reaction {9} occurs with zero activation energy, the activation energy for this mechanism represents the activation energy of the radical addition reaction {8}. The reported value of $E_a \sim 4 \text{ kcal mole}^{-1}$ is in agreement with reported values of $\sim 4.1 \text{ kcal mole}^{-1}$ for the addition of H-atoms to benzene (103) and 3.56 and $4.66 \text{ kcal mole}^{-1}$ for the addition of CF_3 radicals to toluene (104, 105).

Direct abstraction is proposed as the dominant reaction at higher temperatures. This mechanism features a much higher A-factor and an activation energy of $10 \text{ kcal mole}^{-1}$.

Measurements made in this study indicate values of $\log A \sim 10$ $\text{cc mole}^{-1} \text{ sec}^{-1}$ and $E_a \sim 6 \text{ kcal mole}^{-1}$ for the methyl plus ring reaction. An activation energy of approximately 6 kcal mole^{-1} is much too low for direct abstraction from the ring. As mentioned previously, the effect of $-\text{SiD}_3$ substitution on the benzene ring is to reduce the electron density in the ring (27). In this instance, an effect of this nature should show up as a higher activation energy requirement for the methyl addition reaction {10}.



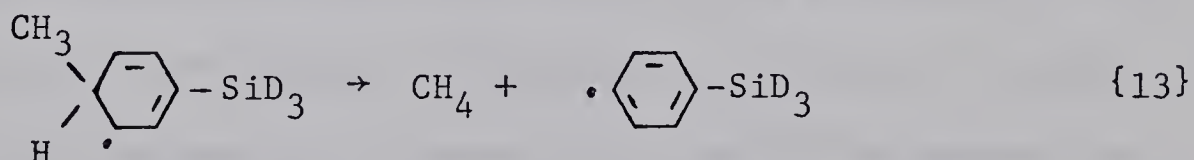
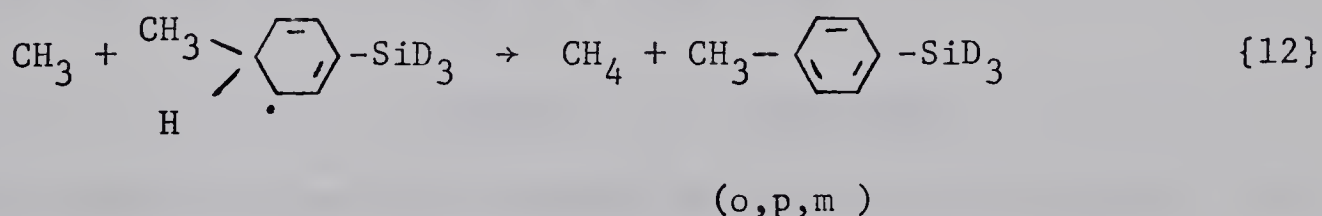
An activation energy of $\sim 6 \text{ kcal mole}^{-1}$ is consistent with this proposal.

It is quite possible that the values reported for the Arrhenius parameters in this study represent the sum of two mechanisms. The addition

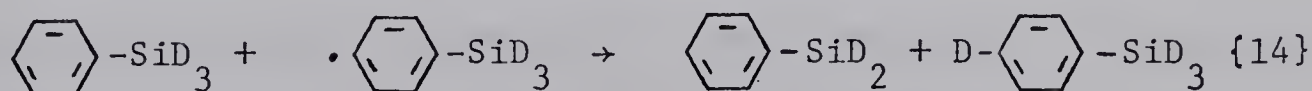
mechanism {10} plus a direct abstraction process {11}.



If two mechanisms are operating, an extensive temperature study should reveal the parameters of the two reaction mechanisms through curvature in the Arrhenius plot as the reaction requiring the higher activation energy begins to prevail at the higher temperature. Due to the thermal instability of phenylsilane at temperatures approaching 300° C, a study at higher temperatures was not carried out. If the Arrhenius parameters for the direct abstraction mechanism are similar to those measured for the analogous reaction of methyl radicals with the aromatic ring of toluene (Table XVIII), reaction {11} will be negligible (Figure 20) in the temperature range studied, and our data will represent the parameters for reaction {10}. These values are meaningful only if reaction {10} is followed entirely by reactions of the following type.



The radical formed by reaction {13} would presumably abstract a deuterium from the side chain.



4) Calculated and Observed Activation Energies:

Table XIX contains values for observed activation energies and calculated potential energies of activation using the BEBO method. A brief outline of the BEBO calculations is given in Appendix E. Comparison of the two values indicate that they are in reasonable agreement. In both cases the calculated and observed values agree within $\pm 2 \text{ kcal mole}^{-1}$ with those for D abstraction showing remarkable agreement. Data for the analogous hydrocarbon reactions are also included in Table XIX so that comparisons could be facilitated.

5) Primary Kinetic Isotope Effect:

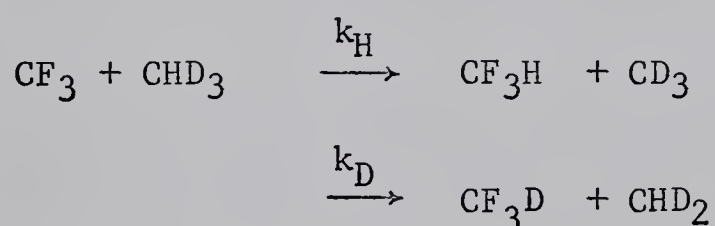
The primary kinetic isotope effect for H and D abstraction based on absolute reaction rate theory (109) is given by.

$$\frac{k_H}{k_D} = \frac{\nu_H^*}{\nu_D^*} \frac{\Gamma_H^*}{\Gamma_D^*} \frac{\prod_{i=1}^{3N-7} \left(\frac{\Gamma_H}{\Gamma_D} \right)_i}{\prod_{i=1}^{3N-6} \left(\frac{\Gamma_D}{\Gamma_H} \right)_i} \frac{\left(\frac{\sigma_H}{\sigma_D} \right)}{\left(\frac{\sigma_D}{\sigma_H} \right)} \quad \{16\}$$

complex
reactants

ν^* is the imaginary reaction frequency of the activated complex, Γ 's are the quantum correction factors for each of the vibrations of the activated complex of the form $\Gamma_i = \frac{1}{2} u_i / \sinh \frac{1}{2} u_i$ with $u_i = h\nu_i/kT$. The reaction path degeneracy is denoted by σ , and Γ^* represents the tunneling correction factor. The present calculations are based upon a three-mass-point model and do not take into account the tunneling factor Γ^* . The BEBO method was used to calculate the properties of the three-mass-point model (Appendix E). These properties are reported in Table XX.

Figures 21 and 22 illustrate the temperature dependence of the experimentally observed and calculated kinetic isotope effects. These diagrams indicate a discrepancy between the observed and calculated values which is of the same order of magnitude as those found by various authors for hydrogen transfer reactions from methane, ethane and H_2 (25), and have been attributed to tunneling effects. For monosilanes this discrepancy is somewhat less than for disilanes and can likely be accounted for by tunneling effects. The three-mass-point model should be a satisfactory approximation of the methyl-monosilanes systems in view of Sharp and Johnston's (110) finding that the computational results for the reactions



depend little on whether a 3,4,5 or 9 mass-point model is considered. For disilanes the three-mass-point model is a less satisfactory approximation and also the input parameters used in the calculations were less reliable. Consequently, the deviation of the calculated curve from the experimental one cannot be assigned entirely to tunneling, as other factors are probably involved also. If this were not the case the calculated and experimental results would show better agreement than for monosilanes because tunneling

effects must be less important for the disilane reactions in view of the smaller activation energies involved.

The data obtained from this study indicates that tunneling phenomena are also implicated in the hydrogen transfer reactions of the silicon hydride molecules. In order to calculate the tunneling correction factors, potential energy surfaces for the reactions would have to be constructed. These calculations were beyond the scope of the present study.

TABLE XIX

Calculated and experimental energies of activation for
H-atoms abstraction by methyl radicals.

	$D_e(R-H)^*$ (kcal mole ⁻¹)	E_a calculated (kcal mole ⁻¹)	E_a experimental (kcal mole ⁻¹)
CH ₃ - H	105.5	13 ^a	14.6 ^b
C ₂ H ₅ - H	100.0	10 ^a	11.8 ^c
SiH ₃ - H	98.2	8.2 ^d	6.99 ^d
SiD ₃ - D			8.19 ^d
Si ₂ H ₅ - H	93.0	6.9 ^d	5.63 ^d
Si ₂ D ₅ - D			6.96 ^d

* Includes zero point energy.

- a. reference 25
- b. reference 107
- c. reference 108
- d. this work

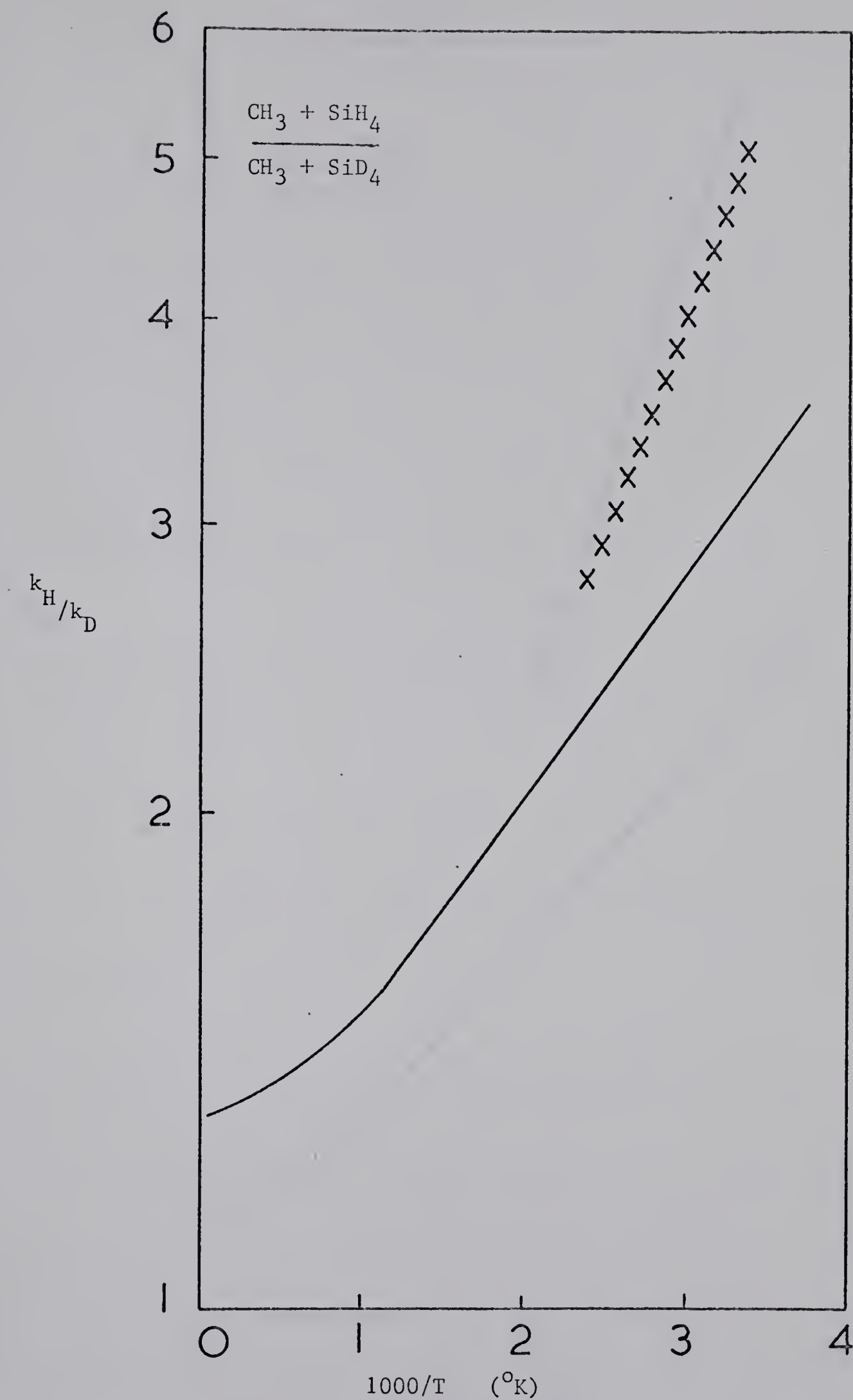


Figure 21. Kinetic isotope effect, $\log k_H/k_D$ vs. $1000/T$, for methyl radical plus monosilane system: (X) calculated from experimental data; solid curve represents theoretical effect calculated by equation {16}.

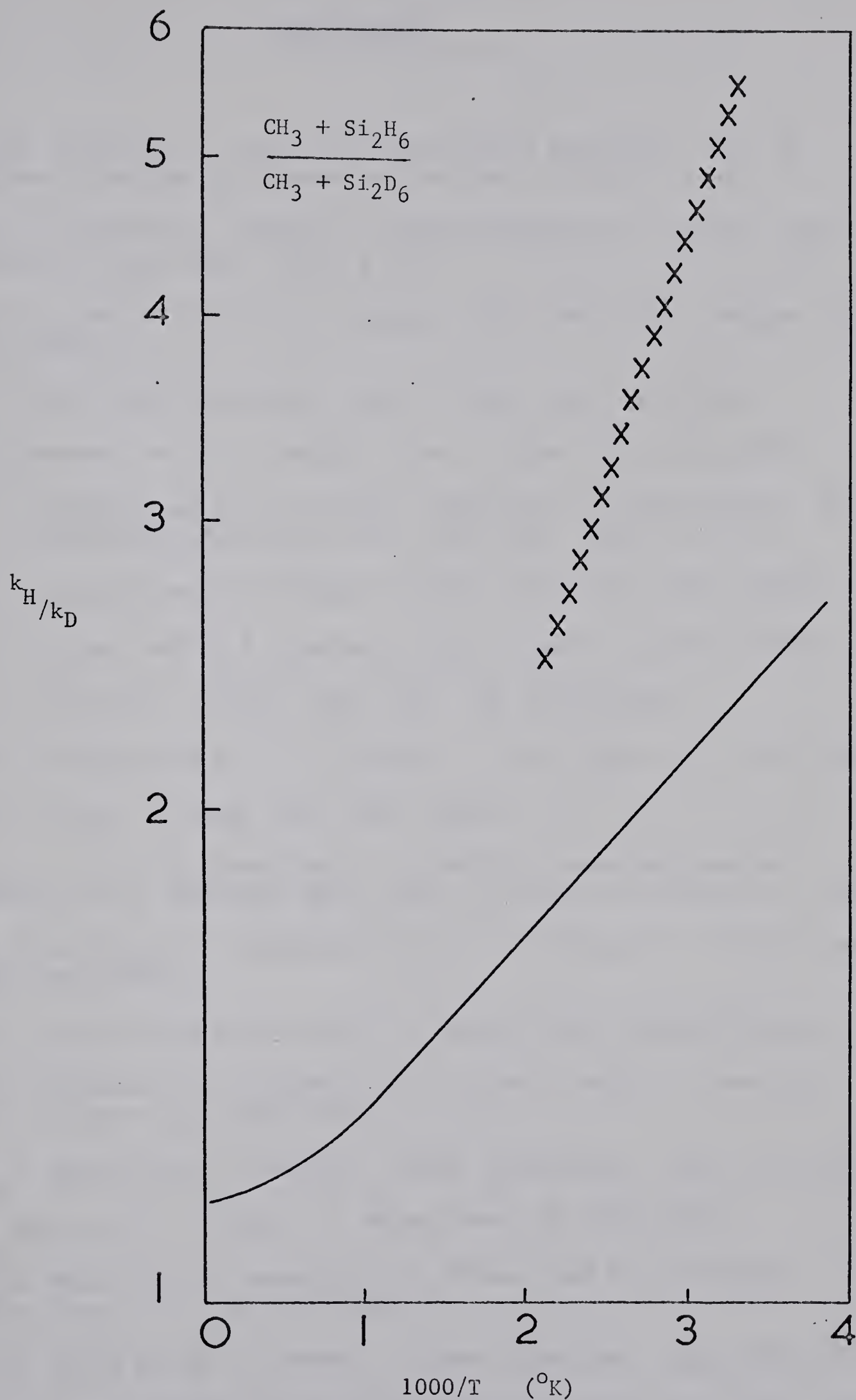


Figure 22. Kinetic isotope effect, $\log k_H/k_D$ vs. $1000/T$, for methyl radical plus disilane system: (X) calculated from experimental data; solid curve represents theoretical effect calculated by equation {16}.

BIBLIOGRAPHY

- 1) E. W. R. Steacie. Atomic and Free Radical Reactions. Vol. I. Reinhold Publishing Corporation, New York. 1954. p. 413.
- 2) R. J. Cvetanovic. Progress in Reaction Kinetics. Vol. II. Macmillan Co., New York. 1964 p. 74.
- 3) G. N. C. Woodall and H. E. Gunning. Bull. Soc. Chim. Belges. 71, 725 (1962).
- 4) P. Kebarle and M. Avrahami. Can. J. Chem. 41, 347 (1963).
- 5) Y. Rousseau and H. E. Gunning. Can. J. Chem. 41, 465 (1963).
- 6) H. E. Gunning and O. P. Strausz. Advances in Photochemistry. Vol. I. Interscience Publishers, Inc., New York. 1963. p. 267.
- 7) R. A. Holroyd and G. W. Klein. J. Phys. Chem. 67, 2273 (1963).
- 8) T. F. Palmer and F. P. Lossing. Can. J. Chem. 41, 2412 (1963).
- 9) J. P. Chesick. J. Amer. Chem. Soc. 86, 3597 (1964).
- 10) H. E. Gunning and E. W. R. Steacie. J. Chem. Phys. 17, 351 (1949).
- 11) K. J. Ivin. J. Chem. Soc. 2241 (1956).
- 12) H. W. Ford, P. J. Kozak and H. E. Gunning. American Chemical Society 137th. Meeting, April, 1960. (Abstracts of papers p. 35R).
- 13) D. W. Sester, B. S. Rabinovitch and E. G. Spittler. J. Chem. Phys. 35, 1840 (1961).
- 14) R. A. Holroyd and G. W. Klein. J. Chem. Phys. 69, 2129 (1965).
- 15) O. P. Strausz, P. J. Kozak, G. N. C. Woodall and H. E. Gunning. Can. J. Chem. 46, 1317 (1968).
- 16) H. J. Emeleus and K. Stewart. Trans. Faraday Soc. 32, 1577 (1936).
- 17) H. Niki and G. J. Mains. J. Phys. Chem. 68, 304 (1964).
- 18) M. A. Nay, G. N. C. Woodall, O. P. Strausz and H. E. Gunning. J. Amer. Chem. Soc. 87, 179 (1965).
- 19) D. G. White and E. G. Rochow. J. Amer. Chem. Soc. 76, 3897 (1954).
- 20) O. P. Strausz, K. Obi and W. K. Duholke. J. Amer. Chem. Soc. 90, 1359 (1968).

- 21) J. A. Kerr, D. H. Slater and J. C. Young. J. Chem. Soc. (A) 104 (1966).
- 22) J. A. Kerr, D. H. Slater and J. C. Young. J. Chem. Soc. (A) 134 (1967).
- 23) W. J. Cheng and M. Szwarc. J. Phys. Chem. 72, 494 (1968).
- 24) T. N. Bell and B. B. Johnson. Aust. J. Chem. 20, 1545 (1967).
- 25) H. S. Johnston. Gas Phase Reaction Rate Theory. Ronald Press, New York. 1966.
- 26) F. G. A. Stone and D. Seyferth. J. Inorg. Nucl. Chem. 1, 112 (1955).
- 27) L. H. Sommer, L. Goodman and A. H. Konstam. J. Amer. Chem. Soc. 87, 1012 (1965).
- 28) F. P. Lossing, D. G. H. Marsden and J. B. Farmer. Can. J. Chem. 34, 701 (1956).
- 29) P. Kebarle. J. Phys. Chem. 67, 351 (1963).
- 30) M. Kasha. J. Opt. Soc. Amer. 38, 929 (1948).
- 31) A. G. Harrison and F. P. Lossing. Can. J. Chem. 37, 1478 (1959).
- 32) J. O. Terry and J. H. Futrell. Can. J. Chem. 45, 2327 (1967).
- 33) J. A. Kerr. Chem. Rev. 66, 465 (1966).
- 34) J. N. Bradley, H. W. Melville and J. C. Robb. Proc. Roy. Soc. A236, 318 (1956).
- 35) R. A. Holroyd and T. E. Pierce. J. Phys. 68, 1392 (1964).
- 36) T. Holstein. Phys. Rev. 72, 1212 (1947).
- 37) T. Holstein. Phys. Rev. 83, 1159 (1951).
- 38) R. Gomer and G. B. Kistiakowsky. J. Chem. Phys. 19, 85 (1951).
- 39) J. Grotewold, E. A. Lissi and M. G. Newmann. J. Chem. Soc. (A) 375 (1968).
- 40) R. A. Marcus. J. Chem. Phys. 20, 355 (1952).
- 41) B. S. Rabinovitch and D. W. Sester. Advances in Photochemistry. Vol. 3. Interscience Publishers, New York. 1964. p. 61.
- 42) R. J. Norstrom, O. P. Strausz and H. E. Gunning. Can. J. Chem. 42, 2140 (1964).

- 43) M. Avrahami and P. Kebarle. J. Phys. Chem. 67, 354 (1963).
- 44) H. M. Frey and G. B. Kistiakowsky. J. Amer. Chem. Soc. 79, 6373 (1957).
- 45) J. N. Butler and G. B. Kistiakowsky. J. Amer. Chem. Soc. 82, 759 (1960).
- 46) J. N. Butler and G. B. Kistiakowsky. J. Amer. Chem. Soc. 83, 1324 (1961).
- 47) D. W. Sester and B. S. Rabinovitch. Can. J. Chem. 40, 1425 (1962).
- 48) F. H. Dorer and B. S. Rabinovitch. J. Phys. Chem. 69, 1952 (1965).
- 49) F. H. Dorer and B. S. Rabinovitch. J. Phys. Chem. 69, 1964 (1965).
- 50) F. H. Dorer and B. S. Rabinovitch. J. Phys. Chem. 69, 1973 (1965).
- 51) J. P. Chesick. J. Amer. Chem. Soc. 82, 3277 (1960).
- 52) D. W. Sester and B. S. Rabinovitch. J. Amer. Chem. Soc. 86, 564 (1964).
- 53) D. G. L. James and G. E. Troughton. Chem. Commun. 94 (1965).
- 54) R. J. Crawford and A. Mishra. J. Amer. Chem. Soc. 87, 3768 (1965).
- 55) R. Hoffmann. J. Amer. Chem. Soc. 90, 1475 (1968).
- 56) D. W. Placzek and B. S. Rabinovitch. J. Phys. Chem. 69, 2141 (1965).
- 57) P. Kebarle and M. Avrahami. Can. J. Chem. 43, 820 (1965).
- 58) J. R. Majer, H. Pinkard and J. C. Robb. Trans. Faraday Soc. 60, 1244 (1964).
- 59) J. R. Majer, B. Mile and J. C. Robb. Trans. Faraday Soc. 57, 1336 (1961).
- 60) G. Greig and J. C. J. Thynne. Trans. Faraday Soc. 63, 1369 (1967).
- 61) G. Greig and J. C. J. Thynne. Trans. Faraday Soc. 63, 2196 (1967).
- 62) J. G. Calvert and J. N. Pitts, Jr. Photochemistry. J. Wiley & Sons Inc., New York. 1966. p. 782.
- 63) H. Ishikawa and W. A. Noyes, Jr. J. Chem. Phys. 37, 583 (1962).

- 64) H. Ishikawa and W. A. Noyes, Jr. J. Amer. Chem. Soc. 84, 1502 (1962).
- 65) J. R. Bates and H. S. Taylor. J. Amer. Chem. Soc. 49, 2438 (1927).
- 66) G. S. Forbes and J. E. Cline. J. Amer. Chem. Soc. 63, 1713 (1941).
- 67) E. J. Y. Scott and E. W. R. Steacie. Can. J. Chem. 29, 233 (1951).
- 68) A. H. Sehon and B. deB. Darwent. J. Chem. Phys. 23, 822 (1955).
- 69) E. Jakubowski, T. Pollock, O. P. Strausz and H. E. Gunning. The Photolysis and Mercury Photosensitization of Phenylsilane-d₃. To be published.
- 70) R. Williams. J. Chem. Phys. 28, 577 (1958).
- 71) S. W. Benson. J. Chem. Ed. 42, 502 (1965).
- 72) G. G. Hess, F. W. Lampe and L. H. Sommer. J. Amer. Chem. Soc. 86, 3174 (1964).
- 73) F. E. Saalfeld and H. J. Svec. Inorg. Chem. 3, 1442 (1964).
- 74) J. N. Pitts Jr., J. K. Foote and J. K. S. Wan. Photochem. and Photobiol. 4, 323 (1965).
- 75) J. K. Foote, M. H. Mallon and J. N. Pitts, Jr. J. Amer. Chem. Soc. 88, 3698 (1966).
- 76) G. Porter and E. Strachan. Trans. Faraday Soc. 54, 1595 (1958).
- 77) C. S. Braun, Shunji Kato and S. Lipsky. J. Chem. Phys. 39, 1645 (1963).
- 78) J. A. Poole. J. Phys. Chem. 69, 1343 (1965).
- 79) M. L. Huggins. J. Amer. Chem. Soc. 75, 4123 (1953).
- 80) S. R. Gunn and L. G. Green. J. Phys. Chem. 65, 779 (1961).
- 81) F. E. Saalfeld and H. J. Svec. Inorg. Chem. 2, 46 (1963).
- 82) R. F. Barrow and J. L. Deutsch. Proc. Chem. Soc. 122 (1960).
- 83) P. C. Jordan. J. Chem. Phys. 44, 3400 (1965).
- 84) P. S. Skell and E. J. Goldstein. J. Amer. Chem. Soc. 86, 1442 (1964).
- 85) K. A. W. Kramer and A. N. Wright. J. Chem. Soc. 3604 (1963).

- 86) J. W. Simons and C. J. Mazac. Can. J. Chem. 45, 1717 (1967).
- 87) C. J. Mazac and J. W. Simons. J. Amer. Chem. Soc. 90, 2484 (1968).
- 88) M. A. Nay, K. S. Sidhu, H. E. Gunning and O. P. Strausz. To be published.
- 89) D. Seyferth and J. M. Burlitch. J. Amer. Chem. Soc. 85, 2667 (1963).
- 90) P. P. Gaspar, B. D. Pate and W. Eckelman. J. Amer. Chem. Soc. 88, 3878 (1966).
- 91) E. Jakubowski. Univ. of Alberta. Unpublished data.
- 92) V. R. Schwarz and F. Heinrich. Z. Anorg. Chem. 221, 277 (1935).
- 93) V. Wartenburg. Z. Anorg. Chem. 79, 76 (1913).
- 94) Unpublished spectra taken by Dr. F. C. James of this laboratory.
- 95) A. Stock and C. S. Someski. Ber. 56, 247 (1923).
- 96) P. Gray and J. C. J. Thynne. Trans. Faraday Soc. 59, 2275 (1963).
- 97) P. Gray, A. Jones and J. C. J. Thynne. 61, 474 (1965).
- 98) J. C. J. Thynne. Trans. Faraday Soc. 60, 2207 (1964).
- 99) R. E. Rebbert and P. Ausloos. J. Phys. Chem. 67, 1925 (1963).
- 100) S. Toby and J. Nimoy. J. Phys. Chem. 70, 867 (1966).
- 101) A. Shepp. J. Chem. Phys. 24, 939 (1956).
- 102) M. Cher, C. S. Hollingsworth and F. Sicilio. J. Phys. Chem. 70, 877 (1966).
- 103) K. Yang. J. Amer. Chem. Soc. 84, 3795 (1962).
- 104) J. L. Holmes and K. O. Kutschke. Trans. Faraday Soc. 58, 333 (1962).
- 105) S. W. Charles and E. Whittle. Trans. Faraday Soc. 56, 794 (1960).
- 106) F. S. Dainton, E. A. Creak and K. J. Ivin. Trans. Faraday Soc. 58, 326 (1962).
- 107) F. S. Dainton, K. J. Ivin and F. Wilkinson. Trans. Faraday Soc. 55, 929 (1959).

- 108) J. R. McNesby. J. Phys. Chem. 64, 1674 (1960).
- 109) S. Glasstone, K. J. Laidler and H. Eyring. Theory of Rate Processes. McGraw-Hill Inc., New York. 1941.
- 110) T. E. Sharp and H. S. Johnston. J. Chem. Phys. 37, 1541 (1962).
- 111) L. Pauling. J. Amer. Chem. Soc. 69, 542 (1947).
- 112) H. S. Johnston and C. Parr. J. Amer. Chem. Soc. 85, 2544 (1963).
- 113) S. Sato. J. Chem. Phys. 23, 2465 (1955).
- 114) P. M. Morse. Phys. Rev. 34, 57 (1929).
- 115) R. E. Wilde. J. Mole. Spect. 8, 424 (1962).
- 116) E. B. Wilson, Jr., J. C. Decius and P. C. Cross. Molecular Vibrations. McGraw-Hill Inc., New York. 1955. p. 175.
- 117) C. A. Heller and A. S. Gordon. J. Phys. Chem. 64, 390 (1960).

APPENDIX A

Quenching Cross sections for Hg $6(^3P_1)$ atoms.

Compound	$\sigma_Q^2 \text{ \AA}^2$	
	Physical	Chemical
C_3H_8	2.86 ^a	2.86 ^b
$CH_3-CD_2-CH_3$	0.99 ^a	0.40 ^b
$CD_3-CH_2-CD_3$	2.50 ^a	2.38 ^b
C_3D_8	0.82 ^a	0.21 ^b
cyclopropane	1.85 ^a	
cyclopropane-d ₆	1.73 ^a	
1-chloropropane	62.30 ^a	
2-chloropropane	60.60 ^a	
SiH_4	45.00 ^d	
SiD_4	46.70 ^a	
$Hg(CH_3)_2$	81.00 ^c	
benzene	73.30 ^c	
propylene	56.00 ^c	
H_2	10.50 ^c	
NO	43.20 ^c	

(a) S. Penzes. Ph.D. Thesis. University of Alberta. "The Energy Transfer Mechanism in Mercury Photosensitization" 1968. p. 90-92.

- (b) J. G. Calvert and J. N. Pitts, Jr. Photochemistry. J. Wiley and Sons Inc., New York. 1966. p. 74-77. ($\sigma_Q^2 \text{ \AA}^2$ Chemical Proc. I x 2.38).
- (c) Ibid, ($\sigma_Q^2 \text{ \AA}^2$ Physical Proc. I x 1.75).
- (d) A. J. Yarwood, O. P. Strausz and H. E. Gunning. J. Chem. Phys. 41, 1705 (1964).

APPENDIX B

Bond Dissociation Energies

Bond	D ₂₉₈ kcal mole ⁻¹	Estimated error kcal mole ⁻¹	Reference
C-H	81		71
CH-H	108	6	33
CH ₂ -H	104	6	33
CH ₃ -H	104	1	33
C ₂ H ₅ -H	98	1	71
C-C ₃ H ₅ -H	101	3	33
CH ₃ CH ₂ CH ₂ -H	98	2	33
(CH ₃) ₂ CH-H	94.5	1	33
C ₆ H ₅ -H	103		71
C ₆ H ₅ -CH ₂ -H	85	1	33
CH ₂ =CHCH ₂ -H	85	1	33
CH ₃ -CH ₃	88	2	33
C ₂ H ₅ -CH ₃	85	2	33
C ₆ H ₅ -CH ₃	93		71
CH ₂ =CHCH ₂ -CH ₃	66 (estimated)		71
<u>n</u> -C ₃ H ₇ -Br	69	2	33
<u>i</u> -C ₃ H ₇ -Br	68	2	33
<u>n</u> -C ₃ H ₇ -Cl	82	2	33
<u>i</u> -C ₃ H ₇ -Cl	81	2	33
CH ₃ Hg-CH ₃	50	2	33
Hg-CH ₃	~7		71

APPENDIX B

(Continued)

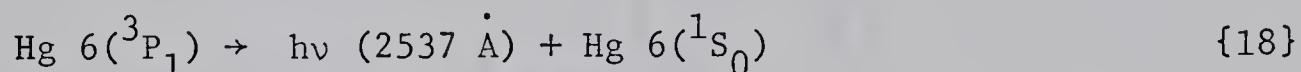
Bond	D_{298} kcal mole ⁻¹	Estimated error kcal mole ⁻¹	Reference
SiH ₃ -H	95.2		73
(CH ₃) ₃ Si-H	83		72
SiH ₃ -SiH ₃	83.7		73
(CH ₃) ₃ Si-CH ₃	79		72
(CH ₃) ₃ Si-C ₂ H ₅	77		72
(CH ₃) ₃ Si-CH(CH ₃) ₂	77		72
(CH ₃) ₃ Si-C(CH ₃) ₃	77		72

APPENDIX C

Secondary Decomposition of Primary Radicals

Imprisonment Lifetime (Trapped radiation)

Due to the large absorption coefficient of mercury for 2537 Å radiation it is possible for a photon of this wavelength entering a reaction vessel to be absorbed, emitted and reabsorbed several times by a mercury atom before emerging from the vessel. The net effect of this phenomena known as "imprisonment of resonance radiation" is to increase the apparent radiative lifetime of the Hg 6(³P₁) atom for the reaction,



The rate of this reaction is given by the inverse of the radiative lifetime, $1/\tau_i$. The imprisonment decay constant can be evaluated using Holstein's experimentally verified formula (36, 37).

$$k_{18} = \frac{1}{\tau_i} = (5/8 k_0 R \{\pi \ln \frac{1}{2} k_0 R\}^{1/2} \tau)^{-1}$$

$$k_0 = 2.23 \times 10^{-12} \text{ N} / \text{T}^{1/2}$$

N = concentration of mercury

$$\text{atoms/cc} = 9.652 \times 10^{18} \text{ P/T}$$

P = pressure in torr

T = absolute temperature = 330° K

$$25 \text{ mtorr} = 7.31 \times 10^{14} \text{ atoms cc}^{-1}$$

R = radius of reaction vessel = 0.45 cm

= mean radiative lifetime of 6(³P₁) atoms

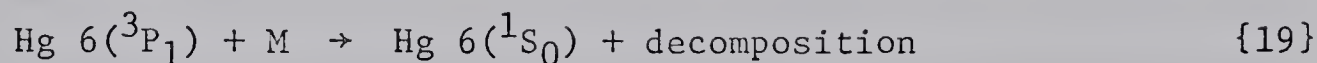
$$= 1.1 \times 10^{-7} \text{ sec}$$

Using these parameters the following values are obtained for τ_i and k_{18} .

$$\tau_i = 8.5 \times 10^{-6} \text{ sec}$$

$$k_{18} = 1.18 \times 10^5 \text{ sec}^{-1}$$

Rate of Quenching, $k_{19} M = k_{19}^*$



The rate of quenching can be calculated from gas kinetic collision theory using the effective quenching cross sections (σ_Q^2), for Hg $6(^3P_1)$ atoms.

$$k_{19} = Z_{(\text{Hg}^*, M)} = \sigma_Q^2(\text{Hg}^*, M) \left[\frac{8 \pi RT}{\mu} \right]^{1/2}$$

$$k_{19}M = \{M\} \sigma_Q^2(\text{Hg}^*, M) \left[\frac{8 \pi RT}{\mu} \right]^{1/2}$$

$$\{M\} = \{\text{Hg}(\text{CH}_3)_2\} = (9.652 \times 10^{18}) (10^{-2}/T)$$

$$= 2.93 \times 10^{14} \text{ molecules cc}^{-1}$$

$$T = 330^\circ \text{ K}$$

$$\sigma_Q^2(\text{Hg}^*, \text{Hg}(\text{CH}_3)_2) = 81 \text{ \AA}^2 \quad (\text{Appendix A})$$

$$\mu = \text{reduced mass} = \frac{m_{\text{Hg}} m_{\text{Hg}(\text{CH}_3)_2}}{m_{\text{Hg}} + m_{\text{Hg}(\text{CH}_3)_2}}$$

$$\mu = 107 \text{ gm mole}^{-1}$$

$$R = 8.317 \times 10^7 \text{ ergs } ^\circ\text{C}^{-1} \text{ mole}^{-1}$$

Using these parameters

$$k_{19}M = k_{19} = 1.9 \times 10^5 \text{ sec}^{-1}$$

Rate of decomposition of $\text{Hg}(\text{CH}_3)_2$, R_d

At 10 torr helium carrier pressure the flow rate through the reaction zone is 1400 cc sec.⁻¹. For reactor tubing having an inner diameter of 9 mm the flow velocity past the lamp is calculated to be 2201 cm sec.⁻¹. Using 4 cm as the contact length of the reaction zone a contact time of 1.8 milliseconds is derived. The illuminated volume of the reactor is 2.5 cc.

At high light intensity conditions 2.5 mtorr of $\text{Hg}(\text{CH}_3)_2$ was decomposed per pass (25% of 10 torr). At the flow rate of 1400 cc sec.⁻¹, 1.22×10^{17} molecules of $\text{Hg}(\text{CH}_3)_2$ were decomposed per second. The reactor volume being 2.5 cc,

$$R_d = \frac{1.22 \times 10^{17} \text{ molecules sec}^{-1}}{2.5 \text{ cc}} = 4.9 \times 10^{16} \text{ molecules cc}^{-1} \text{ sec}^{-1}.$$

Absorbed Light Intensity, I_a

Electronically excited $\text{Hg } 6(^3\text{P}_1)$ atoms revert to the ground state by two main reactions, emission {18}, or quenching {19}. By assuming that every mercury atom quenched by $\text{Hg}(\text{CH}_3)_2$ leads to decomposition of the $\text{Hg}(\text{CH}_3)_2$ the absorbed light intensity I_a , can be calculated. Using the previously calculated values of R_d , k_{18} and k_{19}^* ,

$$R_d = I_a \left[\frac{k_{19}^*}{k_{18} + k_{19}^*} \right].$$

This relationship states that the rate of decomposition is equal to the absorbed light intensity times the fraction decaying by quenching.

$$I_a = R_d \left[\frac{k_{18} + k_{19}^*}{k_{19}^*} \right] = 8 \times 10^{16} \text{ quanta cc}^{-1} \text{ sec}^{-1}$$

Steady State Concentrations of Hg^* , CH_3 and C_3H_7

Under steady-state conditions the radiation absorbed by mercury is equal to the radiative and non-radiative decay of excited mercury atoms.

$$I_a = \{\text{Hg}^*\} (k_{18} + k_{19}^*)$$

$$\{\text{Hg}^*\} = I_a / (k_{18} + k_{19}^*)$$

$$\{\text{Hg}^*\} = \frac{8 \times 10^{16} \text{ quanta cc}^{-1} \text{ sec}^{-1}}{(1.18 \times 10^5 + 1.9 \times 10^5) \text{ sec}^{-1}} = 2.6 \times 10^{11} \text{ atoms cc}^{-1}$$

Assuming steady-state conditions under which the production of methyl radicals via decomposition of $\text{Hg}(\text{CH}_3)_2$ is equal to their rate of disappearance by recombination to form ethane,

$$2 R_d = k_r \{\text{CH}_3\}^2$$

$$\{\text{CH}_3\} = \{2 R_d / k_r\}^{1/2} = 3.6 \times 10^{13} \text{ radicals cc}^{-1}$$

$$k_r = 4.5 \times 10^{13} \text{ cc mole}^{-1} \text{ sec}^{-1} \text{ Ref. (38)}$$

$$k_r = 7.5 \times 10^{-11} \text{ cc molecule}^{-1} \text{ sec}^{-1}$$

At high light intensities and approximately 2 mtorr of propane about 2 - 4% decomposition is observed. These observations plus the fact that only one propyl radical is produced per quenching reaction indicate

that the rate of production of propyl radicals in the system is at least 100 times slower than that of methyl radicals. Using this approximation plus the assumption of an identical rate constant for the combination of propyl with methyl radicals as for methyls, the steady-state concentration of propyl radicals can be estimated.

$$R_{\text{CH}_3} = 2 R_d = 100 R_{\text{C}_3\text{H}_7}$$

$$R_{\text{C}_3\text{H}_7} = k_r \{ \text{C}_3\text{H}_7 \} \{ \text{CH}_3 \} = R_d / 50$$

$$\{ \text{C}_3\text{H}_7 \} = R_d / 50 k_r \{ \text{CH}_3 \}$$

$$\begin{aligned} \{ \text{C}_3\text{H}_7 \} &= \frac{4.9 \times 10^{16} \text{ molecules cc}^{-1} \text{ sec}^{-1}}{50 (7.5 \times 10^{-11} \text{ cc molecules}^{-1} \text{ sec}^{-1}) (3.6 \times 10^{13} \text{ radicals cc}^{-1})} \\ &= 3.6 \times 10^{11} \text{ radicals cc}^{-1} \end{aligned}$$

Assuming an effective quenching cross section of 40 \AA^2 for propyl and methyl radicals the rates of secondary reactions with Hg^* can be calculated.

$$R_{(\text{Hg}^*, \text{C}_3\text{H}_7)} = \{ \text{Hg}^* \} \{ \text{C}_3\text{H}_7 \} \sigma_Q^2 \left[\frac{8 \pi R T}{\mu} \right]^{1/2}$$

$$\{ \text{Hg}^* \} = 2.6 \times 10^{11} \text{ atoms cc}^{-1}$$

$$\{ \text{C}_3\text{H}_7 \} = 3.6 \times 10^{11} \text{ radicals cc}^{-1}$$

$$\sigma_Q^2 = 40 \text{ \AA}^2$$

$$R = 8.317 \times 10^7 \text{ erg } ^\circ\text{C}^{-1} \text{ mole}^{-1}$$

$$T = 330^\circ \text{ K}$$

$$\mu_{(\text{Hg}^*, \text{C}_3\text{H}_7)} = \frac{8.6 \times 10^3}{243} \text{ gm}$$

Then,

$$R_{(\text{Hg}^*, \text{C}_3\text{H}_7)} = 5.24 \times 10^{13} \text{ collisions cc}^{-1} \text{ sec}^{-1}$$

Using the same equation with,

$$\{\text{CH}_3\} = 3.6 \times 10^{13} \text{ radicals cc}^{-1}$$

$$\mu_{(\text{Hg}^*, \text{CH}_3)} = \frac{3 \times 10^3}{215} \text{ gm}$$

$$R_{(\text{Hg}^*, \text{CH}_3)} = 8.31 \times 10^{15} \text{ collisions cc}^{-1} \text{ sec}^{-1}$$

Using Gomer and Kistiakowsky's rate constant for both radical radical reactions,

$$R_{(\text{CH}_3, \text{C}_3\text{H}_7)} = k_r \{\text{CH}_3\} \{\text{C}_3\text{H}_7\}$$

$$= 9.72 \times 10^{14} \text{ molecules cc}^{-1} \text{ sec}^{-1}$$

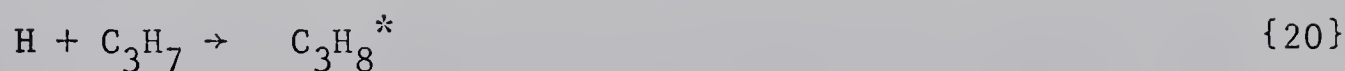
$$R_{(\text{CH}_3, \text{CH}_3)} = k_r \{\text{CH}_3\}^2$$

$$= 9.72 \times 10^{16} \text{ molecules cc}^{-1} \text{ sec}^{-1}$$

APPENDIX D

Calculations Involving the Reactions of $H + C_3H_7$.

Taking the rate of {20}



to equal

$$\{C_3H_8^*\} = \{C_3H_6\} - \{C_3H_6\} \text{ from } \{25\} - \{C_3H_8\} \{+C_2H_5 \cdot CD_3\}$$

the relative amounts of H-atoms reacting with n- and isopropyl radicals can be calculated from the data in Table VIII.

 $H + i-C_3H_7$

$$\{C_3H_6\} \text{ from } \{25\} = 0.15 \quad \{\underline{i}-C_4H_{10}\} = 0.12$$

$$\{C_3H_8^*\} = 2.00$$

$$\{\text{total products}\} = 2.91$$

$$\{C_3H_8^*\} / \{\text{total products}\} = 0.69$$

 $H + n-C_3H_7$

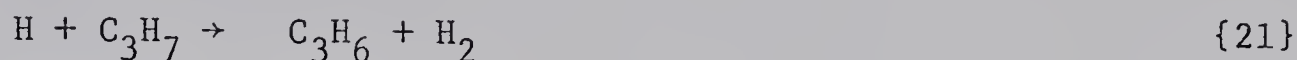
$$\{C_3H_6\} \text{ from } \{25\} = 0.06 \quad \{\underline{n}-C_4H_{10}\} = 0.08$$

$$\{C_3H_8^*\} = 1.64$$

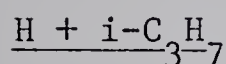
$$\{\text{total products}\} = 2.97$$

$$\{C_3H_8^*\} / \{\text{total products}\} = 0.55$$

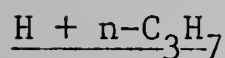
Values for the disproportionation to recombination ratios for H-atoms plus propyl radicals were approximated by taking the propylene produced via {21}.



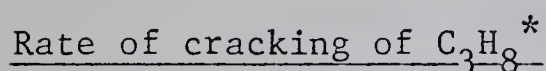
(Total C_3H_6 - that calculated arising from {25}) and dividing by the measured C_3H_8 .



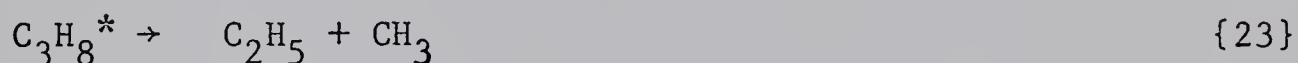
$$k_d/k_r = 1.39$$



$$k_d/k_r = 0.58$$



The gas kinetic expression for collision frequency has been used to calculate the rate of {23}.



Identical rates for the propyl + H and ethyl + H reactions. The fraction of C_3H_8^* decomposing via {25} is calculated by dividing the corrected $\text{C}_2\text{H}_5 \cdot \text{CD}_3$ product (Table VIII) by the $\text{C}_3\text{H}_8 + \text{C}_2\text{H}_5 \cdot \text{CD}_3$ total. This gives, 35% cracking of n-propyl and 17% cracking of isopropyl. The collision frequency is,

$$Z_{(\text{He}, \text{C}_3\text{H}_8^*)} = \frac{N_{\text{He}}}{4} (\sigma_{\text{He}} \sigma_{\text{C}_3\text{H}_8^*})^2 \lambda \left[\frac{8 \pi RT}{\mu} \right]^{1/2}$$

$$N_{\text{He}} = 2.9 \times 10^{17} \text{ atoms cc}^{-1}$$

$$\sigma_{\text{C}_3\text{H}_8} = 6 \times 10^{-8} \text{ cm}$$

$$\sigma_{\text{He}} = 2 \times 10^{-8} \text{ cm}$$

$$\lambda = \text{collision efficiency} = .25$$

$$\mu = \frac{m_{\text{He}} m_{\text{C}_3\text{H}_8}}{m_{\text{He}} + m_{\text{C}_3\text{H}_8}}$$

$$T = 330^\circ\text{K}$$

These parameters give a collision frequency of $Z_{(\text{He}, \text{C}_3\text{H}_8^*)} = 4.8 \times 10^7 \text{ sec}^{-1}$. The cracking rates are,

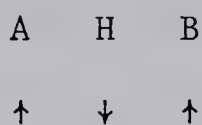
$$\underline{\text{n-propyl}} = 0.35 Z = 1.7 \times 10^7 \text{ sec}^{-1}$$

$$\text{isopropyl} = 0.17 Z = 8.2 \times 10^6 \text{ sec}^{-1}$$

APPENDIX E

Bond - Energy - Bond - Order Calculations.⁵a) Potential energy of activation:

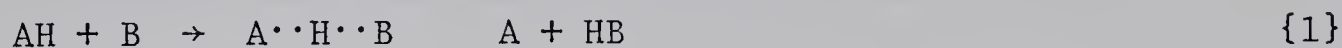
For two radicals to form a stable bond the respective electrons must have opposite spins, $\uparrow\downarrow$, if the spins are parallel, $\uparrow\uparrow$, an unstable pair is formed. For the complex $A\cdot H\cdot B$ the relatively stable pattern is



or



For a general reaction of the type



it is assumed that during all stages of the collision, the formation of the bond HB is "paying" for the breaking of bond AH. The bond orders in AH and HB are both one. This relationship leads to the assumption that the path of lowest energy between reactant and product is that along which the sum of bond orders is unity:

$$n_1 + n_2 = 1 \quad \{2\}$$

⁵

For a complete discussion of the BEBO method see reference (25).

The energy of the linear A·H·B complex is assumed to be composed of three parts E_{AH} , E_{HB} and E_{AB} . E_{AH} represents the bond energy of the AH bond, E_{HB} represents that of the HB bond and E_{AB} represents the triplet repulsive energy. Using these assumptions, the energy of the system relative to zero for the reactants can be expressed as:

$$V = D_e (A-H) - E_{AH} - E_{HB} + E_{AB} \quad \{3\}$$

Where D_e is the single bond energy (including zero point energy) of the reactant molecule. Under these conditions the maximum V along the path of constant total bond order is defined as the potential energy of activation for the reaction {1}.

To evaluate {3}, Pauling's empirical relationships between bond distance - bond order and bond energy - bond order are used (111).

$$R = R_e - 0.26 \ln n \quad \{4\}$$

Where R_e is the length of a single bond and R is the length of any other bond between the two atoms. If a log - log plot of bond energy vs. bond order is constructed the empirical relationship

$$D = D_e n^p \quad \{5\}$$

is obtained, where D is the bond energy of any bond other than a single bond and p is the empirical slope of the curve obtained from the plot (112). A plot of log bond energy vs. bond length indicates an empirical relationship exists between single-order bonds and Lennard-Jones molecules (112). This relationship is expressed as

$$\ln D/D_e = C (R_e - R) \quad \{6\}$$

where C is found to equal $p/0.26$. By use of equations {4}, {5} and {6} the index p can be evaluated from the data available for stable reactant molecules and noble-gas Lennard-Jones molecules.

$$p = \frac{0.26 \ln (D_e / \epsilon_x)}{R_x - R_e} \quad \{7\}$$

ϵ_x = Depth of Lennard-Jones potential for diatomic noble-gas cluster.

R_x = Equilibrium internuclear distance of noble-gas cluster.

With these relationships, equation {3} transforms to

$$V = D_{AH} - D_{AH} n^p - D_{HB} (1-n)^q + E_{AB} \quad \{8\}$$

To evaluate the triplet repulsion term E_{AB} , Sato's anti-Morse function can be used (113).

$$E_{AB} = D_{AB} \frac{1}{2} \exp(-\beta r_3) \{1 + \frac{1}{2} \exp(-\beta r_3)\} \quad \{9\}$$

Where

$$r_3 = R_{AH} + R_{HB} - R_{AB} - 0.26 \ln n_1 n_2 \quad \{10\}$$

$$n_2 = 1 - n_1$$

β = Morse parameter calculated from the expression (114):

$$\beta = 1.2177 \times 10^7 \omega_e (\mu / D_{AB})^{1/2}$$

$$\omega_e = \text{AB stretching frequency in cm}^{-1}$$

$$\mu = \text{Reduced mass in units of gram/mole}$$

By defining two constant terms

$$B = \frac{1}{2} \exp(-\beta \Delta R_e) \quad \{11\}$$

$$\gamma = 0.26 \beta \quad \{12\}$$

Where $\Delta R_e = R_{AH} + R_{HB} - R_{AB}$ and substitution of {9-12} into {8} the final expression is obtained.

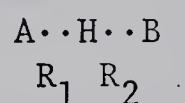
$$V = D_{AH} (1-n^p) - D_{HB} (1-n)^q + D_{AB} B (n-n^2)^\gamma \{1 + B (n-n^2)^\gamma\} \quad \{13\}$$

Input parameters for the final calculations are summarized in Table XXI.

B) Properties of the activated complex:

The derivation of the force constants and other properties of the activated complex by the BEBO method is quite lengthy and only the essential expressions will be presented here.

The algebraic equations for the vibrational frequencies of the linear three-atom-model,



are:

$$\lambda_\alpha = \frac{1}{2} \{Y + (Y^2 - 4Z)^{\frac{1}{2}}\} \quad \{14\}$$

$$\lambda_\beta = \frac{1}{2} \{Y - (Y^2 - 4Z)^{\frac{1}{2}}\} \quad \{15\}$$

$$Y = \frac{F_{11}}{m_A} + \frac{F_{22}}{m_B} + \frac{F_{11} + F_{22} - 2F_{12}}{m_H} \quad \{16\}$$

$$Z = \frac{(F_{11}F_{22} - F_{12}^2) (m_A + m_H + m_B)}{m_A m_H m_B} \quad \{17\}$$

$$\lambda_{\phi} = F_{\phi} \left[\frac{1}{R_{1A}^2} + \frac{1}{R_{2B}^2} + \left(\frac{1}{R_1} - \frac{1}{R_2} \right)^2 \frac{1}{m_H} \right] \quad \{19\}$$

$$\begin{aligned} F_{11} &= \\ F_{22} &= \\ F_{12} &= \end{aligned} \left\{ \begin{array}{l} \text{Single-bond force constants of} \\ \text{activated complex in units of} \\ 10^5 \text{ dynes/cm.} \end{array} \right.$$

$$F_{\phi} = \text{Bending force constant in units of } 10^{-11} \text{ ergs/radian}^2.$$

$$\begin{aligned} R_1 &= \\ R_2 &= \end{aligned} \left\{ \begin{array}{l} \text{Single-bond length in activated complex} \\ \text{in angstrom units.} \end{array} \right.$$

$$R_1 = R_{1e} - 0.26 \ln n$$

$$R_2 = R_{2e} - 0.26 \ln m$$

$$R_3 = R_1 + R_2$$

$$\begin{aligned} R_{1e} &= \\ R_{2e} &= \\ R_{3e} &= \end{aligned} \left\{ \begin{array}{l} \text{Single-bond length} \\ \text{in angstrom units.} \end{array} \right.$$

$$\begin{aligned} n &= \\ m &= \end{aligned} \left\{ \begin{array}{l} \text{Bond orders in activated} \\ \text{complex where } m = 1-n. \end{array} \right.$$

$$\begin{aligned} m_A &= \\ m_B &= \\ m_H &= \end{aligned} \left\{ \begin{array}{l} \text{Reactant masses in gram-molar} \\ \text{mass units.} \end{array} \right.$$

The vibrational frequencies of the activated complex are evaluated from the expression:

$$\omega = 1301.9 \lambda^{\frac{1}{2}} \text{ cm}^{-1} \quad \{19\}$$

The bending force constant is given by:

$$F_{\phi} = \frac{R_1 R_2 \dot{F}_{AB}}{4 \beta_{AB} R_{AB}} (n \ m)^{\gamma} \exp (-\beta \Delta R) \quad \{20\}$$

$$\left. \begin{array}{l} F_{AB} \\ F_{AH} \\ F_{HB} \end{array} \right\} \begin{array}{l} \text{Single-bond force constants in} \\ \text{units of } 10^5 \text{ dynes/cm.} \end{array}$$

$$\gamma = 0.26 \beta_{AB}$$

β = Morse parameter.

$$\beta = 1.2177 \times 10^7 \omega_e (\mu/D(A-B))^{\frac{1}{2}}$$

ω_e = Stretching frequencies in cm^{-1}

μ = Reduced mass in units of gram/mole

$$\Delta R_e = R_{1e} + R_{2e} - R_{3e}$$

The single-bond force constants of the activated complex are calculated from the equations:

$$F_{11} = \frac{F_{\rho} m^2 + F_{\sigma} n^2}{n^2 + m^2} \quad \{21\}$$

$$F_{22} = \frac{F_{\rho} n^2 + F_{\sigma} m^2}{n^2 + m^2} \quad \{22\}$$

$$F_{12} = \frac{(-F_{\rho} + F_{\sigma}) n m}{n^2 + m^2} \quad \{23\}$$

F_{ρ} is the force constant along the reaction path ρ and F_{σ} is the force constant perpendicular to ρ . Both are in dynes/cm.

$$-F_{\rho} = \frac{10.27}{\frac{1}{n^2} + \frac{1}{m^2}} \left\{ \frac{D_{AH} p(p-1)}{n^{2-p}} + \frac{D_{HB} q(q-1)}{m^{2-q}} + \frac{D_{AB}^2 B \gamma}{(n m)^{1-\gamma}} \left[1 + \frac{(1-\gamma)(1-2n)^2}{2 n m} \right] \right\} \quad \{24\}$$

$$F_{\sigma} = \frac{F_{AH} n^3 + F_{HB} m^3 + (F_{AB}/2)(n m)^{\gamma_B}}{n^2 + m^2} \quad \{25\}$$

$\left. \begin{matrix} p \\ q \end{matrix} \right\}$ Bond energy indexes.

$\left. \begin{matrix} D_{AH} \\ D_{HB} \\ D_{AB} \end{matrix} \right\}$ Single bond energies in calories/mole.

$$B = \frac{1}{2} \exp(-\beta \Delta R_e)$$

Table XX contains the input parameters for these calculations and Table XXI summarizes the results. The properties of the activated complex obtained by this method were used in equation {16} chapter 6 to obtain the kinetic isotope effect.

TABLE XX
Input parameters for BEBO calculations.

Parameter	Value	Reference
<u>Bond distance</u> (Å)		
Si - H	1.48	115
C - H	1.09	115
C - Si	1.87	115
<u>Bond energies</u> ^(a) (kcal mole ⁻¹)		
CH ₃ - H	105.5	110
SiH ₃ - H	98.2	73
Si ₂ H ₅ - H	93.0	estimated
H ₃ C - SiH ₃	78.0	72
<u>Bond energy index</u> (p, q)		
C - H	1.087	110
Si - H	1.004 ^(b)	
<u>Force constants</u> (x 10 ⁻⁵ dynes/cm)		
C - H	5.1	116
Si - H	2.9	116
C - Si	3.4	(ave. of C-C & Si-C)
<u>Morse parameter</u> , β ^(c)		
C - Si	1.60	

(a) Includes zero point energy.

TABLE XX

(Continued)

(b) The bond energy index for Si - H bond was calculated from expression {7}, Appendix E using the Lennard-Jones parameters for the He-Ar diatomic gas molecule.

(c) Calculated using the expression (114)

$$\beta = 1.2177 \times 10^7 \omega_e \{\mu/D(\text{C-Si})\}^{1/2}$$

with

$$\omega_e = 750 \text{ cm}^{-1}$$

$$\mu = 8.4 \text{ gram mole}^{-1}$$

TABLE XXI

Properties of the activated complex for three-atom-model
obtained by BEBO method.

Property	Reaction System	
	$\text{SiH}_4 + \text{CH}_3$	$\text{Si}_2\text{H}_6 + \text{CH}_3$
n_1	0.68	0.75
n_2	0.32	0.25
R_1 (Å)	1.58	1.55
R_2	1.58	1.45
$F_{11} \times 10^{-5}$ (dynes/cm)	1.680	2.030
$F_{22} \times 10^{-5}$	- 0.022	- 0.158
$F_{12} \times 10^{-5}$	1.030	0.821
$F_\phi \times 10^{-11}$ (erg/rad ²)	0.067	0.064
(bending) _H (cm ⁻¹)	463.0 (2)	445.0 (2)
(bending) _D	331.0 (2)	318.0 (2)
(stretching) _H	585.0	912.0
(stretching) _D	537.0	736.5
(imaginary) _H	965.5	589.0
(imaginary) _D	740.0	513.0
<u>Reactants</u>		
(stretching) (Si - H) (cm ⁻¹)	2150	2150
(stretching) (Si - D)	1550	1550

B29904